

MINISTÉRIO DA CIÊNCIA E TECNOLOGIA
INSTITUTO NACIONAL DE PESQUISAS ESPACIAIS

INPE-5543-NTC/311

A COMPUTER MODEL FOR
THE LOW-LATITUDE IONOSPHERE

José Augusto Bittencourt

INPE
São José dos Campos
Abril de 1994

A COMPUTER MODEL FOR THE LOW-LATITUDE IONOSPHERE

J. A. Bittencourt

Instituto Nacional de Pesquisas Espaciais - INPE

Caixa Postal 515

12.201-970 São José dos Campos, SP

ABSTRACT

A fully time-dependent computer model for the low-latitude ionospheric F-region is presented. The spatial and time distribution of the ionospheric particle densities and velocities are computed by numerically solving the time-dependent, coupled, nonlinear system of continuity and momentum equations for the ions O^+ , O_2^+ , NO^+ , N_2^+ and N^+ , taking into account photoionization of the atmospheric species by the solar extreme ultraviolet radiation, chemical and ionic production and loss reactions, and plasma transport processes, including the ionospheric effects of thermospheric neutral winds, plasma diffusion and electromagnetic $\mathbf{E} \times \mathbf{B}$ plasma drifts. The Earth's magnetic field is represented by a tilted centered magnetic dipole. This set of coupled nonlinear equations are solved along a given magnetic field line in a frame of reference moving vertically, in the magnetic meridian plane, with the electromagnetic $\mathbf{E} \times \mathbf{B}$ plasma drift velocity. The spatial and time distribution of the thermospheric neutral wind velocities and the pattern of the electromagnetic drifts are taken as known quantities, given through specified analytical or empirical models. The computed results reproduce the typical ionization distribution normally observed in the low-latitude ionospheric F-region including details of the equatorial Appleton anomaly dynamics. The specific effects on the F-region of changes in the thermospheric neutral winds and the electromagnetic plasma drifts are investigated using different wind and drift models, including the important longitudinal effects associated with magnetic declination dependence and latitudinal separation between geographic and geomagnetic equators.

TABLE OF CONTENTS

1. Introduction	3
2. The Low-Latitude Ionospheric Anomaly	4
3. Physical Processes	5
4. Basic Transport Equations	9
4.1 The Plasma Continuity Equations	9
4.2 The Equations of Motion	11
4.3 The Energy Conservation Equations	13
4.4 The Divergence Terms	13
4.5 Coupling to the Neutral Winds and Electric Fields	15
5. Thermospheric Neutral Winds	17
5.1 Basic Equations	17
5.2 Global Pressure Gradients	19
5.3 Boundary Conditions	20
5.4 Thermospheric Neutral Wind Models	21
6. Electromagnetic Plasma Drifts	24
6.1 Theoretical Models	25
6.2 The Divergence of the Plasma Drift Velocity	25
6.3 Plasma Drift Velocity Models	27
7. Photoionization and Ion Chemistry	28
7.1 Photoionization Rates	28
7.2 Ion Chemistry	30
8. Neutral Atmosphere Model	31
8.1 Temperature Profiles	32
8.2 Neutral Density Profiles	33
9. Diffusion Rates and Collision Frequencies	33
10. Computational Procedure	35
10.1 Variable Transformations	35
10.2 Boundary Conditions	36
10.3 Spatial Grid and Time Step	36
11. Examples of Some Computer Model Results	37
11.1 Electromagnetic Plasma Drift Effects	38
11.2 Thermospheric Neutral Wind Effects	39
12. Summary and Conclusions	40
References	54
Appendix	62

1. INTRODUCTION

The ionosphere is usually defined as the region of the upper atmosphere where ions and electrons exist in quantities sufficient to influence the propagation of radio waves. It is the result of the interaction of solar ionizing electromagnetic and corpuscular radiations with the neutral atmospheric constituents, forming ion-electron pairs which ultimately recombine. It is maintained by a balance of ion-electron production, chemical and physical loss mechanisms and transport processes.

The lower boundary of the Earth's ionosphere, at about 60 *km*, coincides with the region where the ionization is produced by the most penetrating radiation, generally cosmic rays. The upper boundary can be defined by the interaction of the solar wind (the plasma that continually flows outward from the Sun at supersonic speeds as the result of the expansion of the hot solar corona) with the planetary magnetic field.

The symbols D, E, F1 and F2 are used to distinguish the various ionospheric regions in terms of altitude ranges which differ basically in the physical and chemical processes governing the behavior of each layer.

The D-region, below approximately 90 *km*, is a region of weakly-ionized plasma and large neutral species number density, as well as complex ion-interchange and electron attachment and detachment reactions. In the E-region (about 90 to 150 *km*) the major ions are NO^+ and O_2^+ , with N_2^+ and O^+ as minor ions. Both the D and E-regions are primarily controlled by photochemical production and loss processes rather than by transport processes, and the main loss rate is proportional to n_e^2 , where n_e denotes the electron number density.

The daytime F-region is divided into F1 (about 150 to 200 *km*) and F2 (above about 200 *km*) layers. The F1-layer is representative of the maximum of ion production and is controlled by photochemical processes with again a loss rate proportional to n_e^2 , since the recombination rate is limited by a dissociative recombination reaction. At greater heights, plasma transport processes become increasingly important so that, above approximately 250 *km*, a transport regime exists with the geomagnetic field playing a very important role in determining the ionization distribution in the F2-layer. The combined effects of ion-chemistry and plasma diffusion result in the F2-peak which represents the maximum of electron density in the vertical height profile. Recombination in situ is linear (proportional to n_e), since the rate is limited by a chemical charge transfer reaction.

At night, in the absence of the solar ionizing source, the F1 and F2-layers coalesce as the F-region, which decays through recombination reactions.

For an overall description of the Earth's ionosphere and of its relevant physical and chemical processes, as well as of some of the important ionospheric phenomena, refer to Rishbeth and Garriot (1969), Whitten and Poppoff (1971), Ratcliffe (1972), Banks and Kockarts (1973), Bauer (1973), Girard and Petit (1976), Kelley (1989), MacNamara (1991) and Hargreaves (1992). For illustration purposes, Fig. 1 presents the mean vertical distribution of the principal ions in the Earth's ionosphere typical of daytime, under solar minimum conditions, taken from Rishbeth and Garriot (1969).

2. THE LOW-LATITUDE IONOSPHERIC ANOMALY

Since the ionospheric ionization is produced as the result of photoionization of the atmospheric species by the solar extreme ultraviolet (XUV) radiation, a maximum of ionization would be expected around the subsolar point in the low latitudinal regions, where the ionization production is a maximum. However, when measured values of the electron number density at the F2-peak are plotted as a function of magnetic latitude, for a given longitude and local time, a curve is obtained which shows a minimum (trough) over the magnetic dip equator, with two maxima (crests) at dip latitudes which may vary between 10^0 to 20^0 north and south of the dip equator, depending on local time and season. This anomalous ionization distribution extends into the topside ionosphere where it gradually diminishes. At the magnetic equator the F2-peak height is a maximum and the peak electron density is typically about 20 to 50 percent less than at the crests.

The low-latitude ionospheric anomaly was first recognized by Appleton (1946) and has since been investigated by many workers. It shows rather different features depending on longitude, local time, season and period of the sunspot cycle. The diurnal development of the equatorial ionospheric anomaly has been studied in some detail for both sunspot maximum and sunspot minimum conditions (Rao, 1962; Lyon and Thomas, 1963; Thomas, 1968; Rastogi, 1966; Rush et al., 1969). There is also considerable longitudinal variation in the development and decay of the anomaly. It shows marked differences in the various longitudinal sectors, depending on the corresponding magnetic declination of each sector. A latitudinal asymmetry in the electron density, as well as in the F2-peak

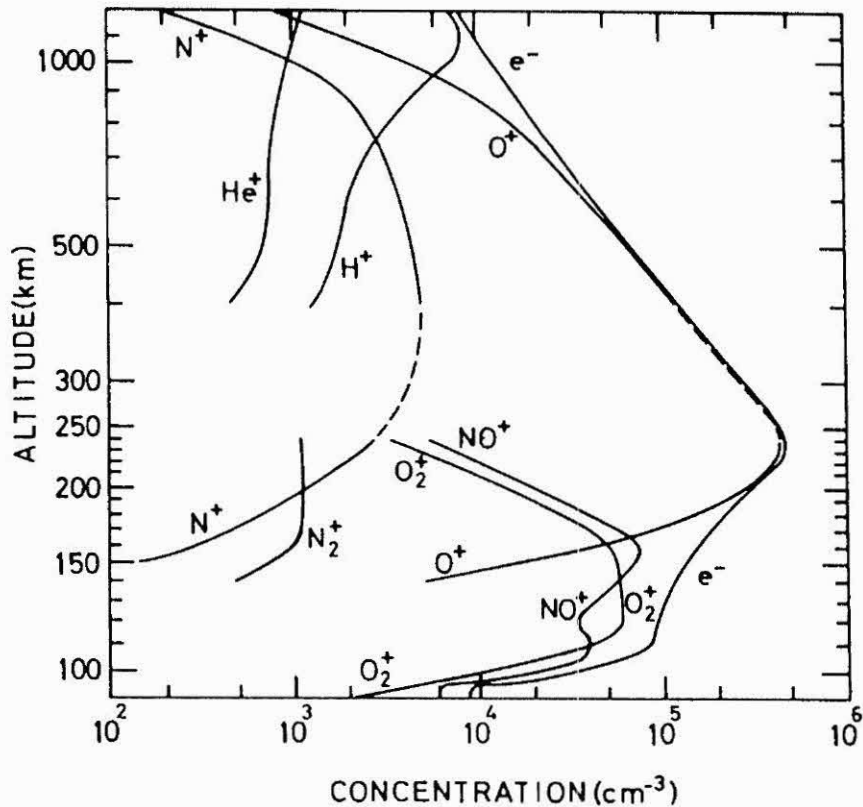


Fig. 1 Vertical distribution of the principal positive ions typical of the low-latitude diurnal ionosphere during solar minimum conditions.

height, at the north-south crests has also been observed, which shows different behavior in the various longitudinal sectors, at the same local time.

This anomalous ionization distribution at low latitudes has been explained in terms of *plasma transport processes* which moves the ionization to regions other than that of its production. It has been investigated theoretically over the past several years by many researchers (e.g. Martyn, 1953; Bramley and Peart, 1965; Hanson and Moffett, 1966; Bramley and Young, 1968; Baxter and Kendall, 1968; Abbur-Robb and Windle, 1969; Sterling et al., 1969; Anderson, 1973a,b; Bittencourt and Tinsley, 1976; Bittencourt et al., 1976). The transport processes affecting the ionization distribution in the low-latitude ionosphere are *plasma diffusion*, *electromagnetic plasma drifts* and *thermospheric neutral wind drag* caused by the meridional and zonal global pressure gradients.

3. PHYSICAL PROCESSES

The physical processes involving *production*, *loss* and *transport* of ionization in the low-latitude ionospheric F-region have different degrees

of importance, depending on the altitude region and local time under consideration.

The sources of ionization in the ionosphere include both electromagnetic and corpuscular radiations. Because of magnetic shielding effects, corpuscular radiation is important only at high latitudes as an ionizing source. Since in the F-region the principal neutral constituent is atomic oxygen, at least 13.6 eV is required for each ion-electron pair created and this energy can be supplied by the solar extreme ultraviolet (XUV) radiation with wavelengths shorter than 911 Å.

The ionization produced in a given elementary volume of the ionosphere may leave it either by being destroyed inside it or by moving outside it. The ion species and electrons may disappear as a result of chemical and ionic reactions such as electron-ion recombination, involving electrons and either atomic or molecular positive ions, or as ion-ion recombination, involving positive and negative ions. This second loss mechanism is small compared to the first one, since few negative ions exist at F-region altitudes due to a low production rate and loss by photodetachment.

In the F1-region and below, a photochemical equilibrium condition exists during the daytime, since the recombination time constant is sufficiently small and transport processes are relatively unimportant. The recombination coefficient (β) decreases with increasing altitude, since it is proportional to the particle density, so that the recombination time constant ($\tau_R \simeq 1/\beta$) increases with altitude.

The time constant for loss by diffusion (τ_D) is approximately given by H_p^2/D_p , where H_p is the plasma scale height and D_p is the plasma diffusion coefficient. Since D_p is proportional to the neutral gas density, τ_D decreases with increasing altitude.

In the F2-region, due to the longer recombination lifetime and smaller diffusion lifetime, transport of ionization plays a dominant role. Laboratory and ionospheric measurements of the recombination rates appropriate to the F2-region indicate that the lifetime of an ion-electron pair is about one to two hours (Ferguson, 1969). At the altitude where $\tau_R \simeq \tau_D$ both processes are comparable and, as a consequence, the electron density as a function of altitude reaches its maximum at approximately this altitude.

As already mentioned, the three relevant transport processes that move the ionization to regions other than that of its formation are plasma diffusion along the magnetic field lines, electromagnetic ($\mathbf{E} \times \mathbf{B}$) plasma drifts, which transport the ionization perpendicularly to the magnetic field lines, and thermospheric neutral winds, which drag the ionization in the direction of the wind component along the field line.

The plasma drift due to an east-west electric field moves the low-latitude ionospheric ionization perpendicularly to the magnetic field lines, in the well-known *fountain effect*. This transport process, combined with plasma diffusion along the magnetic field lines, caused by gravity and pressure gradients, produces a symmetrical ionization distribution about the magnetic dip equator. Two crests of plasma concentration are generated around $\pm 15^\circ$ (north-south) on either side of the magnetic dip equator. The latitudinal position of these ionization crests vary with local time and season, depending on the time variation of the $\mathbf{E} \times \mathbf{B}$ plasma drift, as well as with longitude. Fig. 2, taken from Hanson and Moffett (1966), illustrates the plasma flow associated with the equatorial *fountain effect* as a result of the combined effects of *electrodynamic plasma lifting* ($\mathbf{E} \times \mathbf{B}$ drift) across the magnetic field lines and plasma diffusion along the field lines.

The third process is transport due to thermospheric neutral winds. The neutral-ion collisional drag transports the ionization along the magnetic field lines, in the direction of the wind component along the field, producing an interhemisphere transport of ionization at the same time that it moves the ionization upward in the upwind side and downward in the downwind side of the magnetic field line. This process results in an asymmetrical ionization distribution about the magnetic dip equator, with unequal values of the electron densities and heights of the F2-peak at the ionization crests around $\pm 15^\circ$ either side of the magnetic equator. The ionospheric plasma vertical drift produced by a horizontal thermospheric neutral wind at low latitudes is illustrated schematically in Fig. 3, taken from Bittencourt and Sahai (1978).

At low latitudes these transport processes are greatly dependent on the geometry of the magnetic field lines at a particular region. The longitudinal variations of the *magnetic declination* and of the *latitudinal separation* between the geographic and the geomagnetic equators play important roles in the drift and wind effects on the ionospheric plasma.

For this purpose it very convenient to separate the tropical ionosphere into three longitudinal sectors (Bittencourt et al., 1976, 1992), based on the value of the magnetic declination at a given longitude, namely:

- (a) *Atlantic Sector*, from $-65^\circ W$ to 0° , where the magnetic declination is west and takes its maximum value (about $20^\circ W$) at the magnetic equator.
- (b) *Indian Sector*, from 0° to $150^\circ E$, where the magnetic declination is everywhere near zero at the magnetic equator.
- (c) *Pacific Sector*, from $150^\circ E$ to $-65^\circ W$, where the magnetic declination is close to $10^\circ E$ at the magnetic equator.

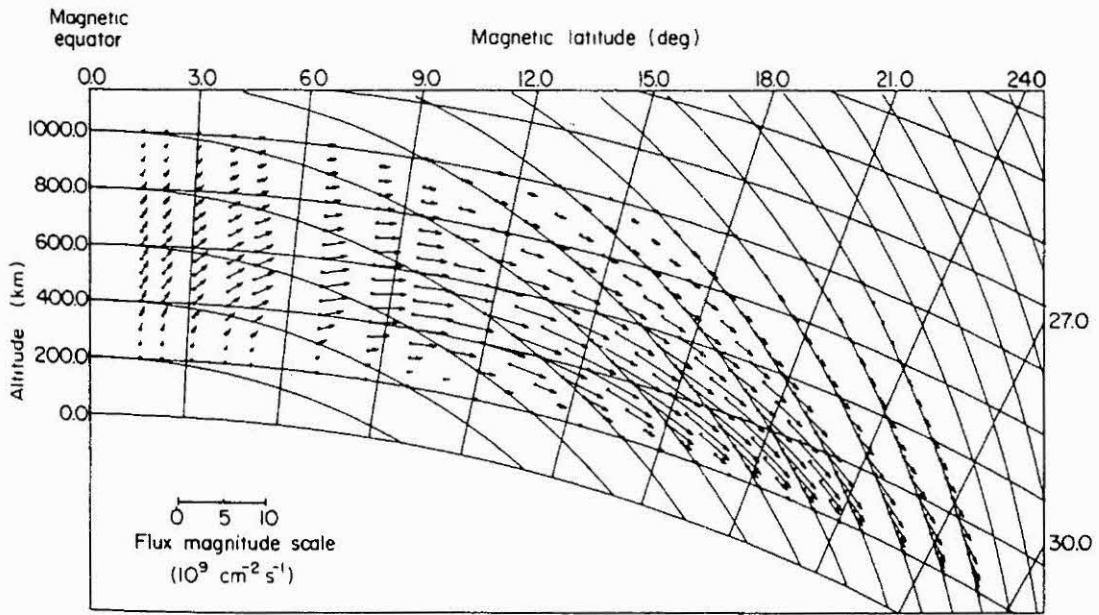


Fig. 2 Schematic illustration of the equatorial fountain effect, showing the plasma flux resulting from the combined effects of vertically upward electromagnetic plasma drift across the field lines and plasma diffusion along the field lines.

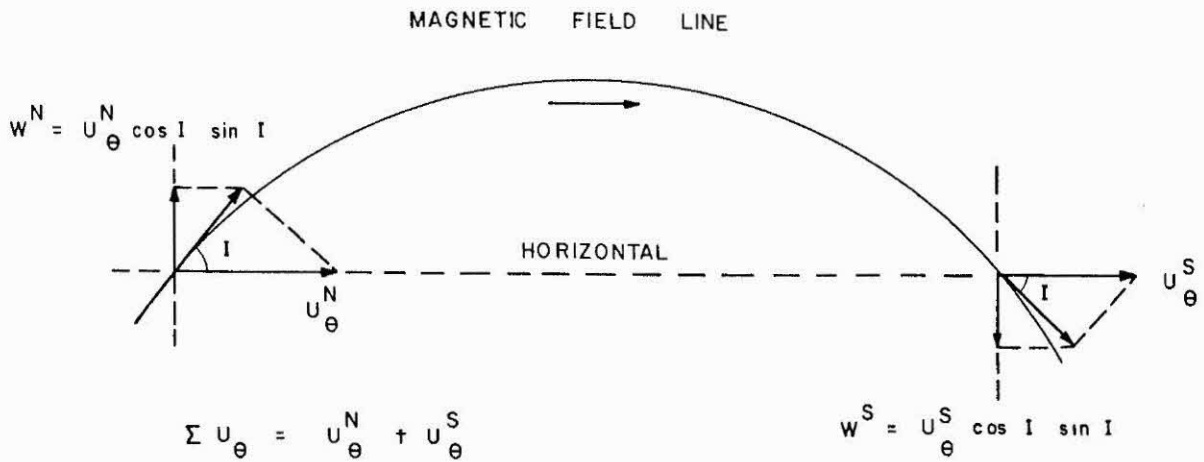


Fig. 3 Schematic diagram illustrating the vertical plasma drift (w) produced by the horizontal thermospheric wind component along the magnetic meridian (u_{θ}). The magnetic dip angle is denoted by I .

The great advantage of using this classification of longitudinal sectors, in terms of magnetic declination, is that it allows us to separate the specific ionospheric effects of the zonal and meridional thermospheric wind components, as well as the effects associated with the seasonal dependences of the vertical electromagnetic plasma drift velocities. Details of these ionospheric wind and drift effects, and their magnetic declination dependences, are discussed in Sections 5 and 6.

4. BASIC TRANSPORT EQUATIONS

The appropriate equations governing the spatial and time distribution of the electron and ion densities in the ionosphere are the time-dependent continuity equation, the momentum conservation equation and the energy conservation equation for each charged particle species. The continuum approximation to the Boltzmann equation holds under the assumption that collisions between the particles are so frequent that the ions and electrons can both be treated as fluids. Normally, this assumption is very well justified for thermal particles in the ionosphere. Above about 600 *km*, in the exosphere, the neutral particles move in ballistic orbits and suffer few collisions. However, the plasma fluid approximation is still applicable to even higher altitudes because of the large Coulomb cross sections.

4.1 The Plasma Continuity Equations

The continuity equation relates the rate of change in the particle number density to the rate of production and loss per unit volume, and to the divergence of the particle flux. If n_i and \mathbf{v}_i denote the number density and the macroscopic (average) velocity of the i^{th} ion species, respectively, then the quantity $n_i\mathbf{v}_i$ represents the flux of this charged particle species and its divergence gives the resulting loss rate per unit volume, due to macroscopic transport.

For the i^{th} ion species, the continuity equation can be expressed as (Bittencourt, 1988)

$$\frac{\partial n_i}{\partial t} + \nabla \cdot (n_i\mathbf{v}_i) = P_i - L_i \quad (4.1.1)$$

where P_i and L_i are the production and loss rates per unit volume, respectively.

The macroscopic charge neutrality plasma condition requires that the electron number density be given by

$$n_e = \sum_i n_i \quad (4.1.2)$$

where only singly charged positive ions are considered, since negative ions are scarce in the ionospheric F-region.

The charged particles in the low-latitude ionosphere may have a common drift velocity due to an external electrostatic field \mathbf{E} , not parallel to the geomagnetic induction field \mathbf{B} , such as that associated with the wind-driven dynamo current system of the E-region, which is very effective in transporting ionization across the magnetic field lines, as well as a diffusion velocity along the magnetic field lines arising from non-electromagnetic forces, namely those due to gravitation, pressure gradients and collisions. The non-electromagnetic forces are unable to transport ionization across the magnetic field lines, since at F-region heights the charged particle magnetic gyrofrequency is much greater than its collision frequency with neutrals, effectively causing it to be guided by the magnetic field. The cyclotron frequency to collision frequency ratio, at F-region altitudes, is estimated to be about 3×10^2 for ions and about 3×10^4 for electrons (Rishbeth and Garriot, 1969).

For calculation purposes, it is therefore convenient to separate the particle macroscopic (average) velocity \mathbf{v}_i into components parallel and perpendicular to the magnetic field lines

$$\mathbf{v}_i = \mathbf{v}_{i\parallel} + \mathbf{v}_\perp \quad (4.1.3)$$

where \mathbf{v}_\perp corresponds to the electromagnetic $\mathbf{E} \times \mathbf{B}/B^2$ plasma drift velocity. In addition, the natural frame of reference for expressing the charged particle motion is a coordinate system moving with the plasma drift velocity \mathbf{v}_\perp with respect to a fixed Earth-centered system.

The divergence of the plasma flux perpendicular to the magnetic field can be separated into two parts

$$\nabla \cdot (n_i \mathbf{v}_\perp) = \mathbf{v}_\perp \cdot \nabla n_i + n_i \nabla \cdot \mathbf{v}_\perp \quad (4.1.4)$$

Adding the advective part to $(\partial n_i / \partial t)$ gives

$$\frac{Dn_i}{Dt} = \frac{\partial n_i}{\partial t} + \mathbf{v}_\perp \cdot \nabla n_i \quad (4.1.5)$$

which is the *total* rate of change in the particle number density in a frame of reference moving with the plasma drift velocity \mathbf{v}_\perp .

The great advantage of using this Lagrangian reference frame is that in this system all plasma motions appear to be field aligned. This approach was first used by Moffett and Hanson (1965) in solving the time-dependent electron continuity equation including the effects of diffusion, plasma drift, production and loss.

Therefore, in the drifting coordinate system, the continuity equation for each ion species becomes

$$\frac{Dn_i}{Dt} + \nabla \cdot (n_i \mathbf{v}_{i\parallel}) + n_i \nabla \cdot \mathbf{v}_\perp = P_i - L_i \quad (4.1.6)$$

An expression for the flux parallel to \mathbf{B} , for each ion constituent, $n_i \mathbf{v}_{i\parallel}$, is derived in the next section starting from the equations of motion for the electrons and ions. The divergence term involving the plasma drift velocity, as well as the production and loss terms, will be considered subsequently.

4.2 The Equations of Motion

The forces acting on the ionospheric plasma include gravitational, collisional and pressure gradient forces, as well as electric and magnetic forces. The equation of motion for each ion species can be expressed as (Bittencourt, 1988)

$$m_i \left[\frac{\partial \mathbf{v}_i}{\partial t} + (\mathbf{v}_i \cdot \nabla) \mathbf{v}_i \right] = e(\mathbf{E} + \mathbf{v}_i \times \mathbf{B}) + m_i \mathbf{g} - \frac{1}{n_i} \nabla (n_i k T_i) - \sum_n m_i \nu_{in} (\mathbf{v}_i - \mathbf{u}) - \sum_j' m_i \nu_{ij} (\mathbf{v}_i - \mathbf{v}_j) \quad (4.2.1)$$

and for the electrons,

$$m_e \left[\frac{\partial \mathbf{v}_e}{\partial t} + (\mathbf{v}_e \cdot \nabla) \mathbf{v}_e \right] = -e(\mathbf{E} + \mathbf{v}_e \times \mathbf{B}) - \frac{1}{n_e} \nabla (n_e k T_e) \quad (4.2.2)$$

where it is assumed that, in the equation for the electrons, both the gravitational and the collisional terms are very small compared to the remaining terms and can be neglected (Rishbeth and Garriot, 1969). Also, a scalar pressure ($p_\alpha = n_\alpha k T_\alpha$, where $\alpha = e, i$) replaces the stress tensor, since

the velocity distribution function is isotropic. Subscripts e , i and n refer to electrons, ions and neutrals, respectively. Mass and temperature are represented by m and T , the acceleration due to gravity is \mathbf{g} , e denotes the electronic charge, k is Boltzmann's constant, \mathbf{u} is the thermospheric neutral wind velocity, and ν_{in} and ν_{ij} are the effective collision frequencies between ions and neutrals, and ions and ions, respectively.

The acceleration term on the left-hand side of the equation of motion for both electrons and ions (in the moving reference frame) can be set equal to zero, being generally negligible for the large scale motions that constitute the main interest here. However, they might not be negligible for small-scale wavelike motions. Taking the component of (4.2.2) parallel to the magnetic field lines, the polarization electric field generated between electrons and ions is obtained as

$$\mathbf{E}_{\parallel} = -\frac{1}{en_e} \nabla_{\parallel} (n_e k T_e) \quad (4.2.3)$$

Adopting the convention previously used by Kendall (1962), we can write

$$\nabla_{\parallel} = \hat{\mathbf{t}} \frac{\partial}{\partial s} \quad (4.2.4)$$

where $\hat{\mathbf{t}}$ represents a unit vector along the magnetic field line, defined such that for points in the northern hemisphere it is above the horizontal and towards the geomagnetic equator, and s is the arc length along the field line measured in the same sense as $\hat{\mathbf{t}}$. Since the cyclotron frequency greatly exceeds the collision frequency with neutrals throughout the F-region, the non-electromagnetic forces will transport the ionization essentially along the field lines. Thus, taking the component of (4.2.1) parallel to the magnetic field, using the expression in (4.2.3) and rearranging, we obtain

$$\begin{aligned} \mathbf{v}_{i\parallel} = & \frac{1}{m_i (\sum_n \nu_{in} + \sum_j' \nu_{ij})} \left[-m_i g \sin I - k \frac{\partial}{\partial s} (T_e + T_i) - \right. \\ & \left. - \frac{kT_e}{n_e} \frac{\partial n_e}{\partial s} - \frac{kT_i}{n_i} \frac{\partial n_i}{\partial s} + \sum_n m_i \nu_{in} |\mathbf{u}_{\parallel}| + \sum_j' m_i \nu_{ij} |\mathbf{v}_{j\parallel}| \right] \hat{\mathbf{t}} \quad (4.2.5) \end{aligned}$$

where $-g \sin I = \hat{\mathbf{t}} \cdot \mathbf{g}$ and I denotes the magnetic dip angle.

4.3 The Energy Conservation Equations

For each ion species the energy conservation equation, considering an isotropic distribution function such that we can replace the stress tensor by a scalar pressure ($p_i = n_i k T_i$), can be expressed in terms of the temperature T_i as (Bittencourt, 1988)

$$\begin{aligned} \frac{3}{2} n_i k \left[\frac{\partial T_i}{\partial t} + (\mathbf{v}_i \cdot \nabla) T_i \right] = & -n_i k T_i (\nabla \cdot \mathbf{v}_i) - \nabla \cdot \mathbf{q}_i + \\ & + M_i - m_i \mathbf{v}_i \cdot \mathbf{A}_i + \left(\frac{1}{2} m_i v_i^2 - \frac{3}{2} k T_i \right) (P_i - L_i) \end{aligned} \quad (4.3.1)$$

where \mathbf{q}_i denotes the heat flux vector, M_i represents the rate of energy density change due to collisions, \mathbf{A}_i stands for the collision terms appearing in the equation of motion (4.2.1), and P_i and L_i are respectively the production and loss terms of the continuity equation (4.1.1).

Equations (4.1.1), (4.2.1) and (4.3.1) constitute a coupled set of nonlinear equations to be solved simultaneously in order to determine the spatial and temporal distribution of the particle number density, macroscopic velocity and temperature, for each species. In order to simplify matters, instead of solving the energy equation (4.3.1), a usual approach consists in considering the temperature distribution for each species, as a function of space and time, as a known quantity. With this approach, the problem reduces to the solution of the coupled nonlinear set of continuity and momentum conservation equations for each charged particle species.

4.4 The Divergence Terms

We shall assume that the Earth's magnetic field can be approximated by a centered magnetic dipole, thus having only radial and meridional components. In a region free from electric currents the magnetic induction field can be described in terms of the gradient of a magnetic scalar potential γ , according to

$$\mathbf{B} = -\nabla \gamma \quad (4.4.1)$$

For the geomagnetic dipole approximation we have

$$\gamma = g_0 r_0^3 \frac{\cos \theta}{r^2} \quad (4.4.2)$$

so that,

$$\mathbf{B} = 2g_0 r_0^3 \frac{\cos \theta}{r^3} \hat{\mathbf{r}} + g_0 r_0^3 \frac{\sin \theta}{r^3} \hat{\boldsymbol{\theta}} \quad (4.4.3)$$

where $\hat{\mathbf{r}}$ and $\hat{\boldsymbol{\theta}}$ are unit vectors along the r and θ directions of a spherical polar coordinate system (r, θ, ϕ) in which θ denotes the colatitude and the axis $\theta = 0^\circ$ passes through the north pole. Here r_0 denotes the Earth's radius and g_0 is the dipole coefficient, approximately equal to -0.31 gauss.

In addition, the equation of a magnetic field line is

$$r = r_e \sin^2 \theta \quad (4.4.4)$$

where r_e represents the radial distance to the point of intersection of the field line with the geomagnetic equatorial plane.

The sense and magnitude of the magnetic dip angle I is taken such that

$$\sin I = \frac{2 \cos \theta}{\sigma^{1/2}} \quad (4.4.5)$$

$$\cos I = \frac{\sin \theta}{\sigma^{1/2}} \quad (4.4.6)$$

where $\sigma = (1 + 3 \cos^2 \theta)$. These expressions can be obtained from equation (4.4.3), noting that $\tan I = B_r/B_\theta$. Therefore, we have

$$\hat{\mathbf{t}} = \sin I \hat{\mathbf{r}} + \cos I \hat{\boldsymbol{\theta}} \quad (4.4.7)$$

$$\nabla_{\parallel} = \hat{\mathbf{t}} \frac{\partial}{\partial s} = \hat{\mathbf{t}} \left(\sin I \frac{\partial}{\partial r} + \frac{\cos I}{r} \frac{\partial}{\partial \theta} \right) \quad (4.4.8)$$

Kendall (1962) has shown that the basic transport equations for the low-latitude ionosphere are greatly simplified by transforming from the spherical coordinate system (r, θ, ϕ) to one whose coordinates define directions parallel and perpendicular to the magnetic field lines. Accordingly, we define a system of orthogonal curvilinear coordinates (p, q, ϕ) by

$$p = \frac{r}{r_0 \sin^2 \theta} \quad (4.4.9)$$

$$q = \frac{r_0^2 \cos \theta}{r^2} \quad (4.4.10)$$

Thus, $p = \text{constant}$ defines the family of curves which represent the magnetic field lines, while the family of constant magnetic potential surfaces is represented by $q = \text{constant}$.

Along a given field line ($p = \text{constant}$) we have

$$\frac{\partial}{\partial r} = \frac{\partial q}{\partial r} \frac{\partial}{\partial q} \quad (4.4.11)$$

$$\frac{\partial}{\partial \theta} = \frac{\partial q}{\partial \theta} \frac{\partial}{\partial q} \quad (4.4.12)$$

and using equations (4.4.9) and (4.4.10), together with (4.4.5) and (4.4.6), the operator ∇_{\parallel} , given in equation (4.4.8), becomes

$$\nabla_{\parallel} = \hat{\mathbf{t}} (\hat{\mathbf{t}} \cdot \nabla) = -\hat{\mathbf{t}} \frac{\sigma^{1/2} r_0^2}{r^3} \frac{\partial}{\partial q} \quad (4.4.13)$$

As Kendall (1962) has shown,

$$\hat{\mathbf{t}} \cdot \nabla = \frac{1}{r \sigma^{3/2}} (9 \cos \theta + 15 \cos^2 \theta) \quad (4.4.14)$$

and using the vector identity

$$\nabla \cdot (n_i \mathbf{v}_{i\parallel}) = (n_i \mathbf{v}_{i\parallel}) \nabla \cdot \hat{\mathbf{t}} + (\hat{\mathbf{t}} \cdot \nabla) (n_i \mathbf{v}_{i\parallel}) \quad (4.4.15)$$

the expression for the divergence of the charged particle flux parallel to the magnetic field lines can be written as

$$\nabla \cdot (n_i \mathbf{v}_{i\parallel}) = \left[\frac{1}{r \sigma^{3/2}} (9 \cos \theta + 15 \cos^2 \theta) - \frac{r_0^2 \sigma^{1/2}}{r^3} \frac{\partial}{\partial q} \right] (n_i \mathbf{v}_{i\parallel}) \quad (4.4.16)$$

The expression for $\mathbf{v}_{i\parallel}$, given in equation (4.2.5), can easily be transformed using equation (4.4.14) and the result incorporated in (4.4.16).

4.5 Coupling to the Neutral Winds and Electric Fields

Since the collisional terms in the charged particle momentum conservation equations involve the thermospheric neutral wind velocity \mathbf{u} , we must consider the corresponding transport equations for the atmospheric neutral species, which are coupled to the charged particle equations through the collisional terms. The ion drag produced by the neutral wind modifies the ionization distribution, which in turn modifies the neutral wind pattern. Thus, for a self-consistent treatment these coupled system of nonlinear equations must be considered simultaneously. The basic equations for the thermospheric neutral wind velocity will be considered in Section 5.

Also, the electric field responsible for the plasma drift in the F-region arises as a result of dynamo action in the E-region, as well as in the F-region. The E-region dynamo is controlled by the atmospheric tides

which moves the ionization across the magnetic field lines, since at E-region altitudes the collision frequency is much higher than the particle cyclotron frequency. The electric field thus generated maps to the F-region through the high electric conductivity along the field lines.

The thermospheric neutral winds are responsible for the F-region dynamo. However, during the daytime, due to the high conductivity of the E-region, the F-region dynamo is short-circuited through coupling with the E-region via the highly conducting magnetic field lines. But, at night, when the E-region conductivity drops drastically, the circuit is open allowing the development of polarization electric fields in the F-region. Again, the electric fields produced modify the ionization distribution in the low-latitude F-region, which in turn modify the pattern of thermospheric neutral winds through ion-neutral drag and, consequently, the electric field.

Therefore, a complete self-consistent formulation requires the inclusion of this *electrodynamical coupling* between the E and F-regions, responsible for the generation of the F-region electric fields. This subject will be considered in more detail in Section 6.

To build a complete *self-consistent* ionospheric model is an extremely complicated task, requiring the simultaneous numerical solution of a large number of coupled nonlinear differential equations. Furthermore, in the usual approach considered so far, the plasma equations are referred to a Lagrangian geomagnetic coordinate system in order to simplify the computational procedure, whereas the neutral gas equations are referred to the normal Eulerian geographic coordinate system. For this reason, up to date, there are no computer models constructed using a complete self-consistent formulation in the sense just described, for the ionosphere-thermosphere system with electrodynamic coupling.

So far, the ionospheric computer models consider the spatial and time variation of both the thermospheric neutral wind velocities and the ionospheric electric fields as known quantities, specified either through analytical formulas or empirical models (e.g. Sterling et al., 1969; Anderson, 1973a; Bittencourt and Tinsley, 1976; Anderson et al., 1987, 1989; Bailey and Sellek, 1990; Batista et al., 1991; Bailey et al., 1993).

Also, the existing thermospheric neutral wind models consider the spatial and time variation of the ionospheric parameters as known quantities, specified either through analytical formulas or empirical models (e.g. Fuller-Rowell and Rees, 1980). Nevertheless, Fuller-Rowell et al. (1987) have constructed a coupled thermosphere-ionosphere computer model for high latitudes but, for low latitudes, they still use analytical formulas for the ionospheric variables, given by the empirical ionospheric model of Chiu

(1975).

Regarding the computation of the ionospheric electric fields, low-latitude computer models have been built which solve the equation of motion for the neutral gas together with the equations for the electric fields considering the electrodynamical coupling of the equatorial E and F regions (e.g. Heelis et al., 1974; Batista et al., 1986). In this case, extremely simplified equations or empirical formulas are used for the ionospheric parameters and conductivities, in order to simplify the computational treatment.

In the low-latitude ionospheric computer model described here we shall consider the spatial and time distribution of both the thermospheric neutral wind velocities and neutral densities, and the ionospheric electric fields as known quantities, specified through analytical formulas or empirical models. Details of these specified models are presented in Sections 5 and 6.

5. THERMOSPHERIC NEUTRAL WINDS

A theoretical description of the global thermospheric neutral wind system requires the numerical solution of a large number of coupled ionospheric and atmospheric equations, involving the time-dependent continuity equations, the momentum conservation equations and the energy conservation equations for each of the ion species as well as for the neutral gas. In addition, to understand also the longitudinal behavior, a three-dimensional solution of this problem is required, taking into account the dependence of the Earth's magnetic field on the geographic coordinates.

The forces acting on the neutral air are the pressure gradient force, gravity, frictional forces due to viscosity of the air and due to collisions between the neutral gas particles and the ions (ion-drag), and the Coriolis and centripetal forces due to the Earth's rotation. Since the ion-drag force is proportional to the collision frequency and to the difference between the wind velocity and the ion drift velocity, the various forces that cause ion motion must also be considered simultaneously in a self-consistent way.

5.1 Basic Equations

The atoms and molecules in the atmosphere collide so frequently that the air can be regarded as a fluid in local thermodynamic equilibrium, described by the usual hydrodynamic conservation equations. Furthermore,

the neutral air can be treated as a single fluid, since the macroscopic differential motion of its various constituents is very much less than the overall macroscopic wind velocity.

The set of equations governing the dynamics of the neutral upper atmosphere are (Rishbeth, 1972):

(a) The continuity equation for the whole neutral gas, which express the law of mass conservation,

$$\frac{\partial \rho}{\partial t} + \nabla \cdot (\rho \mathbf{u}) = 0 \quad (5.1.1)$$

(b) The Navier-Stokes equation of motion, which express the law of momentum conservation, assuming the air to be incompressible and with constant viscosity,

$$\begin{aligned} \frac{\partial \mathbf{u}}{\partial t} + (\mathbf{u} \cdot \nabla) \mathbf{u} + 2(\boldsymbol{\Omega} \times \mathbf{u}) + \boldsymbol{\Omega} \times (\boldsymbol{\Omega} \times \mathbf{r}) = \\ -\frac{1}{\rho} \nabla p - \sum_i \nu_{ni} (\mathbf{u} - \mathbf{v}_i) + \frac{\mu}{\rho} \nabla^2 \mathbf{u} + \mathbf{g} \end{aligned} \quad (5.1.2)$$

(c) The energy conservation equation, neglecting the energy dissipated by viscosity and ion-drag,

$$\rho c_v \left(\frac{\partial T}{\partial t} + \mathbf{u} \cdot \nabla T \right) + p \nabla \cdot \mathbf{u} - \nabla \cdot (K_T \nabla T) = P_E - L_E \quad (5.1.3)$$

(d) The ideal gas equation of state, which relates pressure, density and temperature for the neutral air,

$$p = nkT \quad (5.1.4)$$

In this coupled set of equations, \mathbf{u} denotes the neutral wind velocity, ρ is the neutral air mass density such that $\rho = n\bar{m}$, n is the neutral air number density, \bar{m} is the average neutral particle mass, \mathbf{v}_i is the i^{th} ion drift velocity, $\boldsymbol{\Omega}$ is the Earth's angular rotation velocity, \mathbf{r} is the radius vector from the center of the Earth to the point where the equations are applied, p stands for the scalar pressure, ν_{ni} is the effective neutral-ion collision frequency, μ/ρ is the kinematic viscosity coefficient, \mathbf{g} is the acceleration due to gravity, c_v is the specific heat at constant volume, K_T is the thermal conductivity coefficient, k is Boltzmann's constant and P_E and L_E represent sources and sinks of energy density.

Since the ion-drag term depends on the ion densities (through the collision frequency) and on the ion drift velocities, the continuity, momentum and energy equations for each ion species must be considered simultaneously with the neutral gas conservation equations. Furthermore, the motion of the neutral gas is appropriately represented in terms of geographic coordinates, while that of the ions must be expressed in terms of drifting geomagnetic coordinates. To build a complete and detailed self-consistent model is a formidable task, which requires the simultaneous solution of the three-dimensional system of equations just indicated. At the present time this problem requires the introduction of simplifying approximations.

There have been several numerical model analysis of thermospheric motions. In most of them the temperature field is regarded as a fixed input quantity, usually taken from some phenomenological atmospheric model, such as that of Jacchia (1965, 1971, 1977). In these cases a treatment of the energy conservation equation is not required.

Simplifying approximations are also made regarding the ion densities and the ion drift velocities. So far, all present models for the low latitude thermospheric neutral wind considers the ion densities and ion velocities as known fixed quantities, specified as a function of space and local time, through a parametric model. Hence, only the set of simplified conservation equations for the neutral air is solved, so that these models are not self-consistent in the sense that the wind pattern modifies the ionization distribution through ion-drag which in turn modifies the wind pattern.

5.2 Global Pressure Gradients

In general the thermospheric neutral winds blow away from the hottest part of the thermosphere, in the afternoon sector, towards the coldest part, in the early morning sector, across the polar regions and zonally around the Earth in low latitudes. This behavior is quite different from that of winds in the lower atmosphere (troposphere), which are controlled by the Coriolis force and the difference is attributed mainly to the importance of ion-drag and viscosity in the upper atmosphere (thermosphere).

To calculate the thermospheric wind velocities from (5.1.2) it is necessary to know the horizontal pressure gradients which provide the driving force for the winds. Clearly, the pressure gradient involves the additive effects of a density gradient and a temperature gradient, as can be seen from equation (5.1.4), so that a specified numerical model giving the spatial and time variations of these quantities is required.

The global models of the thermosphere assume fixed boundary conditions (temperature and neutral species densities) at a lower boundary, often taken as 120 *km*. The neutral temperature vertical profile is assumed to have a certain shape, tending at great heights to a limiting value, the exospheric temperature (T_∞), which is a function of local time, latitude, longitude, season, solar activity and magnetic disturbances. The number density vertical profile of each neutral constituent is computed using the diffusive equilibrium equation.

One of the most well known global neutral atmosphere models is that of Jacchia (1965, 1971, 1977), whose general approach is to determine empirical temperature profiles which yield density distributions in agreement with satellite drag measurements. Jacchia's model provides the global distribution and vertical profiles of the temperature and neutral species densities, with their corresponding time dependences, solar cycle variations, as well as geomagnetic storm atmospheric effects.

Other neutral atmosphere models, based on satellite and ground-based observations, are available today, such as the MSIS-86 thermospheric model (Hedin, 1987), as well as models which give the thermospheric neutral wind velocity distribution (e.g. Hedin et al., 1988, 1991) and theoretical global thermospheric models such as that of Fuller-Rowell and Rees (1980).

5.3 Boundary Conditions

Many atmospheric models used for wind computations assume that the pressure, density and temperature are fixed at some lower boundary level, often taken at 120 *km*, so that the horizontal pressure gradient vanishes at this boundary. It is therefore generally assumed that the horizontal wind components are equal to zero at this level, viscosity being too weak to vertically transmit any significant horizontal velocity from greater heights.

This assumption of unvarying conditions at the lower boundary cannot be expected to be realistic (Chandra and Stubbe, 1970). If the atmospheric parameters p , ρ and T were assumed to vary at the lower boundary, as they probably do in reality, some effect would be observed in the computed winds at greater heights.

Since the kinematic viscosity (μ/ρ) becomes very large at great heights, the derivative ($\partial^2 \mathbf{u}/\partial z^2$) must become small at these heights, in order that the viscosity term in the equation of motion (5.1.2) should not become overwhelmingly large. This implies that we must have

$(\partial \mathbf{u} / \partial z) \rightarrow \text{constant}$. Further, to maintain a finite velocity gradient there would have to exist a shearing force which neither the pressure gradients nor the Coriolis force nor ion-drag can provide, so that in fact, $(\partial \mathbf{u} / \partial z) = 0$ at great heights, i.e. \mathbf{u} becomes height-independent, which is the upper boundary condition for the neutral air equation of motion.

5.4 Thermospheric Neutral Wind Models

As mentioned before, in the low-latitude ionospheric computer model described here the horizontal thermospheric neutral wind velocity field is considered to be specified through some analytical or empirical expression.

As the atmosphere undergoes thermal contraction and expansion, the vertical velocity of a surface of constant pressure is given by

$$u_r = \frac{\Omega T}{g} \int_{z_0}^z \frac{g}{T^2} \frac{\partial T}{\partial \phi} dz' \quad (5.4.1)$$

Taking the temperature T as being the exospheric temperature T_∞ , independent of altitude, we have

$$u_r = \frac{\Omega}{T_\infty} \frac{\partial T_\infty}{\partial \phi} \frac{(z - z_0) r}{(R_E + z_0)} \quad (5.4.2)$$

The neutral air wind velocity along \mathbf{B} can be expressed as

$$\mathbf{u}_{\parallel} = (u_r \sin I + u_\theta \cos I) \hat{\mathbf{t}} \quad (5.4.3)$$

Here u_r is the radial velocity of the neutral air due to the diurnal expansion and contraction of the atmosphere, given by expression (5.4.2), and u_θ is the *magnetic* north-south component of the horizontal thermospheric neutral wind velocity, relative to the Earth.

The horizontal wind velocity component along the *magnetic meridian* (u_θ) can be expressed in terms of the *geographic* components of the horizontal thermospheric wind velocity as

$$u_\theta = u'_\theta \cos \delta_m + u'_\phi \sin \delta_m \quad (5.4.4)$$

where u'_θ represents the *geographic* meridional wind component, u'_ϕ represents the *geographical* zonal wind component and δ_m stands for magnetic declination, which is greatly longitudinal dependent.

Notice that the ionospheric plasma equations are solved along a given magnetic field line, so that the proper wind component to be used in the plasma equations is the magnetic meridian component u_θ , with its longitudinal dependence on magnetic declination already included according to (5.4.4).

A number of thermospheric neutral wind models, giving the space and time dependence of u'_θ and u'_ϕ , can be considered for the present ionospheric calculations. The most recent one is the global model of thermospheric winds, based on satellite and ground-based observations, of Hedin et al. (1991, 1988). In the present computations we shall use a very simple analytical expression for the thermospheric wind velocity field, represented by a cosine function in the local time dependence and an amplitude which increases with latitude (Bittencourt and Tinsley, 1976),

$$u_\theta = u_0 \left[\frac{1 - \sin(\theta + \Delta)}{1 - \sin \theta} \right] [\cos(\phi - \phi_0) + \epsilon] \quad (5.4.5)$$

In this expression u_0 is a constant velocity, θ is the colatitude, θ_0 is a normalization constant, the parameter ϕ_0 determines the local time at which the wind achieves its maximum velocity, ϵ permits a choice of smaller velocities during the daytime as compared to the nighttime, allowing for the effect of great ion drag during the day, and Δ represents the latitudinal difference between the position of the magnetic equator at a particular longitude and the latitude to which the winds converge or diverge in their global pattern. Thus, for equinox conditions, Δ represents the geographic latitude of the location of the magnetic equator at a fixed longitude. Further, up to 14° can be considered for the separation between the magnetic and geographic equators, depending on the longitude chosen, and another 23° for the movement of the sub-solar point depending on the season.

Fig. 4 shows the local time and latitudinal dependence of the wind velocity represented by (5.4.5), for the case when $u_0 = -175 \text{ m/s}$, $\theta_0 = 60^\circ$, $\Delta = 0^\circ$, $\phi_0 = -15^\circ$ and $\epsilon = -0.25$. This wind model presents a poleward velocity during the daytime from 08:00 LT to 18:00 LT and equatorward from 18:00 LT to 08:00 LT, achieving a maximum poleward velocity of about 35 m/s and a maximum equatorward velocity of about 55 m/s , at 15° latitude.

An expression similar to (5.4.5) was previously used by Sterling et al. (1969) and Brasher and Hanson (1970) on previous tropical F-region models, but only for the simple case of equinox and coincidence of geomagnetic and geographic equators.

In the results to be presented here we shall consider wind models labeled W1 to W4, based on equation (5.4.5), with different values assigned

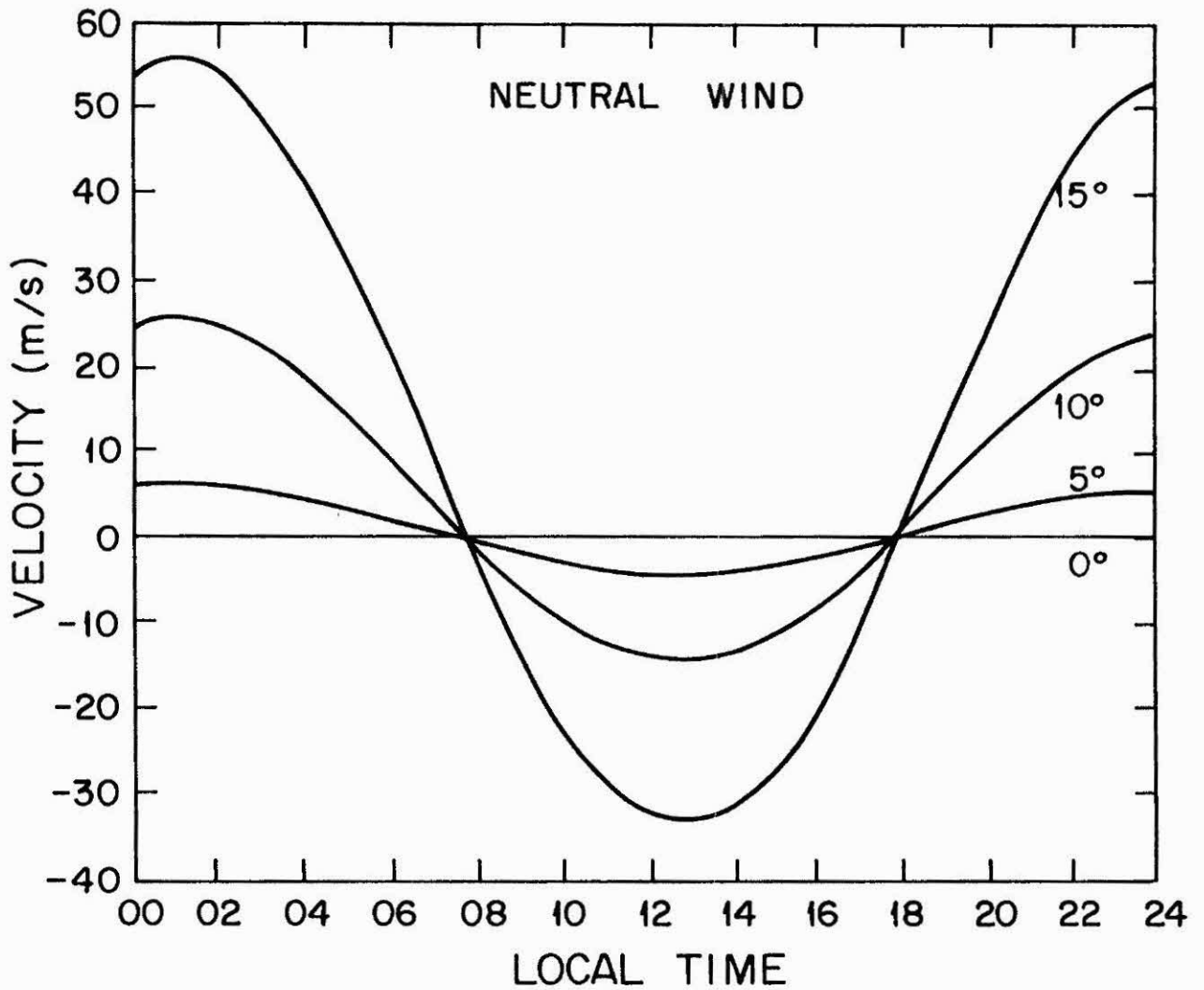


Fig. 4 Neutral wind velocity along the magnetic meridian as a function of local time for various geographic latitudes, according to equation (5.4.5), for equinox. Positive velocities are equatorward.

to the parameters Δ and ϕ_0 in order to represent various conditions. Since the plasma equations are referred to a geomagnetic frame, different magnetic latitude dependence for the wind is obtained by using different values of Δ . For $\Delta = 0^\circ$, for example, the wind is symmetric about the magnetic equator and, therefore, no ionization asymmetry will result in the equatorial ionospheric anomaly.

Wind model W1 has the time of north-south reversal from poleward to equatorward at 18:00 LT ($\phi_0 = -15^\circ$) and corresponds to equinox, with zero solar declination. The magnetic equator is taken at 10° to the north of the geographic equator ($\Delta = 10^\circ$), which corresponds to some longitude

regions in the African-Asian sector.

Wind model W2 is chosen for the dip equator and wind convergence latitude separated by $\Delta = 34^\circ$, corresponding to june solstice at the longitude of Jicamarca (i.e. 23° north for the solar declination plus 11° south for the latitudinal position of the geomagnetic equator). In this case very strong (and probably unrealistic) wind velocities will occur at the magnetic equator and at the southern crest of the Appleton anomaly.

Wind model W3 is the same as W1 except that the time of reversal was delayed three hours ($\phi_0 = -60^\circ$), so that it blows poleward from 11:00 Lt to 21:00 LT. This wind representation is quite similar to some theoretically computed thermospheric winds at low latitudes (e.g. Kohl and King, 1967; Challinor, 1970; Blum and Harris, 1973).

Wind model W4 has wind reversal time at 22:00 LT and a separation of dip equator and convergence latitude of 16° , corresponding to december solstice (solar declination of -23°) in the American sector.

Different wind representations can be used in order to analyze the wind effects on the low-latitude ionospheric ionization distribution at the various longitudes, seasons and solar activity, including geomagnetic disturbances.

6. ELECTROMAGNETIC PLASMA DRIFTS

In the ionospheric E-region the motion of the neutral air, caused by atmospheric tides, are able to transport (through collisions) the ionization across the magnetic field lines causing currents to flow. Polarization fields (electrostatic) are generated which affect the motion of the charged particles in the ionospheric F-region and in the magnetosphere. Since the electrical conductivity along the magnetic field lines is very high, they can be thought of as equipotential wires which transmit electric fields from one region to another (Farley, 1959).

Rishbeth (1971) suggested that thermospheric neutral winds may generate F-region currents (see also Rishbeth 1977, 1981). The resultant polarization fields may or may not be shorted out in the E-region. During the day the E-region ionization is sufficient to short circuit these polarization fields, but at night the very low E-region electron densities allow the field to develop. Consequently, a vertical electric field is established in the equatorial F-region, by the zonal thermospheric winds, causing the ionization to drift in the east-west direction. This plasma drift is in the same direction as the neutral wind which produces the polarization field.

The electrostatic component \mathbf{E} of the *total* electric field ($\mathbf{E} + \mathbf{u} \times \mathbf{B}$)

gives rise to the drifts of the F-region plasma. At the magnetic equator, the east-west component of \mathbf{E} generates the vertical $\mathbf{E} \times \mathbf{B}$ ionization drift, which is upwards during the daytime and downwards at night. The north-south component of the E-region electric field when transmitted to the F-region, over the magnetic equator, points in the vertical direction giving rise to an east-west $\mathbf{E} \times \mathbf{B}$ plasma drift.

Review articles on the equatorial ionospheric electric fields and on low-latitude electrodynamic plasma drifts have been published by Fejer (1981, 1991).

6.1 Theoretical Models

Some theoretical models involving the calculation of electric fields (and the corresponding electric potentials) in the low-latitude ionosphere have been developed (e.g. Heellis et al. 1974; Batista et al., 1986). These models consider that the equatorial F-region electric field is generated by the atmospheric tides, through the E-region dynamo, and by the thermospheric winds, through the F-region dynamo and the electrodynamic coupling between the E and F-regions.

The basic equations include the conservation equations for the neutral air and for the ionospheric ionization, Maxwell equations and the equation for the electric current flow which provides the electrodynamic coupling between the E and F-regions. The models developed by Heellis et al. (1974) and by Batista et al. (1986) assume various simplifying approximations for this set of equations in order to reduce the complexity of its numerical solution.

In the low-latitude ionospheric model described here we shall assume that the F-region $\mathbf{E} \times \mathbf{B}$ plasma drifts are known as a function of space and time, and specified through analytical or empirical formulas based on observations and modelling results.

6.2 The Divergence of the Plasma Drift Velocity

In the F-region, the electric field \mathbf{E} which exists normal to the magnetic field as a result of dynamo action in the E-region, produces a drift velocity of the plasma across the magnetic field lines given by

$$\mathbf{v}_\perp = \frac{\mathbf{E} \times \mathbf{B}}{B^2} \quad (6.2.1)$$

The electric field responsible for this drift can be separated into two parts

$$\mathbf{E} = \mathbf{E}_{cor} + \mathbf{E}_d \quad (6.2.2)$$

where \mathbf{E}_{cor} is such that the velocity $(\mathbf{E}_{cor} \times \mathbf{B})/B^2$ gives corotation with the Earth, i.e.,

$$\frac{\mathbf{E}_{cor} \times \mathbf{B}}{B^2} = r \sin \theta \Omega \hat{\phi} \quad (6.2.3)$$

where Ω denotes the Earth's angular velocity, $\hat{\phi}$ represents a unit vector in the ϕ -direction and \mathbf{E}_d is the electric field normally associated with the ionospheric dynamo system.

The plasma drift velocity can be resolved into the form

$$\mathbf{v}_\perp = v_n \hat{\mathbf{n}} + (v_\phi + r \sin \theta \Omega) \hat{\phi} \quad (6.2.4)$$

where $\hat{\mathbf{n}} = \cos I \hat{\mathbf{r}} - \sin I \hat{\theta}$, which represents a unit vector in the vertical plane, normal to the magnetic field line, and v_n and v_ϕ are the components of \mathbf{v}_\perp in the vertical plane and in the east-west direction, respectively, relative to the Earth. Therefore,

$$v_n \hat{\mathbf{n}} = \frac{1}{B^2} [(\mathbf{E}_d \times \mathbf{B}) \cdot \hat{\mathbf{r}}] \hat{\mathbf{r}} + \frac{1}{B^2} [(\mathbf{E}_d \times \mathbf{B}) \cdot \hat{\theta}] \hat{\theta} \quad (6.2.5)$$

$$v_\phi \hat{\phi} = \frac{1}{B^2} [(\mathbf{E}_d \times \mathbf{B}) \cdot \hat{\phi}] \hat{\phi} \quad (6.2.6)$$

and the divergence of the ϕ -component is

$$\nabla \cdot (r \sin \theta \Omega \hat{\phi} + v_\phi \hat{\phi}) = \frac{1}{r \sin \theta} \frac{\partial v_\phi}{\partial \phi} \quad (6.2.7)$$

Sterling et al. (1969) showed that the effect of v_ϕ in the solutions is negligible so that in the numerical computer calculations it can be assumed that $v_\phi = 0$.

The divergence of the component of \mathbf{v}_\perp in the vertical plane can be expressed as (Baxter, 1964; Moffett and Hanson, 1965)

$$\nabla \cdot (v_n \hat{\mathbf{n}}) = \frac{\partial v_n^0}{\partial r_e} + \frac{4v_n^0}{r\sigma^2} (6 \cos^6 \theta - 3 \cos^4 \theta - 4 \cos^2 \theta + 1) \quad (6.2.8)$$

where v_n^0 is the equatorial value of v_n , r_e is the radial distance from the center of the Earth to the field line's equatorial crossing point and $\sigma = (1 + 3 \cos^2 \theta)$.

The radial dependence of the vertical drift at the dipole equator is given by (Sterling et al., 1972)

$$v_n^0 = v_0 \frac{r^2}{(h_0 + r_0)^2} \quad (6.2.9)$$

where r_0 denotes the Earth's radius and v_0 is the plasma drift velocity at $h_0 = 300 \text{ km}$ above the surface at the dip equator, i.e., the drift velocity normally measured at Jicamarca with the incoherent scatter radar, for example. This radial squared dependence in v_n^0 is chosen so that the magnetic flux in the field tube is conserved as the plasma moves vertically.

6.3 Plasma Drift Velocity Models

Measurements of vertical plasma drifts at the magnetic equator have been reported by Woodman (1970) and Fejer et al. (1989, 1991), obtained using the incoherent scatter radar at Jicamarca, Peru. Typically, upward velocities of 20 to 25 m/s are observed during the day and downward velocities of about the same magnitude at night. A rapid increase in the upward velocity, commencing around sunset and lasting between one to two hours, is also observed which is a consistent feature appearing every day with regularity, after which the velocities reverse to downward. Typical velocities at this pre-reversal peak are of the order of 40 m/s . The amplitude and duration of this pre-reversal peak in the upward velocities vary from one longitudinal region to another and with season, showing a marked dependence on magnetic declination. Woodman (1970) found that the spread in the velocities at any one time, for different days, is as large as the velocities themselves, even during magnetically quiet days, and that the daily behavior of the drift velocities is far from sinusoidal. Also, Fejer et al. (1979) investigated the effects of geomagnetic disturbances on the vertical electromagnetic plasma drifts, finding that in general, in most cases during geomagnetic storm conditions, the drifts are somewhat inhibited.

Woodman (1972) has measured the east-west $\mathbf{E} \times \mathbf{B}$ plasma drift component, finding that the plasma drifts westward during the day with a typical velocity of about 50 m/s and eastward at night with typical velocities from 100 to 150 m/s .

In the ionospheric computer model described here only drifts in the magnetic meridional plane, due to an east-west electric field, are considered, even though east-west plasma drifts are known to exist. Sterling et al. (1969) found that the east-west component of the electromagnetic drift has little effect on the solutions.

Bittencourt and Abdu (1981) found that when the F-layer is sufficiently high, such that transport processes dominate over recombination (above about 300 km), the vertical plasma drifts can be determined to good accuracy from the vertical motions of the F2-peak height, as deter-

mined from ionosonde measurements. This technique allows the determination of the vertical plasma drifts in different longitudinal regions to investigate their magnetic declination and seasonal dependence, at least in the hours near sunset and early evening when the F-layer is sufficiently high. This method, however, underestimates the vertical plasma drifts when the F-layer is not high enough, due to the effects of plasma recombination (Batista et al., 1990; Fejer et al., 1989).

Four hypothetical vertical drift models are considered in the present model, based on incoherent scatter and ionosonde observations, and numerical modelling. Fig. 5 shows the local time variation of the vertical plasma drift velocities corresponding to the drift models labeled here D1 to D4. The drift model D2 has an earlier time of reversal as compared to D1. Model D3 is the same as D1, except that the rapid increase in the upward velocity of the pre-reversal peak just after sunset was decreased from a peak velocity of 40 *m/s* to 25 *m/s*. Drift model D4 has smaller velocities during the daytime, as compared to the previous ones, but the same downward velocities at night.

Different drift models can be considered in order to provide an adequate representation for the drift dependence on longitude (magnetic declination) and season, as well as on solar activity.

7. PHOTOIONIZATION AND ION CHEMISTRY

7.1 Photoionization Rates

The photoionization rate per unit volume for each of the absorbing atmospheric species, produced by the solar ionizing radiation, can be expressed as

$$Q_j(r, \chi) = \sum_k \Phi_\infty(\lambda_k) \exp[-\tau(\lambda_k, r, \chi)] \sigma_j^{(i)}(\lambda_k) n_j(r) \quad (7.1.1)$$

where $\Phi_\infty(\lambda_k)$ represents the incident solar extreme ultraviolet (XUV) radiation flux, in the wavelength band specified by λ_k , at the top of the atmosphere where the optical depth $\tau(\lambda_k, r, \chi)$ is zero, $\sigma_j^{(i)}$ denotes the photoionization cross section in the wavelength band λ_k for the j^{th} absorbing atmospheric species, r is the radial distance, $n_j(r)$ is the number density of the j^{th} species, χ is the solar zenith angle and the summation applies over all wavelength bands of incident solar XUV radiation. The total photoionization rate per unit volume is obtained by summing equation

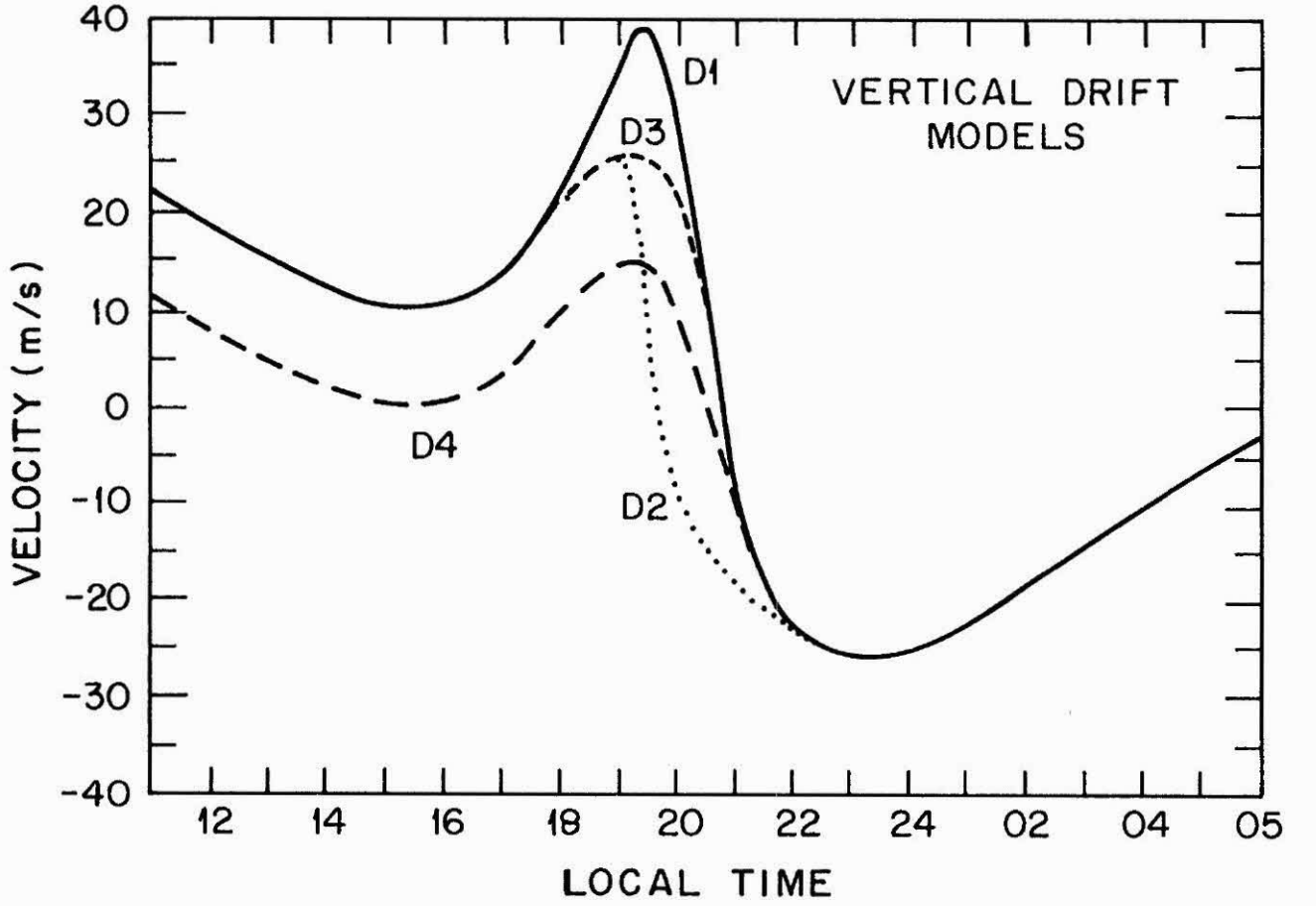


Fig. 5 Local time variation of the vertical electromagnetic plasma drift, at the magnetic equator, corresponding to the drift models D1 to D4.

(7.1.1) over all absorbing species,

$$Q_T(r, \chi) = \sum_j Q_j(r, \chi) \quad (7.1.2)$$

The exponential part in (7.1.1) represents the attenuation of the solar radiation produced by the atmosphere above the altitude considered. The optical depth can be expressed as

$$\tau(\lambda_k, r, \chi) = \sum_j \int_r^\infty \sigma_j^{(a)}(\lambda_k) n_j(r') Ch(r'/H_j, \chi) dr' \quad (7.1.3)$$

where H_j is the scale height of the j^{th} constituent, $Ch(r'/H_j, \chi)$ denotes the geometrical Chapman function which takes into account the Earth's sphericity and $\sigma_j^{(a)}(\lambda_k)$ stands for the absorption cross section in the wavelength band λ_k for the j^{th} absorbing species. Equation (7.1.3) can be replaced by the following approximated simplified expression

$$\tau(\lambda_k, r, \chi) = \sum_j \sigma_j^{(a)}(\lambda_k) n_j(r) H_j Ch(r/H_j, \chi) \quad (7.1.4)$$

For each of the absorbing species, taken to be O , O_2 and N_2 , the photoionization rate per unit volume is computed from expression (7.1.1), considering 62 discrete wavelength intervals in the range from 30 \AA to 1026 \AA . The incident solar XUV radiation flux $\Phi_\infty(\lambda_k)$ and the absorption and ionization cross sections, $\sigma_j^{(a)}(\lambda_k)$ and $\sigma_j^{(i)}(\lambda_k)$, in the present model are taken from the results published by Hinteregger et al. (1965), which are based on satellite and rocket observations. Hinteregger (1970) has suggested that these solar XUV radiation fluxes, measured under solar minimum conditions (in 1963), are probably more representative of solar maximum conditions. Nevertheless, these values constitute the basis for the photoionization rates used in the present ionospheric computer model. More recently, a solar EUV flux model has been published by Tobiska and Barth (1990) and by Tobiska (1991).

The optical depth for each wavelength band is calculated from expression (7.1.4), considering the summation (index j) over the atmospheric species O , O_2 and N_2 . Due to the predominance of atomic oxygen above about 250 km , it constitutes the dominant term in the calculation of the optical depth.

7.2 Ion Chemistry

Loss of ionization in the ionospheric F-region is controlled by recombination processes such as electron-ion and ion-ion recombinations. The pertinent reactions in these loss mechanisms include radiative and dissociative recombinations. Ion-atom interchange and charge exchange reactions are also efficient and must be considered in both production and loss rates for the ion species. Ion-atom interchange reactions are generally more rapid than charge exchange reactions (Bates, 1955).

The ionization production and loss rates per unit volume, resulting from ion chemistry, are governed by the rate coefficients of the relevant ion-ion, ion-neutral and ion-electron processes. The ionic reactions and

TABLE 7.1

Chemical and Ionic Reactions and Their Rates (in $cm^{-3}s^{-1}$).
 (Temperature dependences given by $f(T) = 300/T$ and $g(T) = 700/T$).

Reaction	Rate	Reference
$O^+ + O_2 \rightarrow O_2^+ + O$	$2.0 \times 10^{-11} f(T)$	Donahue (1968)
$O^+ + N_2 \rightarrow NO^+ + N$	$1.0 \times 10^{-12} f(T)$	Donahue (1868)
$O^+ + NO \rightarrow NO^+ + O$	2.0×10^{-11}	Dunkin et al. (1971)
$O^+ + e \rightarrow O + h\nu$	1.7×10^{-12}	Tinsley et al. (1973)
$O_2^+ + N_2 \rightarrow NO^+ + NO$	1.0×10^{-15}	Ferguson (1967)
$O_2^+ + NO \rightarrow NO^+ + O_2$	8.0×10^{-10}	Ferguson (1967)
$O_2^+ + N \rightarrow NO^+ + O$	1.8×10^{-10}	Goldan et al. (1966)
$O_2^+ + e \rightarrow O + O$	$1.0 \times 10^{-7} g(T)$	Biondi (1969)
$NO^+ + e \rightarrow N + O$	$2.0 \times 10^{-7} g(T)$	Biondi (1969)
$N_2^+ + O_2 \rightarrow O_2^+ + N_2$	5.0×10^{-11}	Keneshea et al. (1970)
$N_2^+ + NO \rightarrow NO^+ + N_2$	3.3×10^{-10}	Fehsenfeld et al. (1970)
$N_2^+ + O \rightarrow NO^+ + N$	2.5×10^{-10}	Ferguson et al. (1965)
$N_2^+ + e \rightarrow N + N$	$3.0 \times 10^{-7} f(T)$	Kasner and Biondi (1965)
$N^+ + O_2 \rightarrow NO^+ + O$	3.0×10^{-10}	Dunkin et al. (1968)
$N^+ + O_2 \rightarrow O_2^+ + N$	3.0×10^{-10}	Dunkin et al. (1968)
$N^+ + NO \rightarrow NO^+ + N$	8.0×10^{-10}	Goldan et al. (1966)

the magnitude of their reaction rate coefficients, considered in the present ionospheric computer model, are presented in Table 7.1.

8. NEUTRAL ATMOSPHERE MODEL

Several model atmospheres, based on experimental data from satellites and from the basic equations governing atmospheric structure, have been developed, which provide the spatial and time dependence of the neutral gas temperature and neutral species concentrations in the upper atmosphere, including seasonal, solar cycle and geomagnetic activity dependences (e.g. Jacchia, 1965, 1971, 1977; Hedin, 1987).

The model atmosphere used in the present ionospheric model is similar to that employed by Sterling et al. (1969), Brasher and Hanson (1970), Anderson (1973a,b), Bittencourt and Tinsley (1976), and Bittencourt et al. (1976). It is based on the Jacchia (1977) atmospheric model combined with Walker's (1965) analytic expressions for the temperature and density

profiles. The modification incorporated by Walker (1965) avoids the numerical integration of the diffusive equilibrium equations for each neutral species. Another possible approach is to use the MSIS-86 thermospheric model of Hedin (1987), which is based on satellite data.

8.1 Temperature Profiles

Jacchia's expression for the global distribution of exospheric temperature, T_∞ , is

$$T_\infty = T_0(1 + R \sin^m \psi) \cdot \left[1 + R \frac{(\cos^m \eta - \sin^m \psi)}{(1 + R \sin^m \psi)} \cos^n \left(\frac{\tau}{2} \right) \right] \quad (8.1.1)$$

where T_0 is the minimum nighttime exospheric temperature, $(1 + R)T_0$ is the maximum daytime value of the exospheric temperature, m and n are constants, η and ψ are functions of geographic latitude (Λ) and solar declination (δ_0), defined by

$$\eta = (\Lambda - \delta_0)/2 \quad (8.1.2)$$

$$\psi = (\Lambda + \delta_0)/2 \quad (8.1.3)$$

and the parameter τ is a function of local time defined according to

$$\tau = H + \beta + p \sin(H + \gamma) \quad ; \quad (-\pi < \tau < \pi) \quad (8.1.4)$$

where H represents the solar hour angle measured from noon, in radians, and β , p and γ are constants which specify the phase of maximum exospheric temperature and the shape of the isotherms of exospheric temperature over the globe. The quantity T_0 is dependent on solar activity.

The temperature profile is calculated, according to Walker (1965), from

$$T = T_\infty - (T_\infty - T_{120}) \exp(-\sigma \xi) \quad (8.1.5)$$

where T_{120} is the temperature at 120 km and σ is an analytical function of T_∞ given (in km^{-1}) by

$$\sigma = 0.0291 \exp(-X^2/2) + (r_0 + 120)^{-1} \quad (8.1.6)$$

where r_0 is the Earth's radius (in km) and

$$X = \frac{(T_\infty - 800)}{750 + 1.722 \times 10^{-4}(T_\infty - 800)^2} \quad (8.1.7)$$

The geopotential altitude, ξ , is given (in km) by

$$\xi = \frac{(z - 120)(r_0 + 120)}{(r_0 + z)} \quad (8.1.8)$$

in which z represents the altitude of the point considered, above the Earth's surface.

For all computations in the present model the electron and ion temperatures were taken equal to the neutral gas temperature.

8.2 Neutral Density Profiles

The diffusive equilibrium equation can be integrated analytically using the temperature profile given in (8.1.5). Walker (1965) obtained the following expression for the number density of the α neutral species

$$n_\alpha(z) = n_\alpha(120) \left[\frac{(1-a)}{1-a \exp(-\sigma\xi)} \right]^{(1+\gamma)} \exp(-b_\alpha\sigma\xi) \quad (8.2.1)$$

where

$$a = \frac{(T_\infty - T_{120})}{T_\infty} \quad (8.2.2)$$

$$b_\alpha = \frac{m_\alpha g_{120}}{\sigma k T_\infty} \quad (8.2.3)$$

k is Boltzmann's constant, g_{120} stands for the gravitational acceleration at the 120 km base level and m_α is the mass of the neutral constituent α .

The values of the atmospheric parameters used in the present model are given in Table 8.1. For the concentrations of N and NO needed in this model, the profiles deduced by Norton (1967), which are based on the observations by Barth (1966), are used.

9. DIFFUSION RATES AND COLLISION FREQUENCIES

The general theory for diffusion of ions through a gas was originally developed by Chapman (1939). In the low-latitude ionosphere the relevant ions O^+ , O_2^+ , NO^+ , N_2^+ and N^+ diffuse through the gases of the neutral atmosphere and through each other. The force per unit volume acting on the i^{th} species, due to collisions, is given by

$$\mathbf{f}_{coll}^{(i)} = - \sum_j' m_i n_i \nu_{ij} (\mathbf{v}_i - \mathbf{v}_j) - \sum_n m_i n_i \nu_{in} (\mathbf{v}_i - \mathbf{u}) \quad (9.1)$$

TABLE 8.1

Parameters for the Neutral Atmosphere Model

Parameter	Value
Temperature at 120 km	355 K
O Density at 120 km	$7.6 \times 10^{10} \text{ cm}^{-3}$
O ₂ Density at 120 km	$7.5 \times 10^{10} \text{ cm}^{-3}$
N ₂ Density at 120 km	$4.0 \times 10^{11} \text{ cm}^{-3}$
Minimum Temperature T_0	800 K
m	2.5
n	2.5
R	0.3
p	12 ⁰
β	-45 ⁰
γ	45 ⁰

where the first summation is over all ion species, except the i^{th} , and the second one is over all neutral atmospheric species.

The collision frequencies used in the present computer model are derived from the relationship

$$\nu_{ij} = \frac{kT_i n_j}{m_i b_{ij}} \quad (9.2)$$

where the b_{ij} 's are the binary collision parameters. The values used for the binary collision parameters are presented in Table 9.1 and have been derived from the individual ion mobilities in a neutral gas as given by Dalgarno (1961, 1964).

The temperature dependence of the ion-ion collision parameters was considered, in the present computer model to be $(T_i/1500)^{5/2}$ and the dependence of the ion-neutral collision parameters was $(T_n/300)^{1/2}$, with the temperatures expressed in degrees Kelvin. Furthermore, in all calculations for the present model, we take $T_i = T_e = T_n$.

The ion diffusion coefficient D_i and the collision frequency ν_{ij} are related through the expression

$$D_i = \frac{kT_i}{m_i (\sum_j \nu_{ij})} = \left[\sum_j \left(\frac{n_j}{b_{ij}} \right) \right]^{-1} \quad (9.3)$$

TABLE 9.1

Binary Collision Parameters b_{ij} (in $cm^{-1}s^{-1}$)

	O^+	NO^+	O_2^+	N_2^+	N^+
NO^+	2.5×10^{15}				
O_2^+	2.5×10^{15}	2.1×10^{15}			
N_2^+	2.6×10^{15}	2.1×10^{15}	2.1×10^{15}		
N^+	2.8×10^{15}	2.6×10^{15}	2.6×10^{15}	2.7×10^{15}	
O	3.7×10^{18}	3.3×10^{18}	3.3×10^{18}	3.3×10^{18}	4.7×10^{18}
O_2	3.3×10^{18}	1.0×10^{18}	1.3×10^{18}	1.3×10^{18}	2.9×10^{18}
N_2	3.4×10^{18}	1.8×10^{18}	1.9×10^{18}	1.9×10^{18}	2.8×10^{18}

The summation in equation (9.3) applies to both ions and neutrals.

10. COMPUTATIONAL PROCEDURE

10.1 Variable Transformations

In order to simplify the equations and to put them in a form suitable for numerical solution, three variable transformations are made. These variable transformations are dictated mainly by numerical stability considerations, speed of computation and convenience in interpreting the results.

The first transformation involves the change of the independent variable time t , to longitude ϕ , which allows a straightforward interpretation of the results at specified local times, according to

$$\frac{\partial n_i}{\partial \phi} = \frac{1}{(v_\phi/r + \Omega)} \frac{\partial n_i}{\partial t} \quad (10.1.1)$$

The second transformation maps the parameter q into a parameter Y , defined by

$$Y = \frac{\sinh(\Gamma q)}{\sinh(\Gamma q_{max})} \quad (10.1.2)$$

where Γ is a suitably chosen number and q_{max} is the value of q at the northern end of the field line, where $r = r_b$, and r_b is some base value of r . This base level in the present model is taken at 120 km and $\Gamma = 10$. Baxter and Kendall (1968) and Sterling et al. (1969) found that equal

increments in q give too many points at high altitudes and not enough near the F2-peak. This transformation maps the magnetic field lines into straight lines with $Y = 1$ at the northern end (where $q = q_{max}$), $Y = 0$ at the dipole equator and $Y = -1$ at the southern end (where $q = -q_{max}$).

The third transformation replaces the dependent variable $n_i(\mathbf{r}, t)$ by the variable $G_i(\mathbf{r}, t)$, defined by

$$G_i = n_i \exp \left(\int_{r_0}^r \frac{dr'}{\alpha H_i} \right) \quad (10.1.3)$$

where $\alpha = (T_e + T_i)/T_i$ and H_i is the ion scale height. This transformation was used by Hanson and Moffett (1966) and Baxter (1967) to improve the stability of the numerical solutions since, at great altitudes where n_i varies in an exponential manner, G_i is essentially constant along a magnetic field line. It can be applied to any of the ions considered here, but its use was restricted to the O^+ ions only, which is the dominant ion above the F2-peak in the low-latitude ionospheric F-region.

These transformations are incorporated in the equations according to the details given in Bittencourt and Tinsley (1976) and Sterling et al. (1969). The resultant system of coupled partial differential equations is solved using an iterative, implicit finite-difference method, similar to method three of Crank and Nicolson (1947) (see also Potter, 1980).

10.2 Boundary Conditions

At all times the boundary conditions at $y = \pm 1$ (base level) are $n_i(\phi, y) = 0$, while at $t = 0$ some initial ionization distribution is assumed everywhere along the field line. After a few integration steps in time, the solution becomes independent of the initial values adopted, because of the effects of photoionization, ion chemistry and plasma transport.

10.3 Spatial Grid and Time Step

A usual step in ϕ (local time) is 2.5^0 (corresponding to 10 minutes), but in some cases a step of 7.5^0 (corresponding to 30 minutes) may be adequate. Smaller steps in ϕ may be used depending on the ionospheric phenomena under analysis. Along the magnetic field line 99 steps are used in y (50 in each hemisphere, with one common point at the magnetic equator). It is appropriate to start the time integration around 08:00 local time, cover a full 24-hour period, ending about two or three hours past

08:00 local time of the next day, when the calculation results start to repeat themselves for the same local time. The calculation results for the first two or three hours are then neglected in order to eliminate any possible influence of the initial values adopted.

In order to be able to construct vertical profiles of the particle number densities and velocities, over a latitudinal range between about $\pm 20^\circ$, the integration in ϕ is repeated over the 24-hour period for a given number of magnetic field lines (about twenty or more) with their equatorial crossing altitude chosen such as to cover the altitude range of interest, for all times, in the latitudinal range considered. The distribution in height of the starting magnetic field lines (equatorial crossing altitude) is selected such that the vertical ionization distribution in the region of the equatorial Appleton anomaly (between at least $\pm 15^\circ$ north-south) can be accurately constructed for all ϕ -steps.

For each step in ϕ (local time) a two-dimensional interpolation scheme is employed to transform the particle number densities and velocities along the magnetic field lines into a uniform grid in height and magnetic latitude. A two-dimensional grid is then constructed at 5 km (or less) increments in height and 0.5° increments in magnetic latitude using a three-point Lagrange interpolation scheme. This interpolation is carried out first in height along each field line and then in latitude for each height level using the various field lines. These results are then graphically processed with appropriate graphic softwares in order to generate different types of representations for adequate visualization of the various ionospheric phenomena of interest.

11. EXAMPLES OF SOME COMPUTER MODEL RESULTS

In this section we shall present some examples of results generated by this low-latitude ionospheric computer model in order to illustrate its potential applicability in the study of a variety of important ionospheric phenomena at low latitudes. It also allows the computation of the intensity distribution, in space and time, of various atmospheric airglow recombination emissions, which constitute an important remote diagnostic technique for the study of dynamical processes in the ionosphere. The ionospheric model results presented here are labeled as models M1 to M5 and their main characteristics are summarized in Table 11.1. All these models are computed for average solar activity conditions.

TABLE 11.1
Main Characteristics of Computed Ionospheric Models

Model	Drift	Wind	δ_0	Δ	Wind Reversal
M1	—	—	0^0	0^0	—
M2	D4	—	0^0	0^0	—
M3	D2	—	-23^0	-7^0	—
M4	D2	W4	-23^0	-7^0	12:00-22:00LT
M5	D1	W1	0^0	$+10^0$	08:00-18:00LT

11.1 Electromagnetic Plasma Drift Effects

The electromagnetic vertical plasma drift at low latitudes is the main mechanism responsible for the formation of the Appleton ionospheric equatorial anomaly, as discussed earlier. In general terms, as the vertical upward drift increases, the latitudinal separation of the anomaly north-south crests increases, at the same time that the crest-to-trough ratio in the electron density also increases. The anomaly does not exist in the absence of the vertical plasma drift.

For illustration purposes, we present in Fig. 6 the distribution in space and time of the F2-peak electron density calculated under equinox conditions ($\delta_0 = 0^0$), with the geomagnetic and geographic equators coincident ($\Delta = 0^0$), without an electric field and no thermospheric neutral wind (labeled here as model M1). In this case the F2-peak electron density maximizes at the magnetic (geographic) equator in the late afternoon hours and the ionospheric equatorial anomaly is not generated.

Considering the same conditions as for Fig. 6, except that now we include the vertical drift model D4 (refer to Fig. 5), we obtain the F2-peak electron density distribution shown in Fig. 7 (labeled here model M2), where now two ionization crests are produced, maximizing at about $\pm 12^0$ north-south either side of the magnetic (geographic) equator, around 18:00 LT. Note that in both cases (Figs. 6 and 7) the ionization distribution is symmetric about the equator, since no thermospheric neutral wind was included and the calculations were made for equinox conditions.

Figs. 8 and 9 show, respectively, the F2-peak electron density and F2-peak height distributions calculated for the case of model M3, considering summer solstice in the southern hemisphere or december solstice ($\delta_0 = -23^0$), the geomagnetic equator at 7^0 to the south of the geographic equator ($\Delta = -7^0$), vertical plasma drift model D2 (refer to Fig. 5) and

no thermospheric neutral wind. In this case the equatorial anomaly is enhanced as a result of the larger upward drift velocities of drift model D2 as compared to D4. The very slight north-south asymmetry present in the F2-peak electron density distribution (Fig. 8) is due to the seasonal hemispheric asymmetry in the neutral atmosphere parameters and solar photoionization fluxes. No significant asymmetry is seen in the F2-peak height distribution (Fig. 9) as there are no thermospheric neutral winds in this case.

11.2 Thermospheric Neutral Wind Effects

The results calculated for model M4 are presented in Figs. 10 and 11. In this case the conditions are the same as those selected for model M4, except that now we included a thermospheric neutral wind (model W4). The principal effect of the wind velocity component along the magnetic field is to produce a north-south asymmetry in the F2-peak electron density and F2-peak height distributions. As illustrated in Fig. 3 the wind moves, through ion-drag, the ionization upward in the upwind side of the magnetic field line, into regions where the recombination rate is lower, and downward in the downwind side of the magnetic field line, into regions where the recombination rate is higher, at the same time that it promotes an interhemisphere transport of ionization. As can be seen from Figs. 10 and 11 the ionization is higher (and the peak height is also higher) in the southern crest as compared to the northern one, before the wind reversal which occurred at 22:00 LT. After that the asymmetry in the F2-peak height distribution is also reversed, showing a very fast response of the ionospheric peak height to changes in the wind direction. The same is not true for the electron density distribution due to the effects of recombination.

In Figs. 12 and 13 we present the F2-peak electron density distribution and the F2-peak height distribution, respectively, for the conditions of model M5, i.e. equinox ($\delta_0 = 0^\circ$), the magnetic equator positioned at 10° to the north of the geographic equator ($\Delta = +10^\circ$), plasma vertical drift model D1 and thermospheric wind model W1. In this case the wind reversal occurs at 18:00 LT, when it starts blowing southwards, resulting in lower F-region heights (higher electron densities) in the southern hemisphere as compared to the northern one. It must be noted also that the crests of the Appleton equatorial anomaly are enhanced in this case as compared to the results shown in Fig. 10 (which used drift model D2), due to the higher upward drift velocities of drift model D1 around the

prereversal peak.

To illustrate the vertical profiles generated by this ionospheric computer model we present in Figs. 14 to 17 the height variation of the electron density (in units of 10^5 cm^{-3}), the O_2^+ density (in units of 10^3 cm^{-3}) and the volume emission rate of the OI 630 nm emission (in units of $\text{photons cm}^{-3} \text{ s}^{-1}$) resulting from dissociative recombination of O_2^+ (i.e. $O_2^+ + e \rightarrow O + O$). The profiles are presented for both hemispheres at the equatorial anomaly crests and local times of 18:00, 21:00, 23:00 and 01:00. The north-south asymmetry in these parameters are clearly seen in this direct comparison between profiles taken at magnetically conjugate points. It should be noted that this height asymmetry is due only to the effects of the thermospheric neutral wind, since the effects of the electromagnetic plasma drift are symmetric about the magnetic equator.

12. SUMMARY AND CONCLUSIONS

The low-latitude ionospheric computer model presented here provides the spatial distribution and time evolution of the number density and macroscopic velocity of the electrons and the ions O^+ , O_2^+ , NO^+ , N_2^+ and N^+ in the low-latitude ionospheric F-region, considering various different geophysical conditions. It permits the study of the ionospheric changes related to solar activity, including the solar cycle variation and changes due to geomagnetic storms, to seasonal and neutral atmosphere variations, to plasma dynamical processes such as the electromagnetic plasma drift and to thermospheric neutral wind coupling. Also, from the ion density distributions generated by the model, the intensity of various airglow emission lines due to recombination processes can be calculated as a function of space and time. These emissions constitute a powerful diagnostic technique to study, from the ground, various dynamical processes which occur in the low-latitude ionosphere. The total electron content along a given line of sight can be easily calculated from the ionization distribution generated by the model. Important ionospheric effects on electromagnetic radio wave propagation through the ionosphere can also be investigated.

Different drift models can be used to represent different situations and conditions. As discussed earlier, the amplitude and duration of the prereversal peak in the upward plasma drift velocities is greatly dependent on the season and on the magnetic declination at a particular longitude. This dependence is due mainly to the variation in the low-latitude ionospheric conductivity at magnetically conjugate points near sunset as the terminator crosses the magnetic meridian, since the angle formed between

these two lines depends on season and magnetic declination. These effects can be included in the model through proper selection of the electromagnetic plasma drift velocities appropriate for each longitudinal sector and season.

Since the horizontal wind velocity that goes into the model is the wind component along the *magnetic* meridian, the effects of the *geographic* zonal and meridional wind components will depend on the value of magnetic declination at a specified longitude. According to equation (5.4.4), the effects of the geographic zonal wind component will be just opposite in the longitudinal regions where the magnetic declination is east or west (because of the sign of $\sin \delta_m$). Thus, the effect of the neutral wind on the low-latitude ionosphere is strongly longitudinal dependent, due to the longitudinal variation of magnetic declination. These effects can be included in the calculations through proper selection, for each longitudinal sector, of the wind velocity model (u_θ) along the magnetic meridian.

Comparison of the computer model results with ionospheric measurements and with existent empirical ionospheric models can provide important information for appropriate physical interpretation of ionospheric data and for improvement of empirical models at low latitudes.

F2-PEAK ELECTRON DENSITY

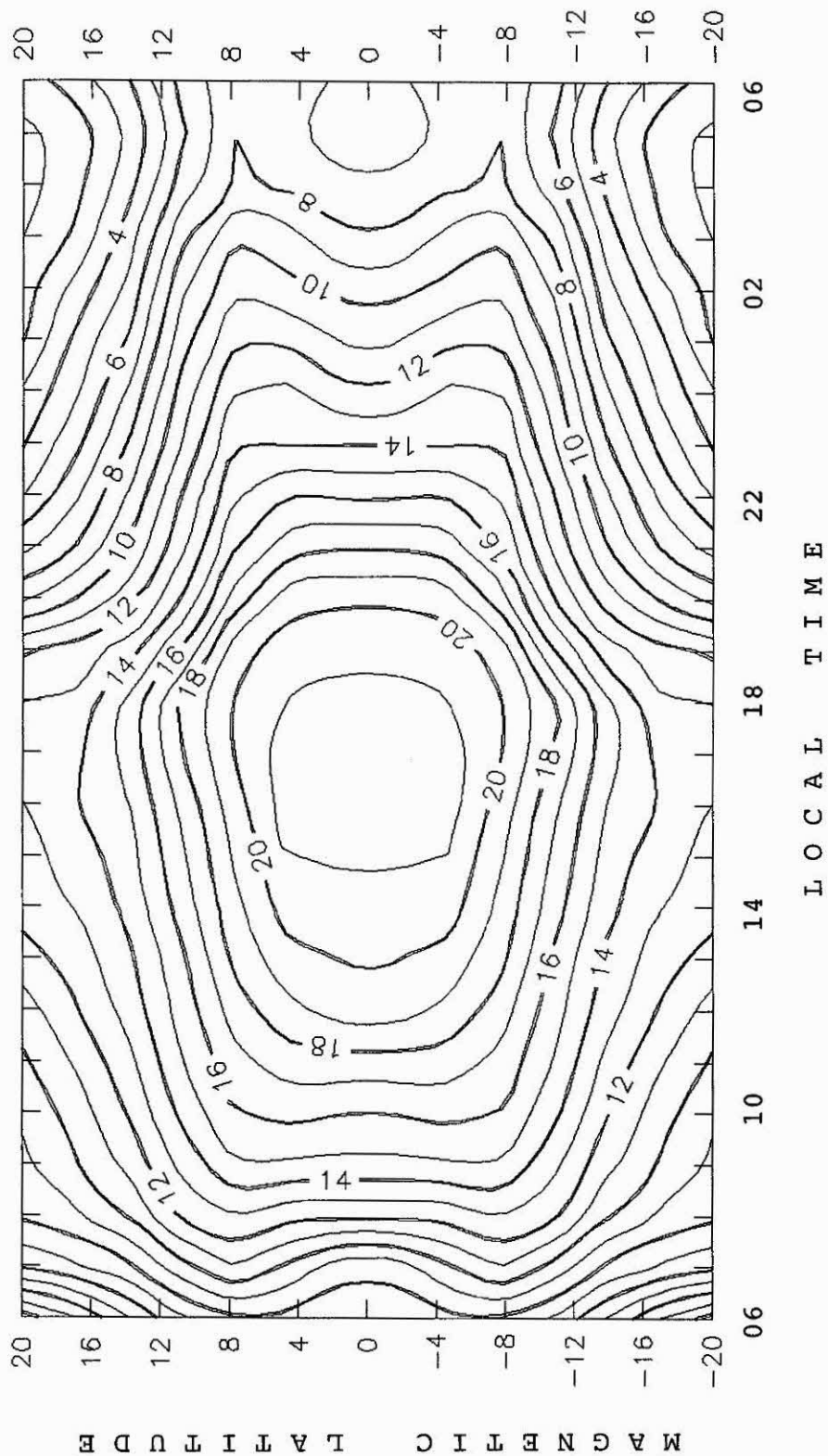


Figure 6. F2-peak electron density distribution for model M1, considering equinox conditions ($\delta_0 = 0^\circ$), $\Delta = 0^\circ$, without an electric field and no thermospheric neutral wind.

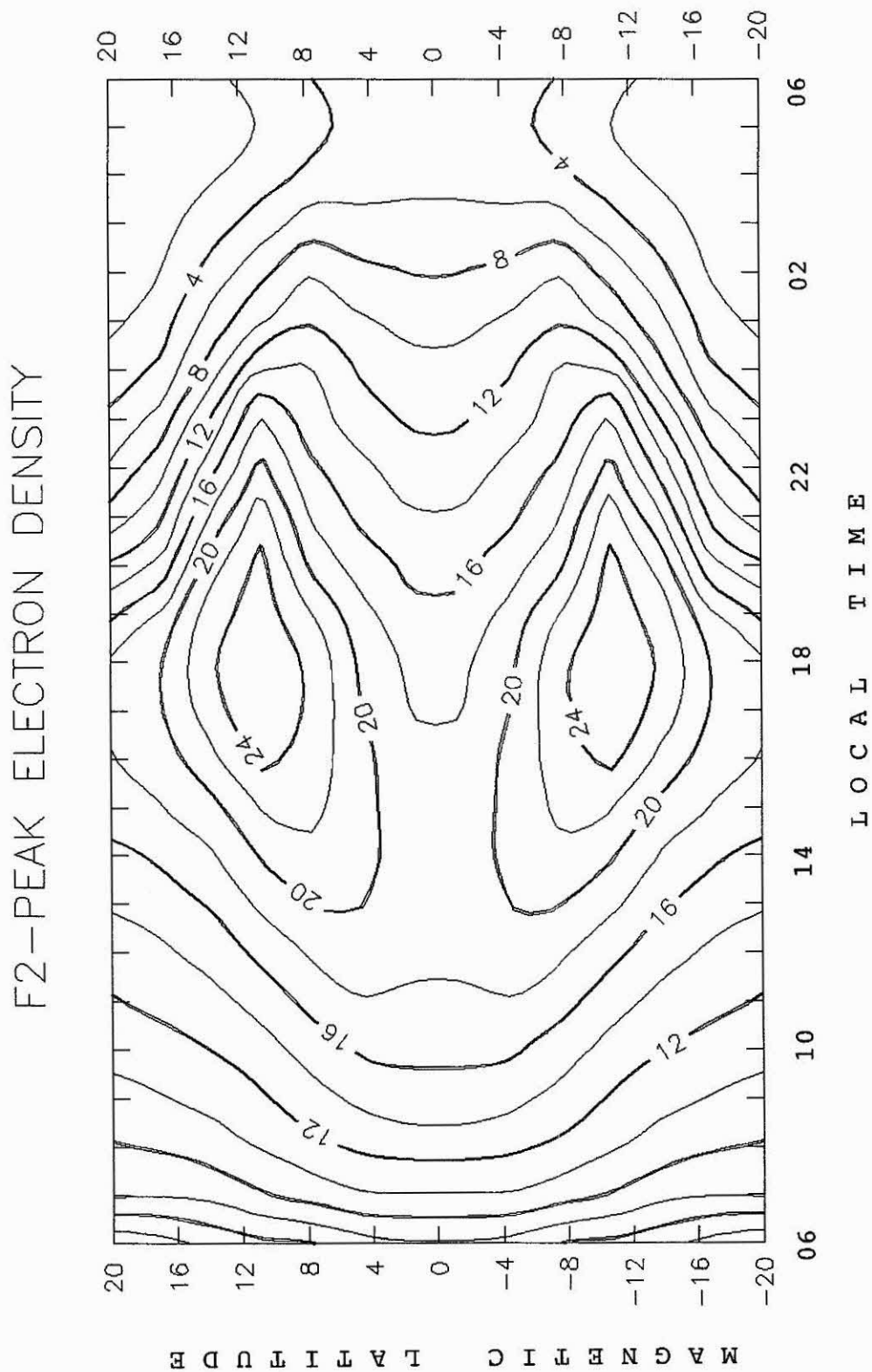


Figure 7. F2-peak electron density distribution for model M2, considering equinox conditions ($\delta_0 = 0^0$), $\Delta = 0^0$, electromagnetic drift model D4 and no thermospheric neutral wind.

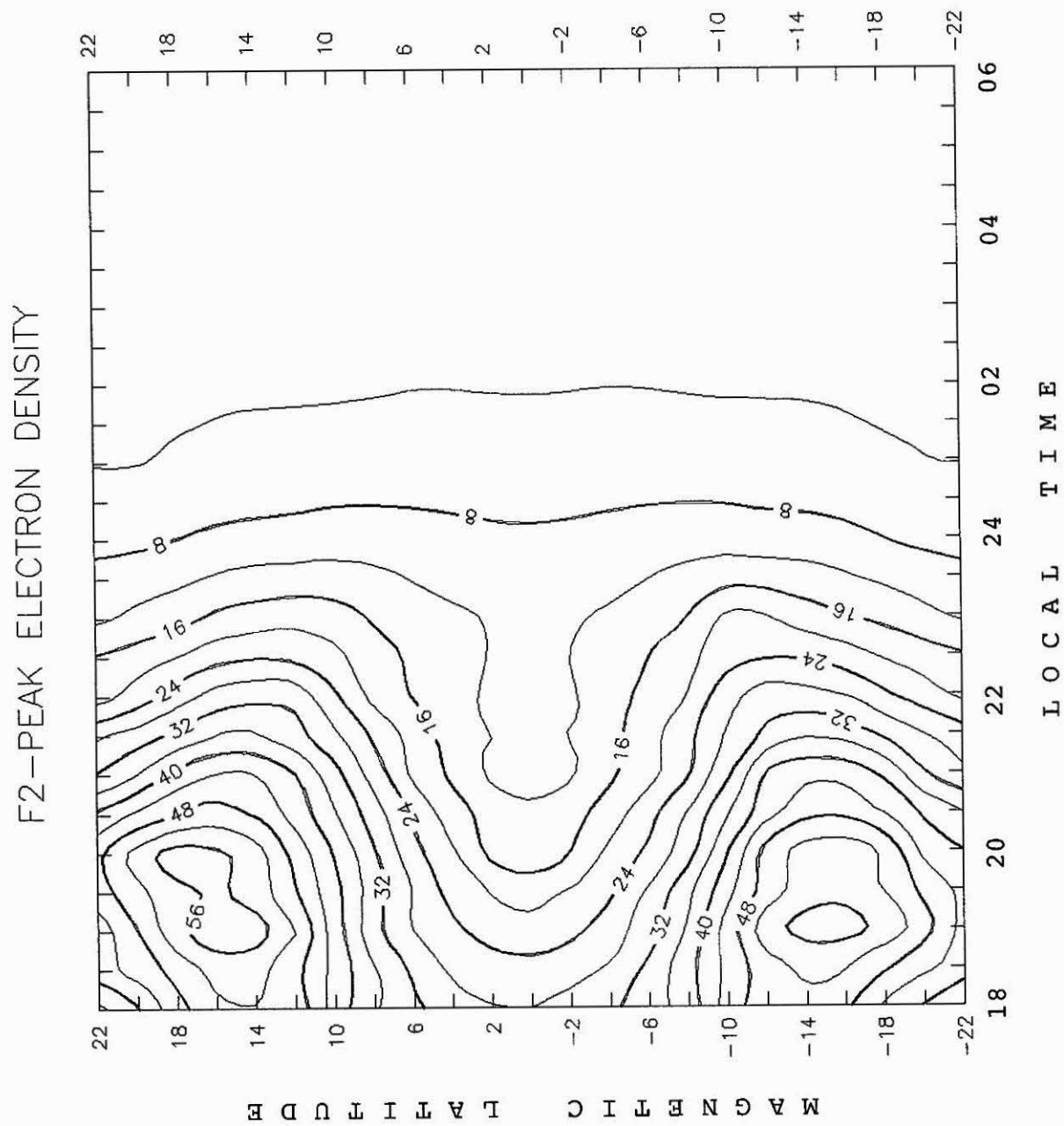


Figure 8. F2-peak electron density distribution for model M3, considering summer solstice in the southern hemisphere ($\delta_0 = -23^\circ$), $\Delta = -7^\circ$, electromagnetic drift model D2 and no thermospheric neutral wind.

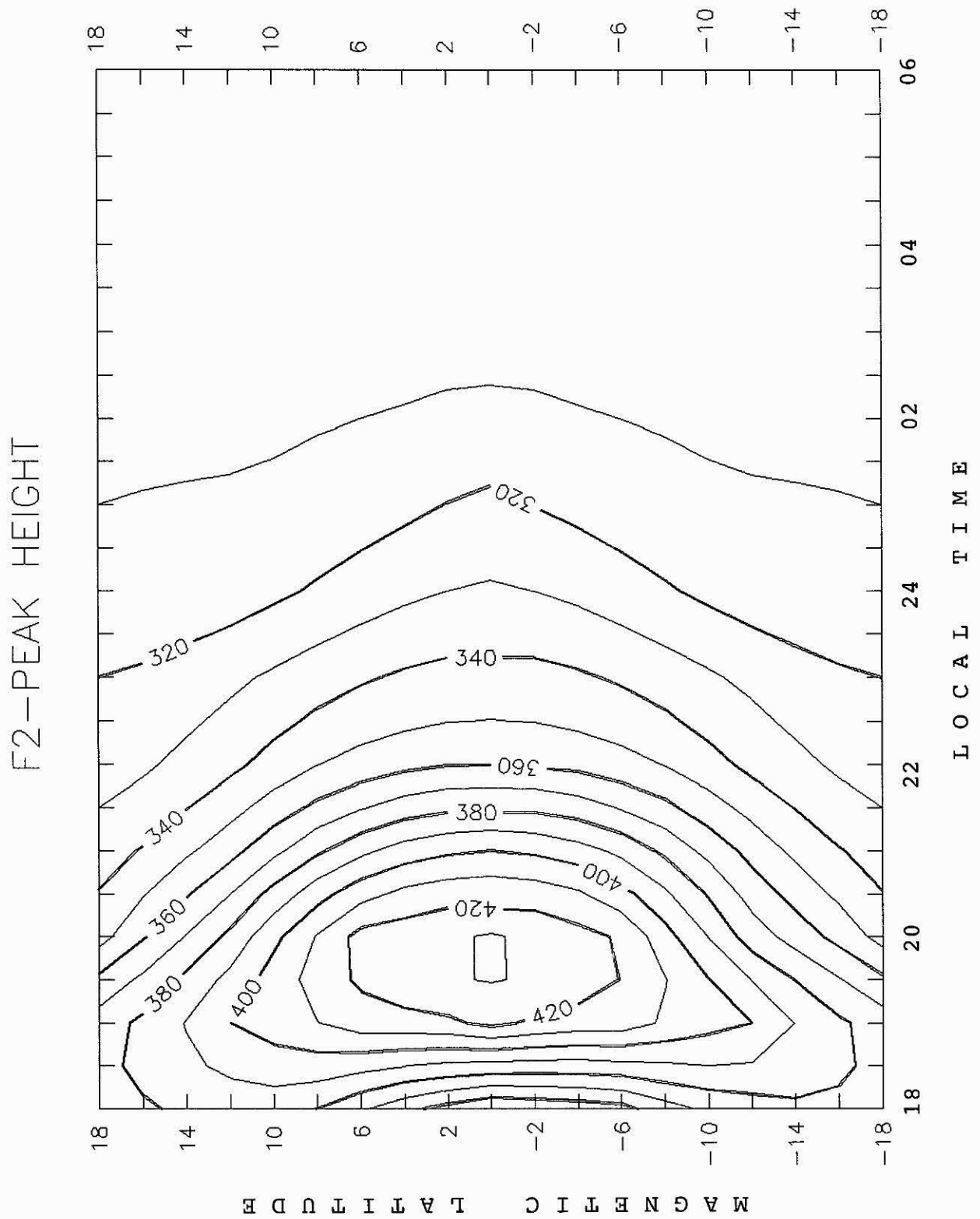


Figure 9. F2-peak height distribution for the same conditions of Figure 8 (model M3).

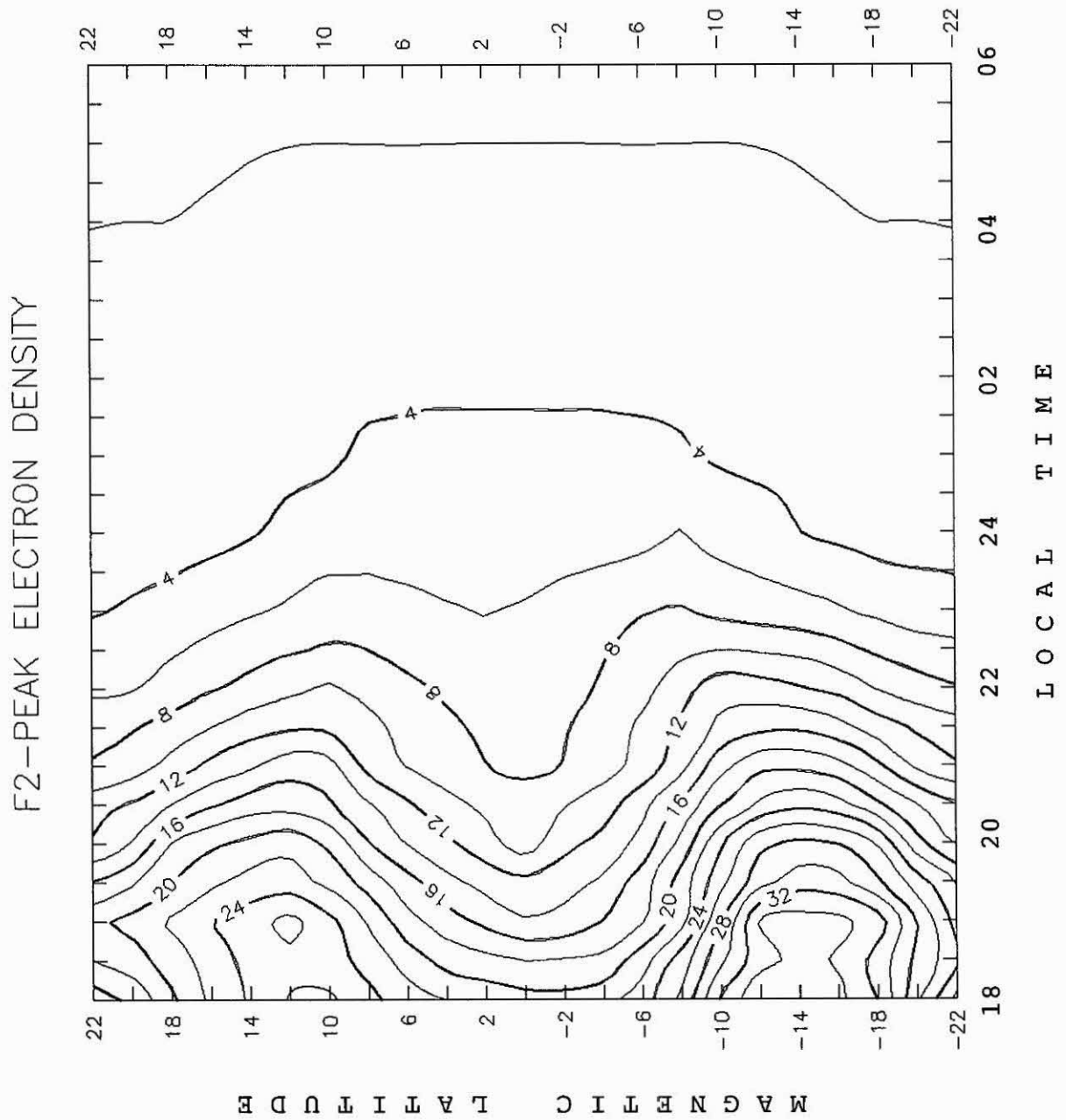


Figure 10. F2-peak electron density distribution for model M4, considering summer solstice in the southern hemisphere ($\delta_0 = -23^\circ$), $\Delta = -7^\circ$, electromagnetic drift model D2 and thermospheric neutral wind model W4.

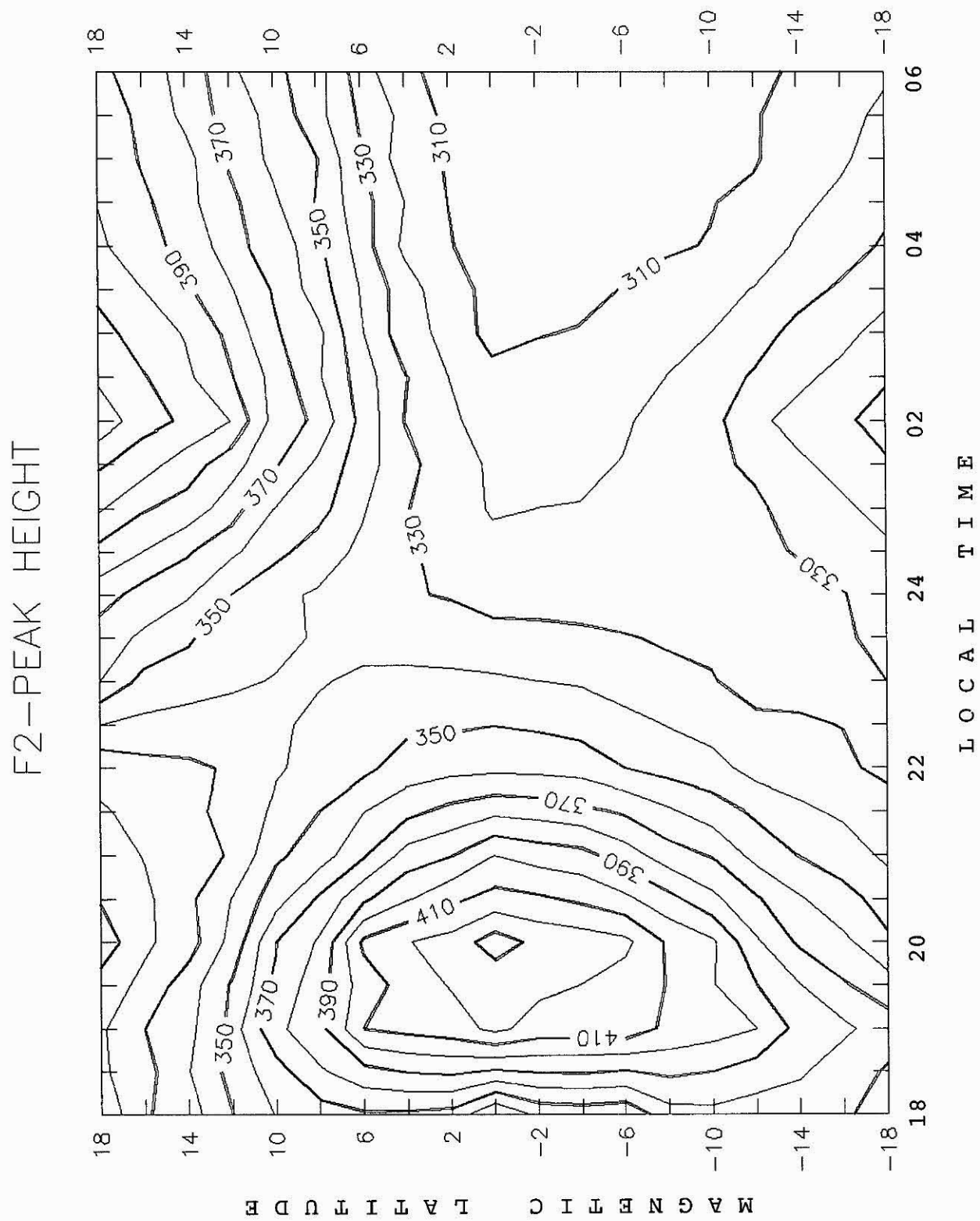


Figure 11. F2-peak height distribution for the same conditions of Figure 10 (model M4).

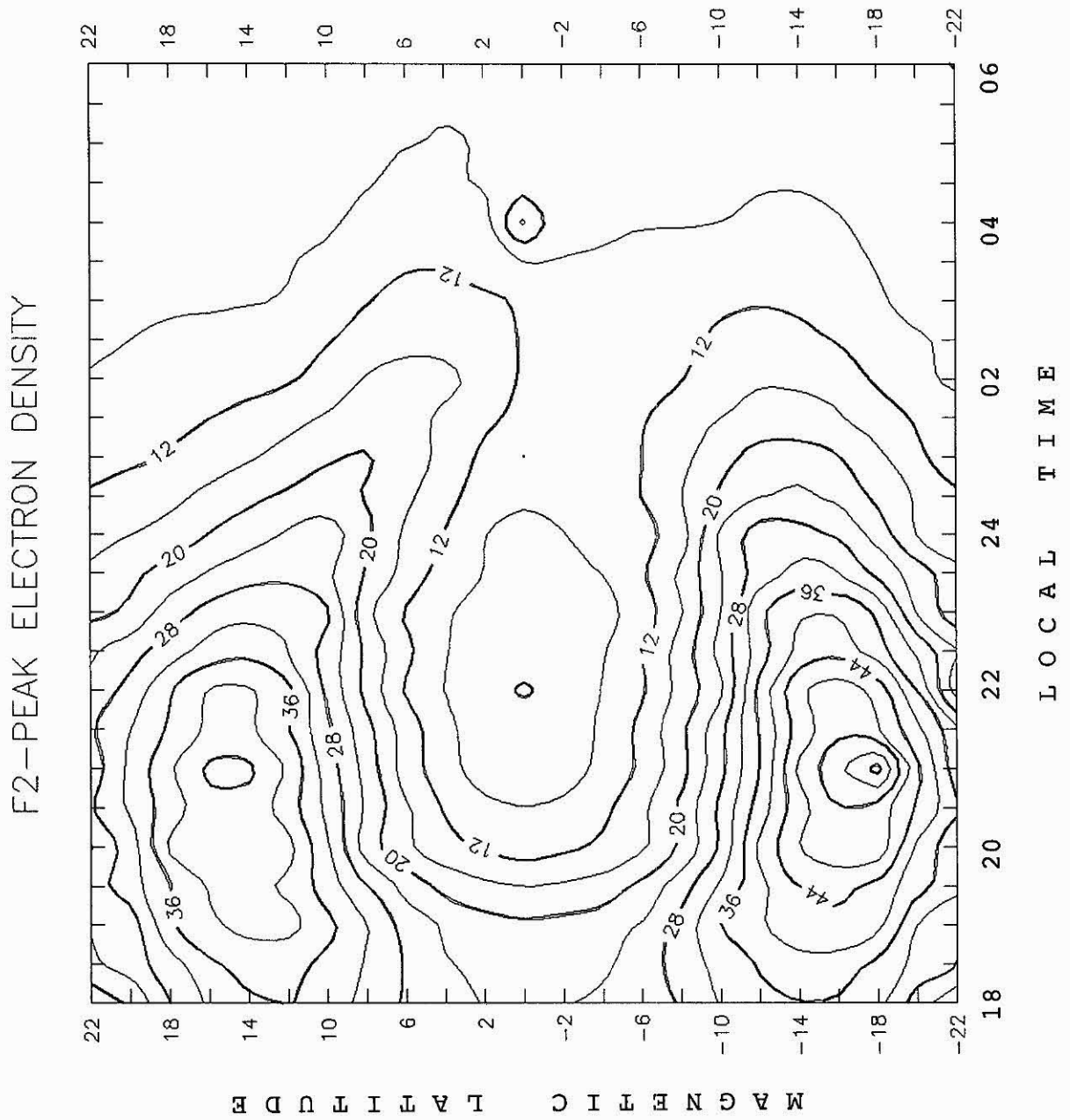


Figure 12. F2-peak electron density distribution for model M5, considering equinox conditions ($\delta_0 = 0^\circ$), $\Delta = +10^\circ$, electromagnetic drift model D1 and thermospheric neutral wind model W1.

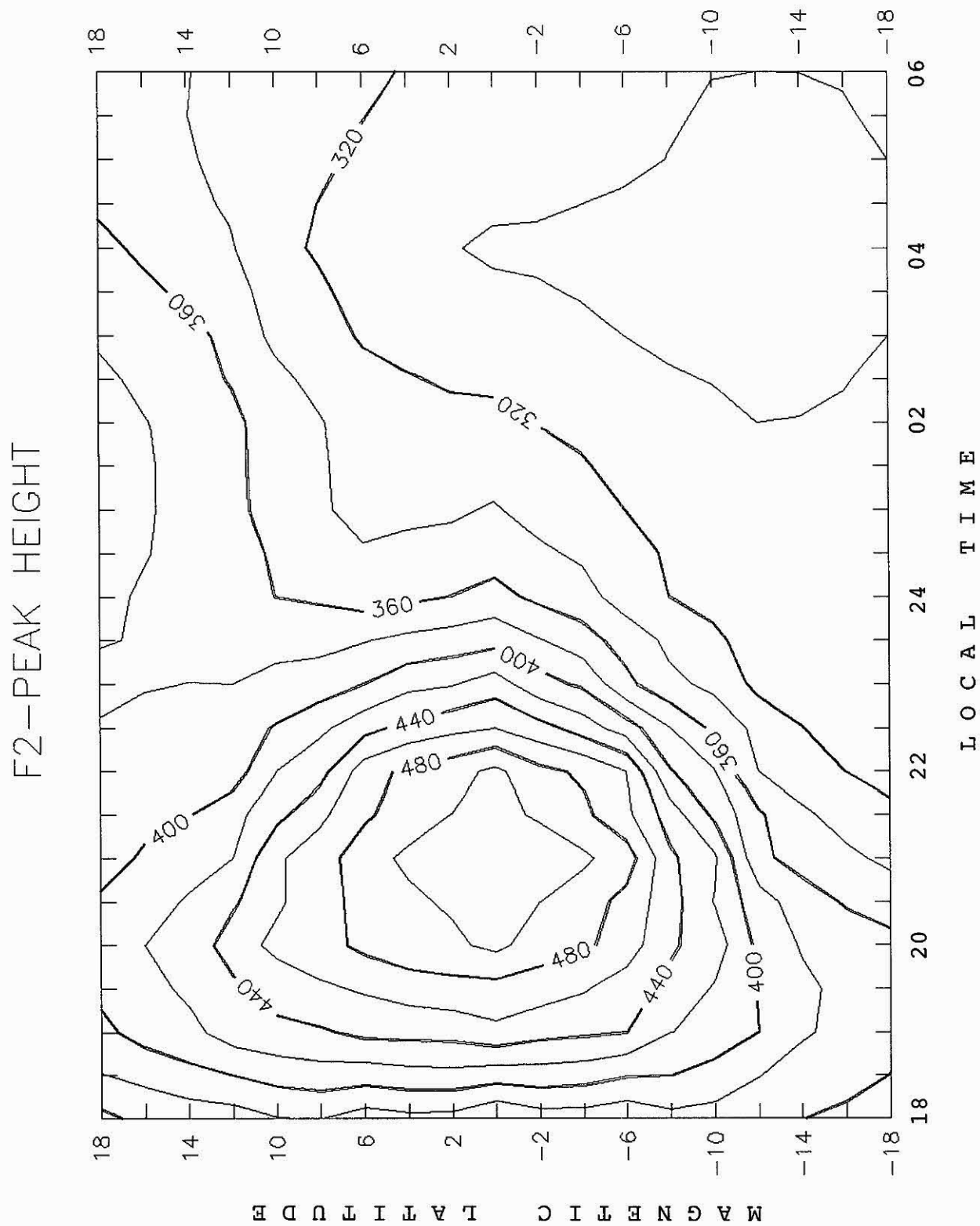


Figure 13. F2-peak height distribution for the same conditions of Figure 12 (model M5).

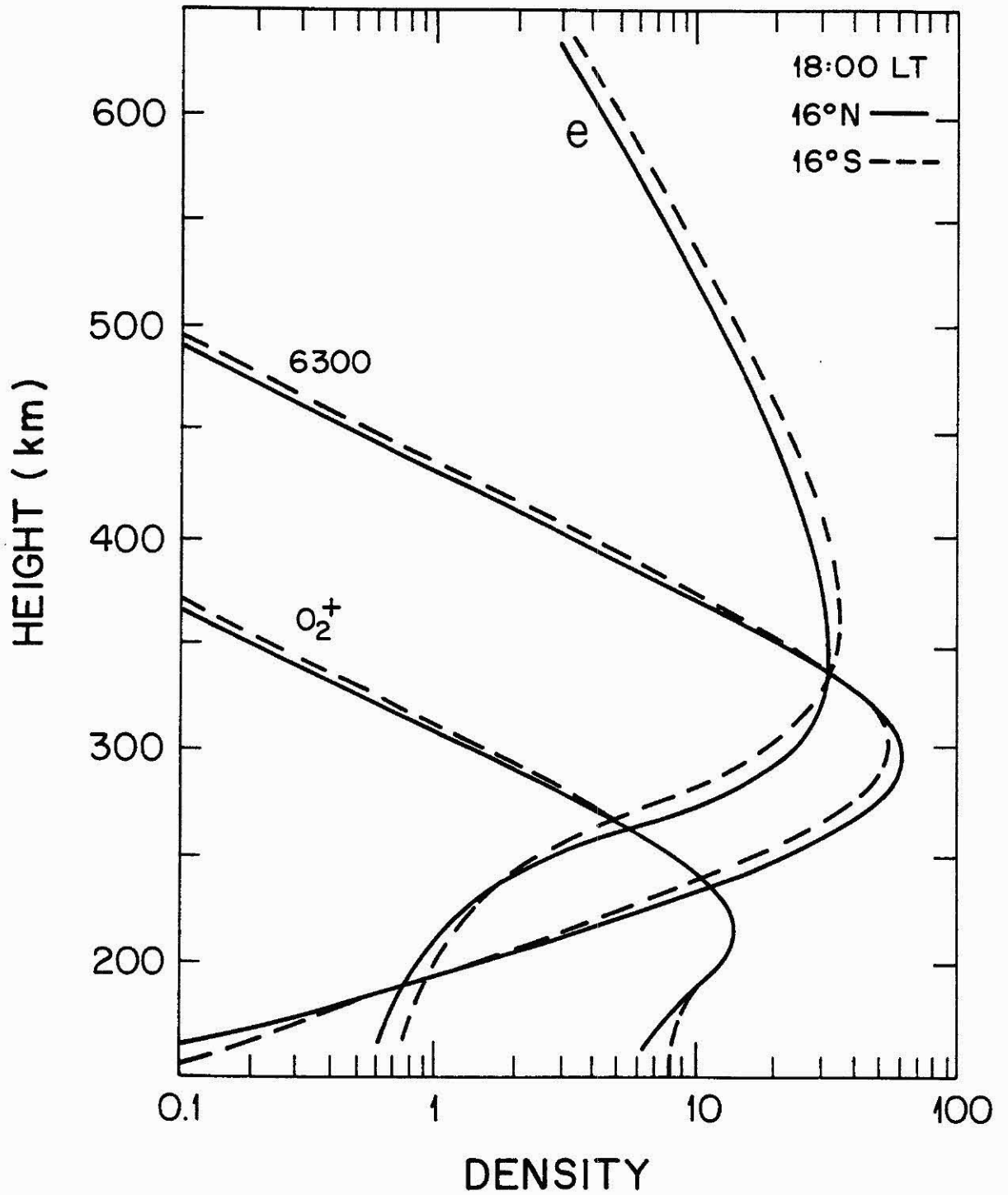


Figure 14. Vertical profiles of electron density (in 10^5 cm^{-3}), O_2^+ density (in 10^3 cm^{-3}) and OI 630 nm volume emission rate (in $\text{photons cm}^{-3} \text{ s}^{-1}$) in both hemispheres at the anomaly crests, for model M5, at 18:00 LT.

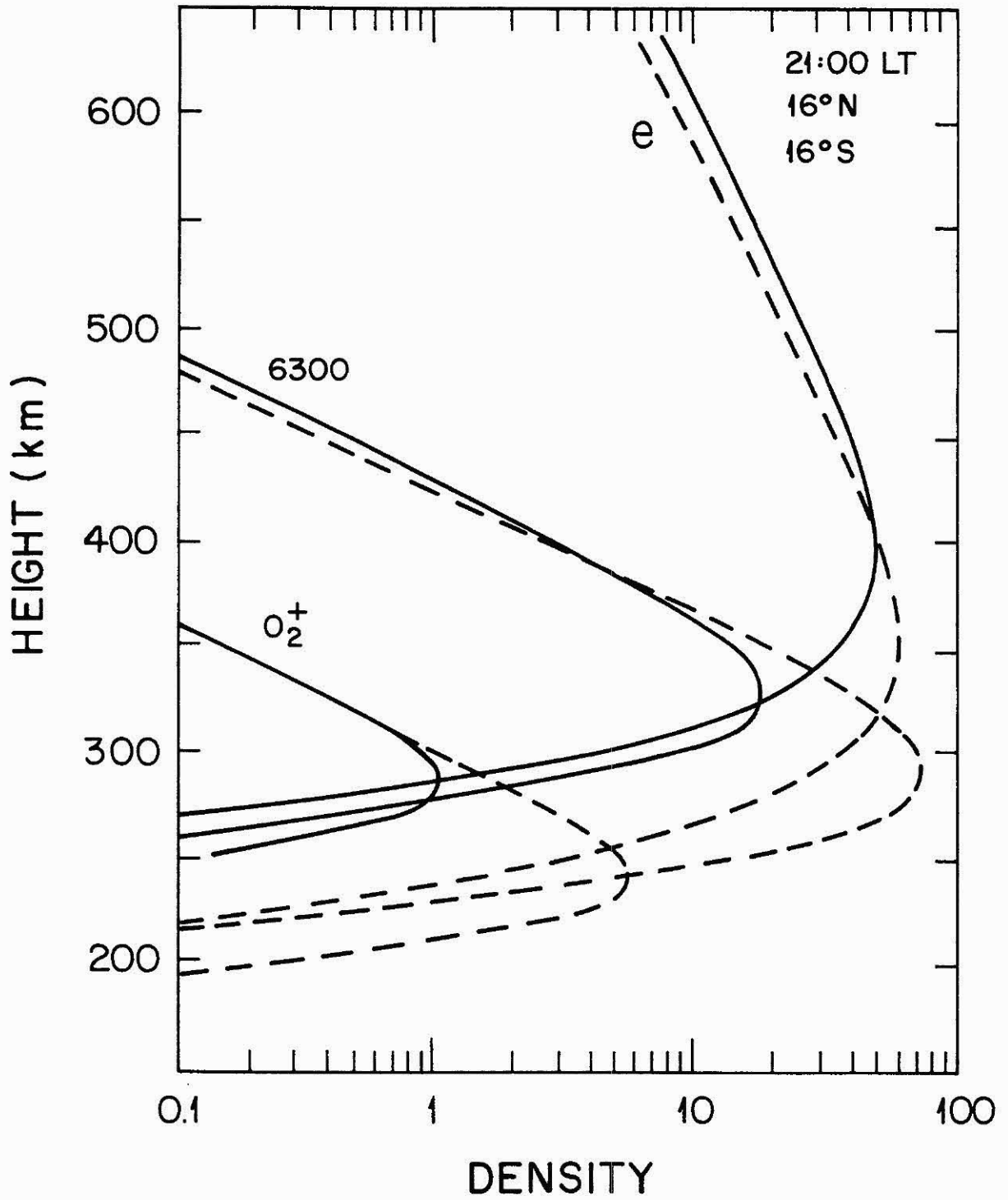


Figure 15. Same as in Figure 14, but at 21:00 LT.

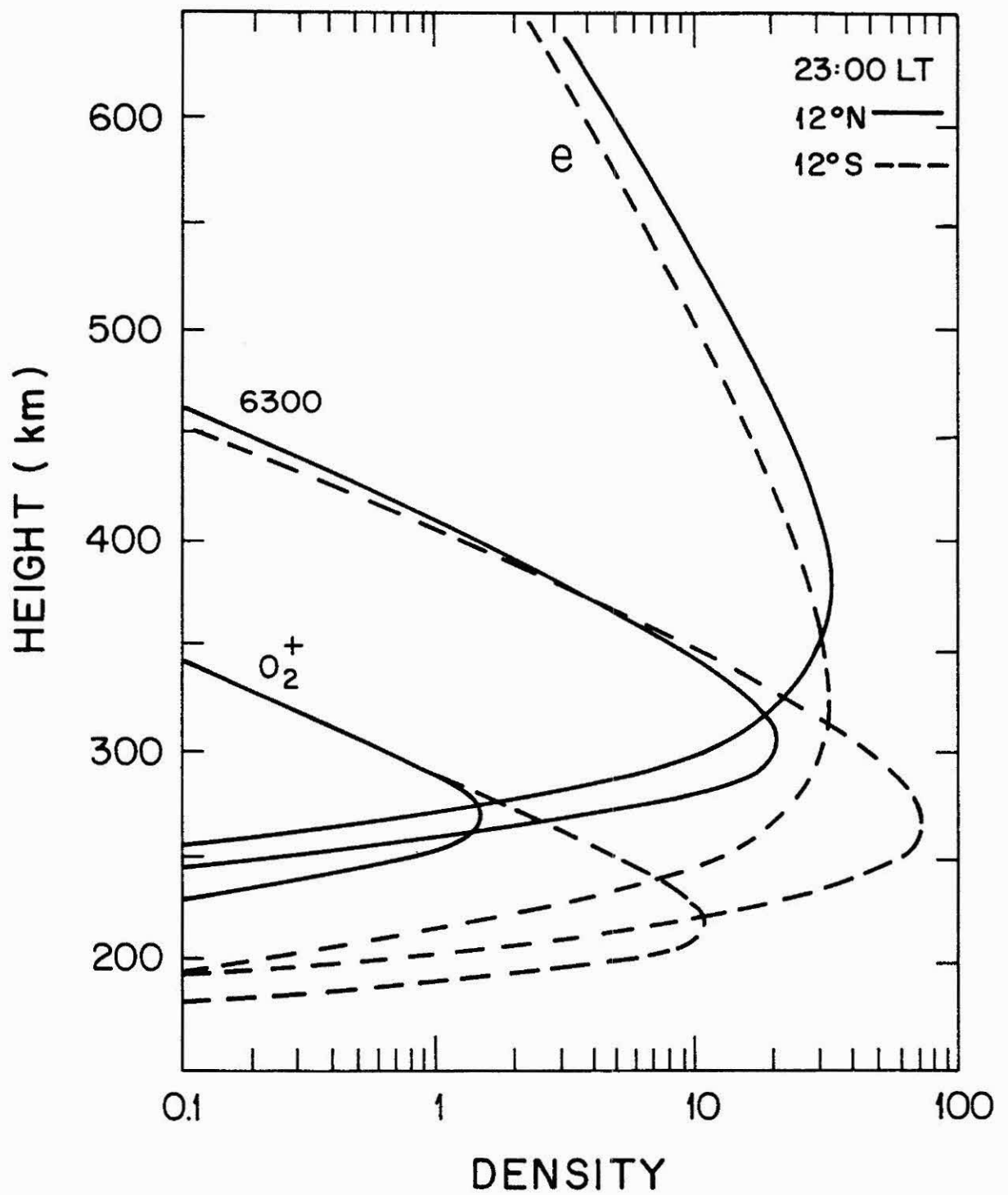


Figure 16. Same as in Figure 14, but at 23:00 LT.

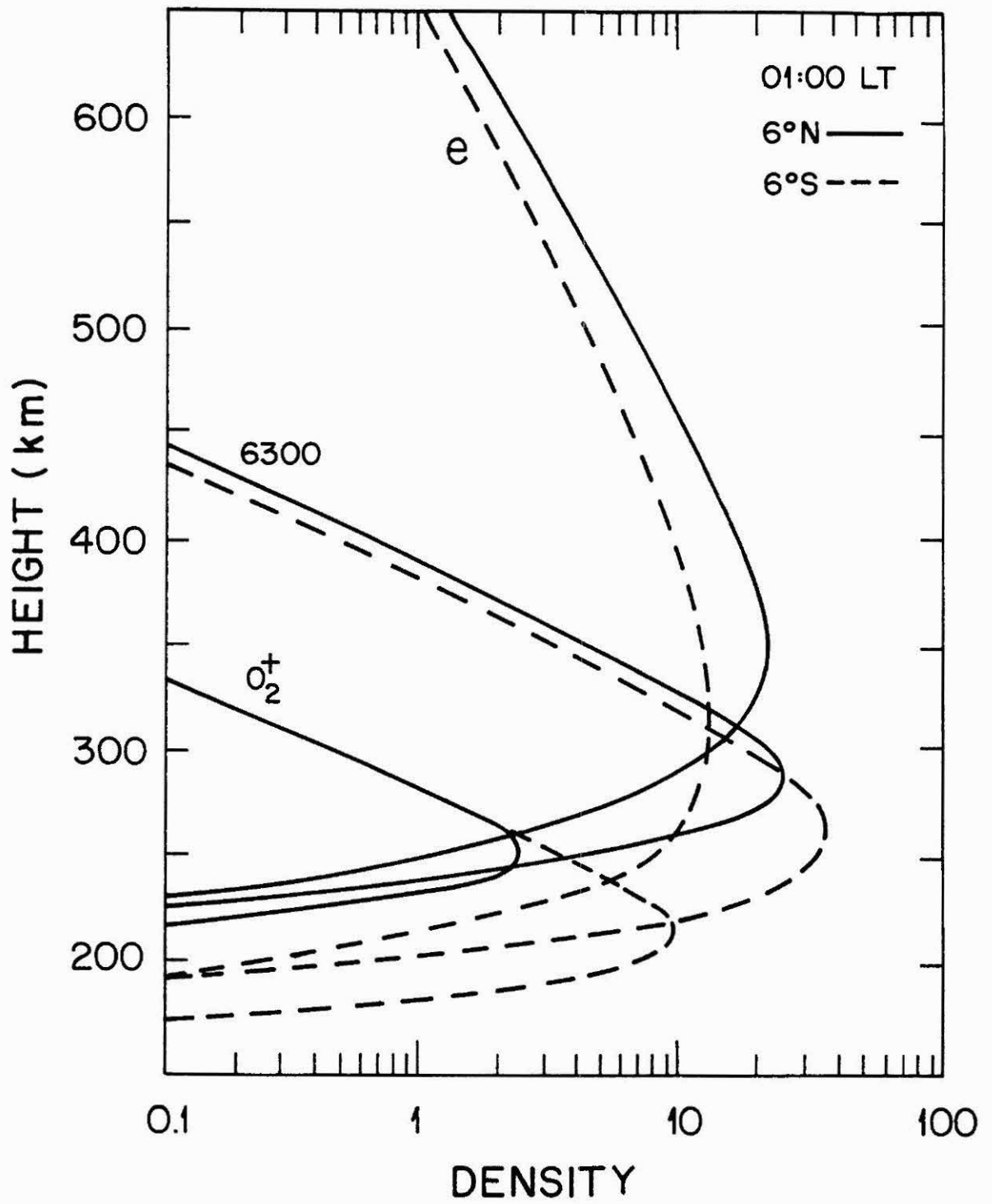


Figure 17. Same as in Figure 14, but at 01:00 LT.

REFERENCES

- ABBUR-ROBB, M.F.K.; WINDLE, D.W.. On the Day and Night Reversal in NmF2 North-South Asymmetry, *Planet. Space Sci.*, 17: 96-106, 1969.
- APPLETON, E.V.. Two Anomalies in the Ionosphere, *Nature*, 157: 691, 1946.
- ANDERSON, D.N.. A Theoretical Study of the Ionospheric F-Region Equatorial Anomaly. I. Theory, *Planet. Space Sci.*, 21: 409-419, 1973a.
- ANDERSON, D.N.. A Theoretical Study of the Ionospheric F-Region Equatorial Anomaly. II. Results in the American and Asian Sectors, *Planet. Space Sci.*, 21: 421-442, 1973b.
- ANDERSON, D.N.; MENDILLO, M.; HERNITER, B.. A Semiempirical Low-Latitude Ionospheric Model, *Radio Sci.*, 22: 292-306, 1987.
- ANDERSON, D.N.; FORBES, J.M.; CODRESCU, M.. A Fully Analytic Low and Middle Latitude Ionospheric Model, *J. Geophys. Res.*, 94(A2): 1520-1524, 1989.
- BAILEY, G.J.; SELLEK, R.. A Mathematical Model of the Earth's Plasmasphere and Its Application in a Study of He^+ at $L = 3.0$, *Ann. Geophys.*, 8: 171-190, 1990.
- BAILEY, G.J.; SELLEK, R.; RIPPETH, Y.. A Modelling Study of the Equatorial Topside Ionosphere, *Ann. Geophys.*, 11: 263-272, 1993.
- BANKS, P.A.; KOCKARTS, G.. *Aeronomy, Parts A and B*, Academic Press, New York, USA, 1973.
- BARTH, C.A.. Nitric Oxide in the Upper Atmosphere, *Ann. Geophys.*, 22: 198-207, 1966.
- BATES, D.R.. Charge Transfer and Ion-Atom Interchange Collisions, *Proc. Phys. Soc. London*, A68: 344-345, 1955.
- BATISTA, I.S.; DE PAULA, E.R.; ABDU, M.A.; TRIVEDI, N.B.; GREENSPAN, M.E.. Ionospheric Effects of the March 13, 1989, Magnetic Storm at Low and Equatorial Latitudes, *J. Geophys. Res.*, 96(A8): 13943-13952, 1991.

BATISTA, I.S.; ABDU, M.A.; MEDRANO, R.A.. Magnetic Activity Effects on Range Type Spread-F and Vertical Plasma Drifts at Fortaleza and Huancayo as Studied Through Ionosonde Measurements and Theoretical Modelling, *Ann. Geophys.*, 8: 357-364, 1990.

BATISTA, I.S.; ABDU, M.A.; BITTENCOURT, J.A.. Equatorial F-Region Vertical Plasma Drifts: Seasonal and Longitudinal Asymmetries in the American Sector, *J. Geophys. Res.*, 91: 12055-12064, 1986.

BAUER, S.J.. *Physics of Planetary Ionospheres*, Springer-Verlag, New York, USA, 1973.

BAXTER, R.G.. A Numerical Solution of the Time-Varying Diffusion Equation for the F2-Layer, *Planet. Space Sci.*, 15: 701-713, 1967.

BAXTER, R.G.. On the Theoretical Effects of Electrodynamical Drift in the Equatorial F2-Layer, *J. Atmos. Terr. Phys.*, 711-720, 1964.

BAXTER, R.G.; KENDALL, P.C.. A Theoretical Technique for Evaluating the Time Dependent Effects of General Electrodynamical Drifts in the F2 Layer of the Ionosphere, *Proc. Royal Soc.*, A304: 171-185, 1968.

BIONDI, M.A.. Atmospheric Electron-Ion and Ion-Ion Recombination Processes, *Can J. Chem.*, 47: 1711-1719, 1969.

BITTENCOURT, J.A.. *Fundamentals of Plasma Physics*, Pergamon Press, Oxford, UK, First Edition, 1986, Second Printing, 1988.

BITTENCOURT, J.A.; ABDU, M.A.. A Theoretical Comparison Between Apparent and Real Vertical Ionization Drift Velocities in the Equatorial F-region, *J. Geophys. Res.*, 86: 2451-2454, 1981.

BITTENCOURT, J.A.; SAHAI, Y.. F Region Neutral Winds from Ionosonde Measurements of hmF2 at Low Latitude Magnetic Conjugate Regions, *J. Atmos. Terr. Phys.*, 40: 669-676, 1978.

BITTENCOURT, J.A.; SAHAI, Y.; TEIXEIRA, N.R.; TAKAHASHI, H.. A Comparative Study of the Low-Latitude Ionospheric and OI 630 nm Nightglow Observations with the SLIM and IRI Models, *Adv. Space Res.*, 12(6): 275-278, 1992.

BITTENCOURT, J.A.; TINSLEY, B.A.. Tropical F Region Winds from OI 1356 A and OI 6300 A Emissions. 1. Theory, *J. Geophys. Res.*, 81(22): 3781-3785, 1976.

BITTENCOURT, J.A.; TINSLEY, B.A.; HICKS, G.T.; REED, E.I.. Tropical F Region Winds from OI 1356 A and OI 6300 A Emissions. 2. Analysis of OGO 4 Data, *J. Geophys. Res.*, 81(22): 3786-3790, 1976.

BLUM, P.W.; HARRIS, I.. The Global Wind System in the Thermosphere, *Space Research*, XIII: 369-375, 1973.

BRAMLEY, E.N.; PEART, M.. Diffusion and Electromagnetic Drift in the Equatorial F2 Region, *J. Atmos. Terr. Phys.*, 27: 1201-1211, 1965.

BRAMLEY, E.N.; YOUNG, M.. Winds and Electromagnetic Drifts in the Equatorial F2 Region, *J. Atmos. Terr. Phys.*, 30: 99-111, 1968.

CHALLINOR, R.A.. Neutral Air Winds in the Ionospheric F-Region for an Asymmetrical Global Pressure System, *Planet. Space Sci.*, 18: 1485-1487, 1970.

CHAPMAN, S; COWLING, T.G.. *The Mathematical Theory of Non-Uniform Gases*, Cambridge University Press, UK, 1939.

CHIU, Y.T.. An Improved Phenomenological Model of Ionospheric Density, *J. Atmos. Terr. Phys.*, 37: 1563-1570, 1975.

CRANK, J.; NICOLSON, P.. A Practical Method for Numerical Evaluation of Solutions of Partial Differential Equations of the Heat Conduction Type, *Cambridge Phil. Soc. Proc.*, 43: 50-67, 1947.

DALGARNO, A.. Ambipolar Diffusion in the F Region, *J. Atmos. Terr. Phys.*, 26: 939, 1964.

DALGARNO, A.. Charged Particles in the Upper Atmosphere, *Ann. Geophys.*, 17: 16-49, 1961.

DONAHUE, T.M.. Ionospheric Composition and Reactions, *Science*, 159: 489-498, 1968.

DUNKIN, D.B.; FEHSENFELD, F.C.; SCHMELTEKOPF, A.L.; FERGUSON, E.E.. Ion-Molecule Reaction Studies from 300 K to 600 K in a

Temperature-Controlled Flowing Afterglow System, *J. Chem. Phys.*, 49: 1365-1371, 1968.

DUNKIN, D.B.; MCFARLAND, M.; FEHSENFELD, F.C.; FERGUSON, E.E.. Rate Constants for the Reactions of O^+ with NO , N_2O and NO_2 , *J. Geophys. Res.*, 76: 3820-3821, 1971.

FARLEY, D.T.. A Theory of Electrostatic Fields in a Horizontally Stratified Ionosphere Subject to a Vertical Magnetic Field, *J. Geophys. Res.*, 64: 1225-1233, 1959.

FEHSENFELD, F.C.; DUNKIN, D.B.; FERGUSON, E.E.. Rate Constants for the Reaction of CO_2^+ with O , O_2 and NO ; N_2^+ with O and NO ; and O_2^+ with NO , *Planet. Space Sci.*, 18: 1267-1269, 1970.

FEJER, B.G.. Low-Latitude Electrodynamic Plasma Drifts: A Review, *J. Atmos. Terr. Phys.*, 53: 677-693, 1981.

FEJER, B.G.. The Equatorial Ionospheric Electric Fields: A Review, *J. Atmos. Terr. Phys.*, 43: 377-386, 1991.

FEJER, B.G.; DE PAULA, E.R.; GONZALEZ, S.A.; WOODMAN, R.F.. Average Vertical and Zonal F-Region Plasma Drifts Over Jicamarca, *J. Geophys. Res.*, 96: 13901-13906, 1991.

FEJER, B.G.; DE PAULA, E.R.; BATISTA, I.S.; BONELLI, E.; WOODMAN, R.F.. Equatorial F-Region Vertical Plasma Drifts During Solar Maxima, *J. Geophys. Res.*, 94: 12049-12054, 1989.

FEJER, B.G.; LARSEN, M.F.; FARLEY, D.T.. Equatorial Disturbance Dynamo Electric Fields, *Geophys. Res. Lett.*, 10: 537-540, 1983.

FEJER, B.G.; GONZALES, C.A.; FARLEY, D.T.; KELLEY, M.C.. Equatorial Electric Fields During Magnetically Disturbed Conditions. 1. The Effect of the Interplanetary Field, *J. Geophys. Res.*, 84: 5797-5802, 1979.

FERGUSON, E.E.. Laboratory Measurements of F Region Reaction Rates, *Ann. Geophys.*, 4: 819-823, 1969.

FERGUSON, E.E.. Ionospheric Ion-Molecule Reaction Rates, *Rev. Geophys.*, 5: 305-327, 1967.

- FERGUSON, E.E.; FEHSENFELD, F.C.; GOLDAN, P.D.; SCHMELTEKOPF, A.L.. Positive Ion-Neutral Reactions in the Ionosphere, *J. Geophys. Res.*, 70: 4323-4329, 1965.
- FULLER-ROWELL, T.J.; REES, D.; QUEGAN S.; MOFFETT, R.J.; BAILEY, G.T.. Interactions Between Neutral Thermospheric Composition and the Polar Ionosphere Using a Coupled Ionosphere-Thermosphere Model, *J. Geophys. Res.*, 92: 7744-7748, 1987.
- FULLER-ROWELL, T.J.; REES, D.. A Three-Dimensional Time-Dependent Global Model of The Thermosphere, *J. Atmos. Sci.*, 37: 2545-2567, 1980.
- GIRARD, A.; PETIT, M.. *Physics of the Earth's Ionosphere*, D. Reidel Pub. Comp., New York, USA, 1976.
- GOLDAN, P.D.; SCHMELTEKOPF, A.L.; FEHSENFELD, F.C.; SCHIFF, H.I.; FERGUSON, E.E.. Thermal-Energy Ion-Neutral Reaction Rates. 2. Some Reactions of Ionospheric Interest, *J. Chem. Phys.*, 44: 4095-4103, 1966.
- HANSON, W.B.; MOFFETT, R.J.. Ionization Transport Effects in the Equatorial F Region, *J. Geophys. Res.*, 71: 5559-5572, 1966.
- HARGREAVES, J.K.. *The Solar Terrestrial Environment*, Cambridge University Press, UK, 1992.
- HEDIN, A.E.. MSIS-86 Thermospheric Model, *J. Geophys. Res.*, 92: 4649-4662, 1987.
- HEDIN, A.E.; BIONDI, M.A.; BURNSIDE, R.G.; HERNANDEZ, G.; JOHNSON, R.M.; KILLEEN, T.L.; MAZAUDIER, C.; MERIWETHER, J.W.; SALAH, J.E.; SICA, R.J.; SMITH, R.W.; SPENCER, N.W.; WICKWAR, V.B.; VIRDI, T.S.. Revised Global Model of Thermosphere Winds Using Satellite and Ground-Based Observations, *J. Geophys. Res.*, 96: 7657-7688, 1991.
- HEDIN, A.E.; SPENCER, N.W.; KILLEEN, T.L.. Empirical Global Model of Upper Thermosphere Winds Based on Atmosphere and Dynamics Explorer Satellite Data, *J. Geophys. Res.*, 93: 9959-9978, 1988.

HEELIS, R.A.; KENDALL, P.C.; MOFFETT, R.J.; WINDLE, D.W.; RISHBETH, H.. Electrical Coupling of the E and F Regions and Its Effects on F Region Drifts and Winds, *Planet. Space Sci.*, 22(5): 743-756, 1974.

HINTEREGGER, H.E.. The Extreme Ultraviolet Solar Spectrum and Its Variation During a Solar Cycle, *Ann. Geophys.*, 26: 547-554, 1970.

HINTEREGGER, H.E.; HALL, L.A.; SCHMIDTKE, G.. Solar XUV Radiation and Neutral Particle Distribution in the July 1963 Thermosphere, *Space Res.*, V: 1175-1190, 1965.

JACCHIA, L.G.. Thermospheric Temperature, Density and Composition: New Models, *Smiths. Astrophys. Obs. Spec. Rep.*, 375, 1977.

JACCHIA, L.G.. Revised Static Models of the Thermosphere and Exosphere with Empirical Temperature Profiles, *Smiths. Astrophys. Obs. Spec. Rep.*, 332, 1971.

JACCHIA, L.G.. Static Diffusion Models of the Upper Atmosphere with Empirical Temperature Profiles, *Smiths. Contrib. Astrophys.* 8: 215-222, 1965.

KASNER, W.H.; BIONDI, M.A.. Electron-Ion Recombination in Nitrogen, *Phys. Rev.*, 137A: 317-329, 1965.

KELLEY, M.C.. *The Earth's Ionosphere - Plasma Physics and Electrodynamics*, Academic Press, San Diego, USA, 1989.

KENDALL, P.C.. Geomagnetic Control of Diffusion in the F2 Region of the Ionosphere. I. The Form of the Diffusion Operator, *J. Atmos. Terr. Phys.*, 24: 805-811, 1962.

KENESHEA, T.J.; NARCISI, R.S.; SWIDER, W., JR.. Diurnal Model of the E-Region, *J. Geophys. Res.*, 75: 845-854, 1970.

KOHL, H.; KING, J.W.. Atmospheric Winds Between 100 and 700 km and Their Effects on the Ionosphere, *J. Atmos. Terr. Phys.*, 29: 1045-1062, 1967.

- LYON, A.J.; THOMAS, L.. The F2 Region Equatorial Anomaly in the African, American and East Asian Sectors During Sunspot Maximum, *J. Atmos. Terr. Phys.*, 25: 373-386, 1963.
- MACNAMARA, L.F.. *Ionosphere: Communications, Surveillance and Direction Finding*, Krieger Pub. Comp., Florida, USA, 1991.
- MARTYN, D.F.. Electric Currents in the Ionosphere. III. Ionization Drift Due to Winds and Electric Fields, *Phil. Trans. Royal Soc.*, A246: 306-320, 1953.
- MOFFETT, R.J.; HANSON, W.B.. Effect of Ionization Transport on the Equatorial F Region, *Nature*, 206: 705-706, 1965.
- NORTON, R.B.. The Ionized Constituents in the 100-300 km Region of the Earth's Upper Atmosphere, *Inst. Envir. Res. Tech. Mem. - ITSA 60*, US Dept. Commerce, 1967.
- POTTER, D.. *Computational Physics*, John Wiley & Sons, Chinchester, UK, 1973, Reprinted 1980.
- RAO, C.S.R.. Study of the Geomagnetic Anomaly During Sunspot Maximum, *J. Atmos. Terr. Phys.*, 24: 729-737, 1962.
- RASTOGI, R.G.. The Equatorial Anomaly in the F2 Region of the Ionosphere, *J. Inst. Telecom. Engrs.*, 12: 245-256, 1966.
- RATCLIFFE, J.A.. *An Introduction to the Ionosphere and Magnetosphere*, Cambridge at the University Press, UK, 1972.
- RISHBETH, H.. Polarization Fields Produced by Winds in the Equatorial F-Region, *Planet. Space Sci.*, 19(3): 357-369, 1971.
- RISHBETH, H.. Thermospheric Winds and the F-Region: A Review, *J. Atmos. Terr. Phys.*, 34:, 1-47, 1972.
- RISHBETH, H.. Dynamics of the Equatorial F-Region, *J. Atmos. Terr. Phys.*, 39(9/10): 1159-1168, 1977.
- RISHBETH, H.. The F-Region Dynamo, *J. Atmos. Terr. Phys.*, 43(5/6): 387-391, 1981.

- RISHBEHT, H.; GARRIOT, O.K.. *Introduction to Ionospheric Physics*, Academic Press, New York, USA, 1969.
- RUSH, C.M.; RUSH, S.V.; LYONS, L.R.; VENKATESWARAN, S.V.. Equatorial Anomaly During a Period of Declining Solar Activity, *Radio Sci.*, 4: 829-841, 1969.
- STERLING, D.L.; HANSON, W.B.; WOODMAN, R.F.. Synthesis of Data Obtained at Jicamarca, Peru, During the September 11, 1969, Eclipse, *Radio Sci.*, 7: 279-289, 1972.
- STERLING, D.L.; HANSON, W.B.; MOFFETT, R.J.; BAXTER, R.G.. Influence of Electromagnetic Drifts and Neutral Air Winds on Some Features of the F2 Region, *Radio Sci.*, 4: 1005-1023, 1969.
- THOMAS, L.. The F2 Region Equatorial Anomaly During Solstice Periods at Sunspot Maximum, *J. Atmos. Terr. Phys.*, 30: 1631-1640, 1968.
- TINSLEY, B.A.; CHRISTENSEN A.B.; BITTENCOURT, J.A.; GOUVEIA, H.; ANGREJI, P.D.; TAKAHASHI, H.. Excitation of Oxygen Permitted Line Emissions in the Tropical Nightglow, *J. Geophys. Res.*, 78: 1174-1186, 1973.
- TOBISKA, W.K.. Revised Solar Extreme Ultraviolet Flux Model, *J. Atmos. Terr. Phys.*, 53: 1005-1018, 1991.
- TOBISKA, W.K.; BARTH, C.A.. A Solar EUV Flux Model, *J. Geophys. Res.*, 95(A6): 8243-8251, 1990.
- WALKER, J.C.G.. Analytic Representation of Upper Atmosphere Densities Based on Jacchia's Static Diffusion Models, *J. Atmos. Sci.*, 22: 462-463, 1965.
- WHITTEN, R.C.; POPPOFF, I.G.. *Fundamentals of Aeronomy*, John Wiley & Sons Inc., New York, USA, 1971.
- WOODMAN, R.F.. East-West Ionospheric Drifts at the Magnetic Equator, *Space Research*, XII: 969-974, 1972.
- WOODMAN, R.F.. Vertical Drift Velocities and East-West Electric Fields at the Magnetic Equator, *J. Geophys. Res.*, 75: 6249-6259, 1970.

APPENDIX

Listing of the
Low-Latitude Ionospheric Computer Program
Written in Fortran 77.

```

$SET OWN
$RESET FREE
FILE 1(KIND=DISK,TITLE="IONDATA2",FILETYPE=7)
FILE 9(KIND=REMOTE)
FILE 3(KIND=PRINTER)
C.....
C JOSE AUGUSTO BITTENCOURT
C INSTITUTO NACIONAL DE PESQUISAS ESPACIAIS - INPE / SCT
C DIVISAO DE AERONOMIA
C.....
C                               MAIN PROGRAM
C
C DYNAMIC BEHAVIOR OF LOW-LATITUDE IONOSPHERIC PLASMA
C CONSIDERING SOLAR PHOTOIONIZATION, ION CHEMISTRY, PLASMA
C DIFFUSION, ELECTROMAGNETIC E X B PLASMA DRIFT AND NEUTRAL
C WIND DRAG, IN A CENTERED, TILTED, DIPOLE MAGNETIC FIELD.
C MULTIPLE ION SPECIES: O+, NO+, O2+, N2+, N+.
C PRINTOUT: VELOCITIES AND DENSITIES FOR EACH SPECIES
C ALONG MAGNETIC FIELD TUBE (100 POINTS) AT EACH TIME STEP.
C.....
      REAL*4 NZAO,NZOO,NZON2,NZOO2,LAMBDA,N(100,10,2),
      1LONG,LNG,LOSS
      REAL*4 NT(100),INTLNG,LNGOBS,LATOBS
      REAL KB,NZO,NZN2,NZO2,LSC
      DIMENSION Y(10),YP(20,6)
      INTEGER*4 IPF,NLH,MOLE,ISYM
      DIMENSION V(100,10,2),G(100,10,2)
      COMMON /PLOT/ IPF,HEAD(40,20),NLH,MOLE(10),ISYM(10)
      COMMON NSET,M,M2,CS(7),DUM1,DUM2,      T0,T120,NZAO
      COMMON CRSCN2,AUO,B0EQ,NZOO,NZOO2,NZON2,DUM3, CK(2),CTH1,
      1DUM4,DUM5
      COMMON CTH4,CTE(2),CDO,DUM6,CRSCO,CRSCPH,DELTA,TILT
      COMMON UPHASE,CUPHI,PHIU,DUM9,DUM10,OFFSET,DELPH,
      1PHFNAL,DPHOUT
      COMMON ZEINIT,PHINIT,DELPHO,LAMBDA,RBASE,RD,
      1DUM11,SPHASE,DUM12
      COMMON SCLN,DB0,ddb
      COMMON R0,DELY,WTH0,WPERPO,OMEGA,B0,DWDRE,DWDPH,TIME
      COMMON INTLNG,DELNG,LNGOBS,UT,LONG,LATOBS,QRA,OMEGA0
      COMMON/SO/ SOL(15,100),SOLE(15,100)
      COMMON /COEFF/X(700)
      COMMON/OPR/IREP,IPUNCH
      COMMON /MOL/ NOMOL,MOL(10,2)
      COMMON/ILOVE/NOOKY,INBED
      COMMON/BETAC/BETAC,ALPHC
      COMMON /NDATA/ N
      COMMON/SUMMO/SUMX(8,100)
C
C INITIALIZATION OF SOME CONSTANTS AND VARIABLES (CGS UNITS)
C IARRAY IS NUMBER OF POINTS ALONG MAGNETIC FIELD LINE
C R0 IS EARTH'S RADIUS (IN CM)
C OMEGA IS EARTH'S ANGULAR VELOCITY OF ROTATION (IN RAD/S)
      IARRAY=100
      1 CONTINUE
      IPF = 0
      ZERO=0.
      ONE=1.
      TWO=2.
      FOUR=4.
      RNDOFF=0.5
      R0=6370.E5
      R200=R0+200.E5

```



```

KB=1.38054E-16
PI=3.1415926535
PI2=PI/2.
RAD=PI/180.
DELPHX=RAD
DEGS=ONE/RAD
CM5=1.E5
CM2=100.
PERIOD=24.*3600.
OMEGA=TWO*PI/PERIOD
OMEGA0=OMEGA
DELRE=5.E5
WPERP0=ZERO
WTH0=ZERO
DWDRE=ZERO
DWDPH=0.
UT=0.
LONG=0.
QRA=1.
BETAC=1.
ALPHC=1.
NOOKY=1

C
C SET UP PARAMETERS FOR CHAPMAN FUNCTION IN A SPHERICALLY
C STRATIFIED ATMOSPHERE FOR PHOTOIONIZATION CALCULATIONS
C (GEOMETRICAL FACTOR)
C   CACA=CH0 (ZERO)

C
C READ IN SOLAR FLUXES AND CROSS SECTIONS (ABSORPTION AND
C IONIZATION),
C FOR ATMOSPHERIC SPECIES; PREPARE VARIABLES FOR SUB PHOTO,
C WHICH CALCULATES SOLAR PHOTOIONIZATION RATES.
C   CALL PHOTO0

C
C INITIALIZE PARAMETERS FOR ECLIPSE CALCULATIONS, IF ANY.
C NOECLP = 1 (READ IN READEC) FOR NO ECLIPSE CALCULATIONS.
C LATOBS IS MAGNETIC LATITUDE OF OBSERVATIONS
C   CALL READEC (INTLNG, DELNG, LNGOBS, LATOBS, NCLP, FSC, LSC)
C   NOECLP=NCLP

C
C SET UP STORAGE ARRAYS SOL AND SOLE, 15 VARIABLES EACH, FOR
C IARRAY ( = 100) POINTS ALONG FIELD LINE.
C   DO 5 J=1, IARRAY
C   DO 5 I=1, 15
C   SOL(I, J)=0.
C   5 SOLE(I, J)=0.

C
C INITIALIZE DENSITIES AND VELOCITIES
C   DO 7 K=1, 2
C   DO 7 J=1, 10
C   DO 7 I=1, IARRAY
C   N(I, J, K)=1.E-5
C   7 V(I, J, K)=1.E-5

C
C READ INPUT PARAMETERS
C   RE=R0
C   PHI=0.
C   6 CALL INPUT(S0, RE, PHI, G, N, V, NCLP)

C
C   ITWOM=2*M
C   RDDIS=RD+10.E5
C   CALL COEF00

```

```

S=S0
CALL ECLPSE(TIME, LNGOBS, PHI, UT, LONG, SINX, COSX,
1PHIM, THT, NENTRY)
NOECLP=NCLP
L=0
LUST=0
CALL RKAM(PHI, TIME, RE, DELPH/NOOKY, 2, LUST)
LFINIS= ABS((PHFNAL-PHI )/DELPH)+.5
SINPH = SIN(PHI)
COSPH = COS(PHI)
CALL COEF0 (RE, PHI, COSPH, SINPH )
CALL COEF2 (RE, PHI, 16., 2.)
LPHOUT=DPHOUT/DELPH + .5
GO TO 26
10 IF(L.GE.LFINIS)GOTO 6
C
C SET UP OLD PROFILES
DO 8 K=1, NOECLP
CALL CONTOG(G, N, 1, K)
IF(NOMOL.EQ.1)GO TO 8
DO 8 J=2, NOMOL
DO 8 I=1, M2
G(I, J, K)=N(I, J, K)
8 CONTINUE
C
L=L+1
DO 11 I=1, NOOKY
LUST=LUST+1
CALL RKAM(PHI, TIME, RE, DELPH/NOOKY, 2, LUST)
11 PHI=PHI+DELPH/NOOKY
IF(RE.LT.RDDIS)GOTO 13
SINPH=SIN(PHI)
COSPH=COS(PHI)
CALL ECLPSE(TIME, LNGOBS, PHI, UT, LONG, SINX, COSX,
1PHIM, THT, NENTRY)
NOECLP=NCLP
CALL COEF0 (RE, PHI, COSPH, SINPH)
CALL COEF2 (RE, PHI, 16., 2.)
CALL GCALC(RE, PHI, DELPH, COSPH, SINPH, LNGOBS, DELY,
1G, N, V, NOECLP)
LOUT=LOUT+1
IF(LOUT.GT.LPHOUT)GO TO 26
GO TO 10
13 PHIX=PHI/RAD
ZE=(RE-R0)/1.E5.
WRITE(3, 130) ZE, PHIX
130 FORMAT(' ZE=', F11.3, ' PHIX=', F11.3)
LOUT=LOUT+1
IF(LOUT.GT.LPHOUT)LOUT=1
IF(L.GE.LFINIS)GOTO 6
L=L+1
DO 14 I=1, NOOKY
LUST=LUST+1
CALL RKAM(PHI, TIME, RE, DELPH/NOOKY, 2, LUST)
14 PHI=PHI+DELPH/NOOKY
IF(RE.LT.RDDIS)GOTO 13
LOUT=LOUT+1
IF(LOUT.GT.LPHOUT)LOUT=1
GO TO 10
C
C OUTPUT.....
26 PH=PHI/RAD

```

```

I=UT/3600.
UTIME=(UT+2400.*I)/60.
TIEMPO=TIME/3600.
LNG=LONG/RAD
ZE =(RE-R0)/CM5
IX=NOMOL
IF(IPUNCH.EQ.0)GOTO 32
C WRITE(2,992)ZE,PH
K=0
KK=1
L1=M2/16
L2=L1*16-M2
IF(L2.LT.0)L2=L2+16
L3=(M2+L2 )*IX
27 DO 30 I=1,IX
DO 28 J=1,M2
K=K+1
X(K)=ALOG10(N(J,I,KK))
28 IF(X(K).LT.0.)X(K)=0.
IF(L2.EQ.0)GOTO 30
DO 29 J=1,L2
K=K+1
29 X(K)=0.
30 CONTINUE
C WRITE(2,993)( X(J),J=1,L3)
IF(NOECLP.EQ.1)GOTO 32
KK=KK+1
IF(KK.GT.2)GOTO 32
K=0
GOTO 27
32 LOUT=1
DO 33 I=1,M2
X(I)=(SOL(1,I)-R0)/1.E5
X(100+I) = (PI2-SOL(4,I))/RAD
X(300+I) = SOLE(2,I)/KB
33 X(400+I) = SOLE(3,I)/KB
C
C WRITE STATEMENTS (IF NEEDED)
C WRITE(2,2003)ZE,PH
2003 FORMAT(1X,F8.3,F9.3)
C
WRITE(3,1003)ZE,PH
DO 57 KK=1,NOECLP
CALL COCONT(CNO,PRD,LOSS,N,1,KK)
RX= (RE/R200)**3/(RE*R0)
CNO=CNO*RX
PRD=PRD*RX
LOSS=LOSS*RX
DO 133 I=1,M2
X(200+I) = 1.0
133 IF(KK.EQ.2.AND.PHI.NE.PHINIT) X(200+I) = SOLE(9,I)
134 CONTINUE
C
C NORTHERN HEMISPHERE OUTPUT
WRITE(3,1009)
WRITE(3,1006)
WRITE(3,1007)
DO 145 I=1,IX
II=MOL(I,2)
GO TO (140,141,142,143,144,1441,1442,1443,1444,1445),II
140 WRITE(3,1108)
GOTO 145

```

```

141 WRITE(3,1109)
   GOTO 145
142 WRITE(3,1110)
   GOTO 145
143 WRITE(3,1111)
   GOTO 145
144 WRITE(3,1112)
   GO TO 145
1441 CONTINUE
   WRITE (3,1113)
   GO TO 145
1442 CONTINUE
   WRITE (3,1114)
   GO TO 145
1443 CONTINUE
   WRITE (3,1115)
   GO TO 145
1444 CONTINUE
1445 CONTINUE
   WRITE(3,1114) II
145 CONTINUE
   DO 35 I=1,M,6
   NL=I
   NU=NL+5
   IF(NU.GT.M)GOTO 36
   DO 34 J=NL,NU
   NT(J)=0.
   DO 34 K=1,IX
34 NT(J)=N(J,K,KK)+NT(J)
C
C WRITE STATEMENTS (IF NEEDED)
C   WRITE(2,2005) (X(J),X(100+J),J=NL,NU)
C   WRITE(2,2004) (NT(J),J=NL,NU),
C   1(N(J,1,KK),J=NL,NU),(N(J,3,KK),J=NL,NU)
2005 FORMAT(1X,6(F7.2,F6.2))
2004 FORMAT(1X,9(6(1PE10.3,1X)/1X))
C
   WRITE(3,1005) (X(200+J),X(J),X(100+J),J=NL,NU)
35 WRITE(3,1004) (SOLE(7,J),NT(J),J=NL,NU),
1 ((V(J,K,KK),N(J,K,KK),J=NL,NU),K=1,IX)
   IF(M.EQ.M2)GO TO 57
   GOTO 39
36 NU=M
   DO 37 J=NL,NU
   NT(J)=0.
   DO 37 K=1,IX
37 NT(J)=N(J,K,KK)+NT(J)
C
C WRITE STATEMENTS (IF NEEDED)
C   WRITE(2,2005) (X(J),X(100+J),J=NL,NU)
C   WRITE(2,2004) (NT(J),J=NL,NU)
C
   WRITE(3,1005) (X(200+J),X(J),X(100+J),J=NL,NU)
   WRITE(3,1004) (SOLE(7,J),NT(J),J=NL,NU)
   DO 38 K=1,IX
C
C WRITE STATEMENTS (IF NEEDED)
   IF(K.EQ.2) GO TO 2000
   IF(K.GT.3) GO TO 2000
C   WRITE(2,2004) (N(J,K,KK),J=NL,NU)
2000 CONTINUE
C

```

```

38 WRITE(3,1004) (V(J,K,KK),N(J,K,KK),J=NL,NU)
   IF(M.EQ.M2)GO TO 57
C
C SOUTHERN HEMISPHERE OUTPUT
39 WRITE(3,1010)
   WRITE(3,1006)
   WRITE(3,1007)
   DO 45 I=1,IX
   II=MOL(I,2)
   GO TO (40,41,42,43,44,1045,1046,1047,1048,1049),II
40 WRITE(3,1108)
   GOTO 45
41 WRITE(3,1109)
   GOTO 45
42 WRITE(3,1110)
   GOTO 45
43 WRITE(3,1111)
   GOTO 45
44 WRITE(3,1112)
   GOTO 45
1045 CONTINUE
   WRITE (3,1113)
   GO TO 45
1046 CONTINUE
   WRITE (3,1114)
   GO TO 45
1047 CONTINUE
   WRITE (3,1115)
   GO TO 45
1048 CONTINUE
1049 CONTINUE
   WRITE(3,1114) II
45 CONTINUE
   DO 53 I=1,M,6
   NL=I
   NU=NL+5
   IF(NU.GT.M)GOTO 54
   DO 51 J=NL,NU
   NT(J)=0.
   DO 51 K=1,IX
51 NT(J)=N( ITWOM-J,K,KK)+NT(J)
C
C WRITE STATEMENTS (IF NEEDED)
C   WRITE(2,2005) (X(ITWOM-J),X(100+ITWOM-J),J=NL,NU)
C   WRITE(2,2004) (NT(J),J=NL,NU),
C   1(N(ITWOM-J,1,KK),J=NL,NU), (N(ITWOM-J,3,KK),J=NL,NU)
C
   WRITE (3,1005) (X(200+ITWOM-J), X(ITWOM-J), X(100+ITWOM-J),
1J=NL,NU)
53 WRITE(3,1004) (SOLE(7,ITWOM-J),NT(J),J=NL,NU),
1((V(ITWOM-J,K,KK),N(ITWOM-J,K,KK),J=NL,NU),K=1,IX)
   GOTO 57
54 NU=M
   DO 55 J=NL,NU
   NT(J)=0.
   DO 55 K=1,IX
55 NT(J)=N( ITWOM-J,K,KK)+NT(J)
C
C WRITE STATEMENTS (IF NEEDED)
C   WRITE(2,2005) (X(ITWOM-J),X(100+ITWOM-J),J=NL,NU)
C   WRITE(2,2004) (NT(J),J=NL,NU)
C

```

```

WRITE(3,1005) (X(200+ITWOM-J),X(ITWOM-J),X(100+ITWOM-J),
1J=NL,NU)
WRITE(3,1004) (SOLE(7,ITWOM-J),NT(J),J=NL,NU)
DO 56 K=1,IX
C
C WRITE STATEMENTS (IF NEEDED)
IF(K.EQ.2) GO TO 3000
IF(K.GT.3) GO TO 3000
C WRITE(2,2004) (N(ITWOM-J,K,KK),J=NL,NU)
3000 CONTINUE
C
56 WRITE(3,1004) (V(ITWOM-J,K,KK),N(ITWOM-J,K,KK),J=NL,NU)
57 CONTINUE
6969 CONTINUE
1015 FORMAT(' ',10(1PE12.3))
IFORT=2
IF(IFORT.EQ.1)GOTO 666
GOTO 10
666 CONTINUE
992 FORMAT(' ZE=',F11.3,' PH=',F11.3)
993 FORMAT(16F5.3)
998 FORMAT(' N=',I5,' NO. OF COUNTS OF DELG')
999 FORMAT(6I5)
1003 FORMAT(' ', ' ZE =',F8.3,' PHI=',F9.3)
1004 FORMAT(' ',9(6(-2PF7.2,1PE10.3,5X)/1X)/)
1005 FORMAT(' ',6(F7.2,0PF7.2,F7.2,1X))
1006 FORMAT('0 ECL Z LAT ECL Z LAT ECL
1 Z
1 LAT ECL Z LAT ECL Z LAT ECL
1 Z
2 LAT')
1007 FORMAT('0 WIND NE WIND NE WIND
1 NE
1 WIND NE WIND NE WIND
1 NE
2 ')
1108 FORMAT(' VO O+ VO O+ VO
1 O+
1 VO O+ VO O+ VO
1 O+
2 ')
1109 FORMAT(' VNO NO+ VNO NO+ VNO
1 NO+
4 VNO NO+ VNO NO+ VNO
1 NO+
5 ')
1110 FORMAT(' VO2 O2+ VO2 O2+ VO2
1 O2+
7 VO2 O2+ VO2 O2+ VO2
1 O2+
8 ')
1111 FORMAT(' VN2 N2+ VN2 N2+ VN2
1 N2+
A VN2 N2+ VN2 N2+ VN2
1 N2+
B ')
1112 FORMAT(' VN N+ VN N+ VN
1 N+
G VN N+ VN N+ VN
1 N+
H ')
1113 FORMAT(' VO O++ VO O++ VO

```

```

1 O++
J VO O++ VO O++ VO
1 O++
K ')
1114 FORMAT(' VO+ O+2D VO+ O+2D VO+
1 O+2D
M VO+ O+2D VO+ O+2D VO+
1 O+2D
N ')
1115 FORMAT(' VH H+ VH H+ VH
1 H+
P VH H+ VH H+ VH
1 H+
Q ')
1009 FORMAT('O',T30,'NORTHERN HEMISPHERE')
1010 FORMAT('O',T30,'SOUTHERN HEMISPHERE')
1011 FORMAT(' HGT=',F8.3,' PHI=',F8.2,' N(PHI)=',1PE11.3)
1013 FORMAT(21F6.0)
STOP
END

```

C

C.....
SUBROUTINE INPUT(S,RE,PHI,G,N,V,NOECLP)

C.....
\$SET OWN

```

IMPLICIT REAL*4 (A-Z)
INTEGER NOX
INTEGER NENTRY
INTEGER WNDMDL,DRFMDL,QTMDL,ATMS71
INTEGER NN,IX,II,JJ,I,J,K,NSET,M,M2,JJW,KOX
INTEGER NOOKY,NOECLP,NL,NU,ITWOM,INBED,MOL,NOMOL,PUNCH,REP
INTEGER*4 IBUF(16000),NLOC
INTEGER*4 IPF,NLH,MOLE,ISYM,IPF1
DIMENSION VVW(50),PHW(50),NEQ(50)
DIMENSION VV(100),PH(100),TE(100),NE(100)
DIMENSION N(100,10,2),G(100,10,2),CC(54),V(100,10,2),
1REQ(50)
COMMON /PLOT / IPF,HEAD(40,20),NLH,MOLE(10),ISYM(10),
1NLOC,IBUF
COMMON NSET,M,M2 ,CS(7),DUM2,DUM3,T0,T120,NZAO
COMMON CRSCN2,AUO ,BOEQ,NZ00,NZ002,NZ0N2,DUM6,
1CK(2),CTH1,A1,A2
COMMON CTH4,CTE(2),CDO,DUM7,CRSCO,CRSCPH,DELTA,TILT
COMMON UPHASE,CUPHI,PHIU,DUM9,DUM10,OFFSET,
1DELPH,PHFNAL,DPHOUT
COMMON ZEINIT,PHINIT,DELPHO,LAMBDA,RBASE,RD,
1DUM11,SPHASE,DUM12
COMMON DUM13,DUM14,DUM15
COMMON RO,DELY,WTHO,WPERPO,OMEGA,B0,DWDRE,DWDPH,TIME
COMMON INTLNG,DELNG,LNGOBS,UT,LONG,LATOBS,QRA,OMEGA0
COMMON/OPR/REP,PUNCH
COMMON /MOL/ NOMOL,MOL(10,2)
COMMON/CHEM/LM(10,5)
COMMON/PROFL/HTT(100),PRF(8,100),NOX
COMMON/CNTRL/WNDMDL,DRFMDL,QTMDL,ATMS71
COMMON/ILOVE/NOOKY,INBED
COMMON /SO/ SOL(15,100),SOLE(15,100)
COMMON /COEFF/ XX(1400)
COMMON/BETAC/BETAC,ALPHC
COMMON/EP SLN/ EPS(100),HGT(100),CNEBYO(100),II
IPF1 = 0
1 READ(1, 999) NN

```

```

C
C PARAMETER NN SPECIFIES SET OF DATA TO BE READ
C NN=1 READ NSET,M,M2
C NN=2 READ PARAMETERS
C NN=3 READ DENSITIES AND CONVERT TO G
C NN=4 EXECUTE
C NN=5 READ ZEINIT PHINIT
C NN=6 READ DELPH,PHFNAL,DPHOUT
C NN=7 STOP
C NN=11 READ IN ATMOSPHERIC PROFILES
C NN=8 READ EQUATORIAL HEIGHT PROFILE AND CONVERT TO PROFILE
C ALONG MAGNETIC FIELD LINE; MAXIMUM ARRAY IS 50.
C NN=9 CONVERT EQUATORIAL PROFILE TO PROFILE ALONG FIELD LINE
C NN=10 CHEMICAL RATES
C NN=12 PHOTOCHEMICAL NORMALIZATION FACTORS
C NN=13 INITIALIZE ECLIPSE FUNCTION
C NN=14 COMPUTE HEATING EFFICIENCIES FROM INPUT PROFILE
C NN=15 READ IN DRIFT VALUES
C NN=16 READ IN WIND VALUES
C NN=17 COMPUTE IRON PROFILE
C NN=18 READ PLOT VALUES
C NN=19 PRODUCTION AND LOSS TERMS
C NN=20 PLOT LEGION
C
      NLOC=64000
      KB=1.38054E-16
      PI=3.1415926535
      RAD=PI/180.
      GO TO (10,20,30,40,50,60,70,80,90,100,110,120,130,140,
1150,161,170,180,190,200),NN
C
10 READ(1,999)NSET,M,M2
   WRITE(3,1010)NSET,M,M2
   READ(1,999)WNDMDL,DRFMDL,QTMDL,ATMS71
   WRITE(3,11)WNDMDL,DRFMDL,QTMDL,ATMS71
11 FORMAT(' WNDMDL=',I5,' DRFMDL=',I5,' QTMDL=',I5,
1' ATMS71=',I5)
   READ(1,999)NOMOL
   READ(1,999)((MOL(I,J),J=1,2),I=1,NOMOL)
   WRITE(3,12)((MOL(I,J),J=1,2),I=1,NOMOL)
12 FORMAT (' MOL1=',2I5,' MOL2=',2I5,' MOL3=',2I5,
1' MOL4=',2I5,
1' MOL5=',2I5,' MOL6=',2I5,' MOL8=',2I5,
1' MOL9=',2I5,' MOL10=',2I5)
   READ(1,999)REP,PUNCH,NOOKY,INBED
   WRITE(3,13)REP,PUNCH,NOOKY,INBED
13 FORMAT(' REP IS # OF ITERATIONS OF SOLUTION IN GCALC'/
1' PUNCH=0 MEANS NO CARDS PUNCHED IN MAIN'/
2' NOOKY IS # OF ITERATIONS OF RKAM IN MAIN'/
3' REP=',I5,' PUNCH=',I5,' NOOKY=',I5,' INBED=',I5)
   ITWOM=2.*M
   GO TO 1
C
20 READ(1,1001)(CC(I),I=1,54)
   WRITE(3,1011)(CC(I),I=1,54)
   CS(1)=CC(1)
   CS(2)=CC(2)
   CS(3)=CC(3)
   CS(4)=CC(4)
   CS(5)=CC(5)
   CS(6)=CC(6)
   CS(7)=CC(7)

```



```

DUM2=CC(8)
DUM3=CC(9)
T0=CC(10)
T120=CC(11)
NZAO=CC(12)
CRSCN2=CC(13)
AUO =CC(14)
BOEQ=CC(15)
B0=B0EQ
NZ00=CC(16)
NZ002=CC(17)
NZ0N2=CC(18)
DUM6=CC(19)
CK(1)=CC(20)
CK(2)=CC(21)
CTH1=CC(22)*RAD
A1=CC(23)
A2=CC(24)
CTH4=CC(25)*RAD
CTE(1)=CC(26)
CTE(2)=CC(27)
CDO=CC(28)
DUM7=CC(29)
CRSCO=CC(30)
CRSCPH=CC(31)
DELTA=CC(32)*RAD
TILT=CC(33)*RAD
UPHASE=CC(34)*RAD
CUPHI=CC(35)*100.
PHIU=CC(36)*RAD
DUM9=CC(37)
DUM10=CC(38)
OFFSET=CC(39)
DELPH=CC(40)*RAD
PHFNAL=CC(41)*RAD
DPHOUT=CC(42)*RAD
ZEINIT=CC(43)*1.E5
PHINIT=CC(44)*RAD
DELPHO=CC(45)*RAD
LAMBDA=CC(46)
RBASE=CC(47)*1.E5+R0
RD=CC(48)*1.E5+R0
DUM11=CC(49)
SPHASE=CC(50)*RAD
DUM12=CC(51)
DUM13=CC(52)
DUM14=CC(53)
DUM15=CC(54)
READ(1,1000) OMEGA
WRITE(3,21) OMEGA
21 FORMAT (' OMEGA = ',1PE11.3)
DELY=1./M
PHI=PHINIT
RE=ZEINIT+R0
CALL SS(S,COS(PHI+SPHASE),SIN(PHI+SPHASE),RE)
IF(RE.LT.RD)RE=RD
CALL COEF00
GO TO 1
C
30 READ(1,999)J
DO 34 K=1,NOECLP
DO 31 I=1,M,6

```

```

NL=I
NU=NL+5
IF (NU.GT.M) NU=M
31 READ (1,1002) (N (IX,J,K) , IX=NL,NU)
IF (M.EQ.M2) GO TO 33
DO 32 I=1,M,6
NL=I
NU=NL+5
IF (NU.GT.M) NU=M
32 READ (1,1002) (N (ITWOM-IX,J,K) , IX=NL,NU)
33 DO 34 I=1,M2
34 V (I,J,K)=0.
GO TO 1
C
50 READ (1,1000) ZEINIT,PHINIT
WRITE (3,51) ZEINIT,PHINIT
51 FORMAT (' ZEINIT=',F11.3,' PHINIT=',F11.3)
ZEINIT=ZEINIT*1.E5
PHINIT=ZEINIT*RAD
RE=ZEINIT+R0
PHI=PHINIT
CALL SS (S,COS (PHI+SPHASE) , SIN (PHI+SPHASE) , RE)
IF (RE.LT.RD) RE=RD
GO TO 1
C
60 READ (1,1000) DELPH,PHFNAL,DPHOUT
WRITE (3,62) DELPH,PHFNAL,DPHOUT
62 FORMAT (' DELPH=',F11.3,' PHFNAL=',F11.3,' DPHOUT=',F11.3)
DELPH=DELPH*RAD
PHFNAL=PHFNAL*RAD
DPHOUT=DPHOUT*RAD
GO TO 1
C
70 STOP
C
80 READ (1,1004) ((REQ(J),NEQ(J),KOX),J=1,KOX)
C
90 J=1
K=KOX
R=RBASE
CALL QR1 (SINHQM,COSHQM,P,QMAX,RE)
Y=1.
DO 83 I=1,M
Y=Y-DELY
IF (I.EQ.M) Y=0.
CALL QR (Y,Q,R,SINHQM,COSHQM,P,QMAX,RE)
81 NQ=NEQ(J)
RQ=REQ(J)*1.E5+R0
IF (J.EQ.K) GO TO 82
IF (R.LE.RQ) GO TO 82
J=J+1
IF (J.GT.K) J=K
GO TO 81
82 N (I,1,1)=NQ
N (I,1,2)=NQ
IF (M.EQ.M2) GO TO 83
N (ITWOM-I,1,1)=NQ
N (ITWOM-I,1,2)=NQ
83 CONTINUE
GOTO 1
C
100 READ (1,101) ((LM(I,J),J=1,5),I=1,10)

```

```

101 FORMAT(5E11.3)
    WRITE (3,102) ((LM(I,J),J=1,5),I=1,10)
102 FORMAT(' CHEMICAL RATE COEFFICIENTS'/
1      ' O+',5(1PE11.3)/
2      ' NO+',5(1PE11.3)/
3      ' O2+',5(1PE11.3)/
4      ' N2+',5(1PE11.3)/
5      ' N+',5(1PE11.3)/
6      ' O++',5(1PE11.3)/
7      ' HE+',5(1PE11.3)/
8      ' H+',5(1PE11.3)/
9      5(1PE11.3)/
A      5(1PE11.3))
    GOTO 1

```

C

```

110 READ (1,999) NOX
    READ(1,111) (HTT(I), (PRF(J,I),J=1,8),I=1,NOX)
111 FORMAT((5E13.5/4E13.5))
    WRITE(3,112) (HTT(I), (PRF(J,I),J=1,8),I=1,NOX)
112 FORMAT(' HGT =',E13.5,
2      ' TZ =',E13.5,
3      ' N2 =',E13.5,
4      ' O2 =',E13.5,
5      ' O =',E13.5/
6      ' NZNO=',E13.5,
7      ' NZN =',E13.5,
8      ' NZHE=',E13.5,
9      ' NZH =',E13.5)
    GOTO 1
999 FORMAT(6(8X,I5))
1000 FORMAT(3(8X,E11.3))
1001 FORMAT(17(3(8X,E11.3)/),3(8X,E11.3))
1010 FORMAT('1 NSET=',I5,' M=',I5,' M2=',I5)
1011 FORMAT('0 CS(1)=' ,1PE11.3,' CS(2)=' ,E11.3,
1' CS(3)=' ,E11.3//
1      ' CS(4)=' , E11.3,' CS(5)=' ,E11.3,
1' CS(6)=' ,E11.3//
2      ' CS(7)=' , E11.3,' DUM2=' ,E11.3,
1' DUM3=' ,E11.3//
3      ' TO=' , E11.3,' T120=' ,E11.3,
1' NZAO=' ,E11.3//
4      ' CRSCN2=' , E11.3,' AUO=' ,E11.3,
1' BOEQ=' ,E11.3//
5      ' NZOO=' , E11.3,' NZOO2=' ,E11.3,
1' NZON2=' ,E11.3//
6      ' DUM6=' , E11.3,' K(O2)=' ,E11.3,
1' K(N2)=' ,E11.3//
7      ' CTH1=' , E11.3,' A1=' ,E11.3,
1' A2=' ,E11.3//
8      ' CTH4=' , E11.3,' CTE(1)=' ,E11.3,
1' CTE(2)=' ,E11.3//
9      ' CDO=' , E11.3,' DUM7=' ,E11.3,
1' CRSCO=' ,E11.3//
A      ' CRSCPH=' , E11.3,' DELTA=' ,E11.3,
1' TILT=' ,E11.3//
B      ' UPHASE=' , E11.3,' CUPHI=' ,E11.3,
1' PHIU=' ,E11.3//
C      ' DUM9=' , E11.3,' DUM10=' ,E11.3,
1' OFFSET=' ,E11.3//
D      ' DELPH=' , E11.3,' PHFNAL=' ,E11.3,
1' DPHOUT=' ,E11.3//
E      ' ZEINIT=' , E11.3,' PHINIT=' ,E11.3,

```

```

1' DELPHO=' ,E11.3//
F      ' LAMBDA=' , E11.3, ' ZBASE=' ,E11.3,
1'      ZD=' ,E11.3//
G      ' DUM11 =' , E11.3, ' SPHASE=' ,E11.3,
1' DUM12=' ,E11.3//
H      ' DUM13=' , E11.3, ' DUM14=' ,E11.3,
1' DUM15=' ,E11.3//)
1002 FORMAT(6E11.3)
1003 FORMAT(6F5.1)
1004 FORMAT(2E11.3,I3)
C
C COMPUTE SOLAR FLUX FACTOR
120 READ(1,1000)HGTQ0,PHIQ0,LATQ0,Q0
WRITE(3,121)HGTQ0,PHIQ0,LATQ0,Q0
121 FORMAT(' HGTQ0=' ,F11.3, ' PHIQ0=' ,F11.3, ' LATQ0=' ,F11.3,
1' Q0=' ,F11.3)
HGTQ0=HGTQ0*1.E5
PHIQ0=PHIQ0*RAD
LATQ0=LATQ0*RAD
READ(1,1000)BETAC,ALPHC
WRITE(3,122)BETAC,ALPHC
122 FORMAT(' BETAC=' ,1PE11.3, ' ALPHC=' ,1PE11.3)
CALL RATES
QRA=1.
IF(HGTQ0.EQ.0.)GOTO 1
CALL PRDCT(HGTQ0,PHIQ0,LATQ0 ,DELTA,NZ00,NZ002,NZ0N2 ,
1NZO,NZO2,NZN2,TZ,QRA,QO,QN,HO,BETA)
QRA=QO/QO
WRITE(3,123) QRA,QO,HO,BETA,TZ
123 FORMAT(' QRATIO=' ,F11.3, ' QO=' ,F11.3, ' HO=' , -5PF11.3,
1' BETA=' ,
11PE11.3, ' TZ=' ,0PF11.3)
GO TO 1
C
130 TIME=0.
CALL ECLINT(PHINIT)
CALL ECLPSE(TIME,LNGOBS,PHINIT,UT,LON,SINX,COSX,
1PHIM,THT,NENTRY)
GOTO 1
C
C READ TE AND NE PROFILES
140 READ(1,141)LHADTA,II
141 FORMAT(8X,F11.3,8X,I5)
WRITE(3,142)LHADTA
142 FORMAT(' LHADTA=' ,F11.3)
LHADTA=LHADTA*RAD
READ(1,143) (HGT(I),NE(I),TE(I),I=1,II)
143 FORMAT(F5.1,E10.1,F5.0)
WRITE(3,144) (HGT(I),NE(I),TE(I),I=1,II)
144 FORMAT(' HGT=' ,F7.1, ' NE=' ,1PE11.3, ' TE=' ,0PF7.1)
DO 145 I=1,II
HGT(I)=HGT(I)*1.E5
CALL PRDCT(HGT(I),LHADTA,LATOBS,DELTA,NZ00,NZ002,NZ0N2 ,
1NZO,NZO2,NZN2,TZ,QRA,QO,QN,HO,BETA)
XX(I)=QO
XX(100+I)=BETA
IF(TZ.GT.TE(I))TZ=TE(I)
QEI=4.8E-7*NE(I)*NE(I)*(TE(I)-TZ)/TE(I)**1.5+
1 3.E-12*NZO*NE(I)*(TE(I)-TZ)/TZ
EPS(I)=QEI/QN
145 CNEBYO(I)=NE(I)/NZO
WRITE(3,146) (HGT(I),EPS(I),CNEBYO(I),XX(I),XX(100+I),

```

```

    1I=1,II)
146 FORMAT(' HGT=',-5PF11.3,' EPSILON=',0PF11.3,
    1' NE/N(O)=',1PE11.3,
    1' QO=',0PF11.3,' BETA=',1PE11.3)
    CALL QUNT(2)
    GOTO 1
C
C READ DRIFT VELOCITIES IN M/S AND LOCAL HOUR ANGLE IN DEGREES
150 READ(1,151)HGTV,JJ
151 FORMAT(8X,F11.3,8X,I5)
    WRITE(3,152)HGTV
152 FORMAT(' HGTV=',F11.3)
    READ(1,153)(PH(J),VV(J),J=1,JJ)
153 FORMAT(16F5.0)
    WRITE(3,154)(PH(J),VV(J),J=1,JJ)
154 FORMAT(' PH=',F7.0,' DRIFT=',F7.0)
    DO 155 J=1,JJ
    VV(J)=VV(J)*100.
155 PH(J)=PH(J)*RAD
    HGTV=HGTV*1.E5
    GOTO 1
C.....
    ENTRY VPERP(HGTVV,PHI,WPERP )
    HGTVV=HGTV
    PHIX=PHI
    WPERP=VV(1)
    IF(PHIX.LT.PH(1))GOTO 160
156 IF((PHIX-2.*PI).LT.PH(1))GOTO 157
    PHIX=PHIX-2.*PI
    GOTO 156
157 DO 158 J=2,JJ
    IF(PHIX.LT.PH(J))GOTO 159
158 CONTINUE
    WPERP =VV(JJ)
    GOTO 160
159 WPERP = VV(J-1)+(VV(J)-VV(J-1))*
    1(PHIX-PH(J-1))/(PH(J)-PH(J-1))
C
160 RETURN
C READ DIURNAL VARIATION OF WIND. NORMALIZATION IS 1
161 READ(1,999)JJW
    READ(1,162)(PHW(J),VVW(J),J=1,JJW)
162 FORMAT(16F5.0)
    WRITE(3,163)(PHW(J),VVW(J),J=1,JJW)
163 FORMAT(' PHW=',F7.0,' WIND=',F7.0)
    DO 164 J=1,JJW
164 PHW(J)=PHW(J)*RAD
    GOTO 1
C.....
    ENTRY VWIND(PHI,VW)
    PHIX=PHI
    VW=VVW(1)
    IF(PHIX.LT.PHW(1))GOTO 169
165 IF((PHIX-2.*PI).LT.PHW(1))GOTO166
    PHIX=PHIX-2.*PI
    GOTO 165
166 DO 167 J=2,JJW
    IF(PHIX.LT.PHW(J))GOTO 168
167 CONTINUE
    VW=VVW(JJW)
    GOTO 169
168 VW = VVW(J-1)+(VVW(J)-VVW(J-1))*

```

```

      1(PHIX-PHW(J-1))/(PHW(J)-PHW(J-1))
169 RETURN
C
C READ IN PARAMETERS FOR FUNCTION PROFILE, USED IN FE+ ANALYSIS
170 READ(1,1002)NFE0,CFE
      READ(1,171 )LAT0,LAT1,LAT2
171 FORMAT(6E11.3)
      WRITE(3,172) NFE0,CFE
172 FORMAT(' NFE=',1PE11.3,' CFE=',0PF11.3)
      WRITE(3,173) LAT0,LAT1,LAT2
173 FORMAT(' LAT0=',F11.3,' LAT1=',F11.3,' LAT2=',F11.3)
      CFE=(CFE*RAD)**2
      LAT0=LAT0*RAD
      LAT1=LAT1*RAD
      LAT2=LAT2*RAD
      R=RBASE
      CALL QR1(SINHQM,COSHQM,P,QMAX,RE)
      Y=1.
      DO 177 I=1,M
      Y=Y-DELY
      IF(Y.LT.0.)Y=0.
      CALL QR(Y,Q,R,SINHQM,COSHQM,P,QMAX,RE)
      COS2=R/RE
      COS1=SQRT(COS2)
      LAT=ARCOS(COS1)
      IF(LAT.LT.LAT0)GO TO 174
      IF(LAT.LT.LAT1)GO TO 175
      IF(LAT.LT.LAT2)GO TO 175
174 N(I,2,1)=NFE0
      GO TO 176
175 Z1=(LAT-LAT0)**2/CFE
      Z2=(LAT-LAT1)**2/CFE
      Z3=(LAT-LAT2)**2/CFE
      IF(Z1.GT.20.)Z1=20.
      IF(Z2.GT.20.)Z2=20.
      IF(Z3.GT.20.)Z3=20.
      N(I,2,1)=NFE0*(EXP(-Z1)
1          +EXP(-Z2)
2          +EXP(-Z3))
176 IF(M.NE.M2)N(ITWOM-I,2,1)=N(I,2,1)
177 CONTINUE
C
180 CONTINUE
190 CONTINUE
200 CONTINUE
      GOTO 1
1100 FORMAT (20A4)
1110 FORMAT (10I4)
C
40 RETURN
      END
C
C.....
      SUBROUTINE COEF00
$SET OWN
C.....
C SET UP PARAMETERS THAT DEPEND ON DIPOLE COORDINATES ONLY.
C THIS SUBROUTINE USES FOR G TRANSFORM A LATITUDE INDEPENDENT
C SCALE HEIGHT. THE TEMPERATURE TINF IS TAKEN AT THE EQUATOR.
C.....
      IMPLICIT REAL*4 (A-Z)
      REAL*8 C11,C12,C13

```

```

INTEGER MOLECC
INTEGER WNDMDL,DRFMDL,QTMDL
INTEGER NSET,M,M2,I,J,ITWOM,I1,I2,I3,I4,NOTRAN
INTEGER L0,L00,JJ,J0,J1,K,NENTRY,ITYPE
INTEGER MOLEC
INTEGER * 4 IM(10),NOMOL
DIMENSION VX(9)
DIMENSION CD(10,15),SOUP(2,100)
DIMENSION LMB(10,5)
DIMENSION UAN(3),UPRO(3),ULOSS(3),UDELNV(3)
DIMENSION N(100,10,2),V(100,10,2),ALF(100),G(100,10,2)
COMMON NSET,M,M2,CS(7),DUM1,DUM2,T0,T120,NZAO
COMMON CRSCN2,AUO,DUM3,NZ00,NZ002,NZ0N2,
1DUM4,CK(2),CTH1,D5,D6
COMMON CTH4,CTE(2),CDO,DUM7,CRSCO,CRSCPH,DELTA,TILT
COMMON UPHASE,CUPHI,PHIU,DUM9,DUM10,
1OFFSET,DELPH,PHFNAL,DPHOUT
COMMON ZEINIT,PHINIT,DELPHO,LAMBDA,RBASE,RD,
1DUM12,SPHASE,DUM13
COMMON DUM14,DB0,DDB
COMMON R0,DELY,WTH0,WPERP0,OMEGA,B0,DWDRE,DWDPH,TIME
COMMON INTLNG,DELNG,LNGOBS,UT,LONG,LATOBS,QRA,OMEGA0
COMMON /MOL/ NOMOL
COMMON /CNTRL/ WNDMDL,DRFMDL,QTMDL
COMMON /COEFF/ X(7,100)
COMMON /SO/ SOL(15,100),SOLE(15,100)
COMMON /SOSO/ SOOL(6,100)
COMMON /SUMMO/ SUMX(8,100)
INTR(X1,X2,X3)=(C11*X1-C12*X2+C13*X3)/DELY2
DER9(X4,X3,X2,X1)=(41.13*X1+63.00*X2+46.35*X3-28.07*X4)/
1(387.8*DELY)
C SOL(1)=R
C SOL(2)=SIN1
C SOL(3)=COS1
C SOL(4)=THETA
C SOL(5)=SQRSIG
C SOL(6)=-SQRSIG*R02/R3
C SOL(7)=DEL.T
C SOL(8)=DEL.VEM
C SOL(9)=L
C SOL(10)=GRAV
C SOL(11)=Y
C SOL(12)=NTOG1
C SOL(13)=ALFH0
C SOL(14)=GTRAN
C SOLE(1)=TINF
C SOLE(2)=KTE
C SOLE(3)=KTI
C SOLE(4)=N(O)
C SOLE(5)=N(O2)
C SOLE(6)=N(N2)
C SOLE(7)=U*COSI+VTH*SINI
C SOLE(8)=DDS(KTE+KTI)
C SOLE(9)=E
C SOLE(10)=TZ
C SOLE(11)=QO
C SOLE(12)=QO2
C SOLE(13)=QN2
C SOLE(14)=QN
C SOLE(15)=QOO
C SOOL(1)=NO
C SOOL(2)=N

```

```

C SOOL(3)=HE
C SOOL(4)=H
C SOOL(6)=NZN2D
  LAMBD2=LAMBDA**2
  DELY2=DELY*DELY
  TWODY=2.*DELY
  PROTON=1.67252E-24
  KB=1.38054E-16
  G0=980.655
  PI=3.1415926535
  PI2=PI/2.
  TWOPI=2.*PI
  RAD=PI/180.
  R120=R0+120.E5
  H120=120.E5
  ITWOM=2*M
  R02=R0*R0
  SNDEL=SIN(DELTA)
  CSDEL=COS(DELTA)
  SINOBS=SIN(LATOBS)
  COSOBS=COS(LATOBS)
  R02POB=R02*SINOBS
  COSOB2=COSOBS**2
  COSTIL=COS(TILT)
  SINTIL=SIN(TILT)
  NZNO=0.
  NZN=0.
  NZHE=0.
  NZH=0.
  RETURN

```

C

C.....

```

ENTRY COEF0(RE, PHI, COSPH, SINPH)
R=RBASE
OMEGA0=WTH0/RE+OMEGA
GMULT=1./OMEGA0
CALL ATMS(RE, PHI)
CALL UU0(PHI)
CALL QR1(SINHQM, COSHQM, P, QMAX, RE)
Y=1.
DO 1 I=1, M
Y=Y-DELY
IF(I.EQ.M) Y=0.
  CALL QR(Y, Q, R, SINHQM, COSHQM, P, QMAX, RE)
R2=R*R
R3=R2*R
COS2=R/RE
COS1=SQRT(COS2)
SIN2=1.-COS2
SIN1=SQRT(SIN2)
SIN3=SIN2*SIN1
THETA=PI2-ARSIN(SIN1)
SIG=1.+3.*SIN2
SQRSIG=SIG**.5
GRAV=G0*R02/R2
STOQ=-SQRSIG*R02/R3
DIVWT=DWDRE+4.*WPERP0/(R*SIG**2)*(6.*SIN2**3-3.*SIN2**2-
14.*SIN2+1.)
DIVWPH=DWDPH/RE
SOL(1, I)=R
SOL(2, I)=SIN1
SOL(3, I)=COS1

```



```

SOL(4,I)=THETA
SOL(5,I)=SQRSIG
SOL(6,I)=STOQ
SOL(7,I)=(9.*SIN1+15.*SIN3)/(R*SIG**1.5)
SOL(8,I)=DIVWT+DIVWPH
SOL(9,I)=LAMBDA*COSH(LAMBDA*Q)/SINHQM
SOL(10,I)=GRAV
SOL(11,I)=Y
IF(M.EQ.M2)GO TO 1
SOL(1,ITWOM-I)=R
SOL(2,ITWOM-I)=-SIN1
SOL(3,ITWOM-I)=COS1
SOL(4,ITWOM-I)=PI-THETA
SOL(5,ITWOM-I)=SQRSIG
SOL(6,ITWOM-I)=STOQ
SOL(7,ITWOM-I)=-SOL(7,I)
SOL(8,ITWOM-I)=SOL(8,I)
SOL(9,ITWOM-I)=SOL(9,I)
SOL(10,ITWOM-I)=GRAV
SOL(11,ITWOM-I)=-Y
1 CONTINUE
C
C...SET UP PARAMETERS THAT DEPEND ON BOTH HEMISPHERES.....
E=1.
DO 8 I=1,M2
R=SOL(1,I)
GRAV=SOL(10,I)
Z=R-R0
SIN1=SOL(2,I)
COS1=SOL(3,I)
SQRSIG=SOL(5,I)
SN1=SIN1*COSTIL+COS1*SINTIL
CS1=COS1*COSTIL-SIN1*SINTIL
CALL ATMST(TINF,TZ,Z,CS1,SN1)
CALL ATMSD(DTDPH,DTDTH,DTDR)
CALL ATMSN(NZ00,16.,NZ0)
CALL ATMSN(NZ002,32.,NZ02)
CALL ATMSN(NZ0N2,28.,NZN2)
HO=KB*TZ/(16.*PROTON*GRAV)
HO2=HO*16./32.
HN2=HO*16./28.
DTDZ=DTDR/TZ
HO=1./(1./HO+DTDZ)
HO2=1./(1./HO2+DTDZ)
HN2=1./(1./HN2+DTDZ)
CALL UU(SN1,CS1,U)
VT=OMEGA*DTDPH/(TINF*R120)*(Z-H120)*R
C
C...COMPUTE ELECTRON PRODUCTION.....
IF(Z-1.E8)2,5,5
2 COSCHI=SNDEL*SN1+CSDEL*CS1*COSPH
CHI=ARCOS(COSCHI)
SINCHI=SIN(CHI)
IF(CHI-PI2)6,6,4
4 IF(R*SINCHI-RBASE)5,5,6
5 QO4S=0.
QO2D=0.
QOO=0.
QO2=0.
QN2=0.
QN=0.
GO TO 7

```

```

6 NHCHO=NZO*HO*CH(R/HO,CHI,SINCHI)
  NHCHO2=NZO2*HO2*CH(R/HO2,CHI,SINCHI)
  NHCHN2=NZN2*HN2*CH(R/HN2,CHI,SINCHI)
  OPLUS=1.E6
  CALL PHOTO(NHCHO,NHCHO2,NHCHN2,OPLUS,QN,QO4S,QO2D,
1QOO,QO2,QN2,QRA,NZO,NZO2,NZN2,Z)

```

C.....

```

7 SINI=2.*SIN1/SQRSIG
  COSI=COS1/SQRSIG
  SOLE(1,I)=TINF
  SOLE(4,I)=NZO
  SOLE(5,I)=NZO2
  SOLE(6,I)=NZN2
  SOLE(7,I)=U*COSI+VT*SINI
  SOLE(10,I)=TZ
  SOLE(11,I)=QO4S
  SOLE(12,I)=QO2
  SOLE(13,I)=QN2
  SOLE(14,I)=QO2D
  SOLE(15,I)=QOO
  CALL ATMSUP(NZNO,NZN,NZHE,NZHEP)
  SOOL(1,I)=NZNO
  SOOL(2,I)=NZN
  SOOL(3,I)=NZHE
  SOOL(4,I)=0.0
  SOOL(5,I)=NZHEP
8 SOOL(6,I)=.4*NZN
  DYDT=-WPERPO/R0*LAMBDA*COSHQM/(SINHQM*2.0*P*P*QMAX)*
1(R0/RBASE)**3
  ZE=RE-R0
  R=RE*COSOB2
  R2=R*R
  ZD=R-R0
  PHIX=PHI/RAD
  Q=R02POB/R2
  Y0=SINH(LAMBDA*Q)/SINHQM
  L00=1
  DO 9 I=1,M2
9 IF(SOL(2,I).GT.SINOBS)L00=I
  Y=SOL(11,L00)
  IF((Y-Y0).LT.DELY/2.)L00=L00-1
  IF(L00.LT.1)L00=1
  IF(L00.GT.(M2-2))L00=M2-2
  Y1=SOL(11,L00)
  Y2=SOL(11,L00+1)
  Y3=SOL(11,L00+2)
  C11=(Y0-Y2)*(Y0-Y3)/2.
  C12=(Y0-Y1)*(Y0-Y3)
  C13=(Y0-Y1)*(Y0-Y2)/2.
  IF(QTMDL.EQ.0)CALL QUNT(2)
  RETURN

```

C

C...COMPUTE CONTENT.....

```

  ENTRY COCONT(CONTNT,PRD,LOSS,N,J,K)
  CONTNT=0.
  PRD=0.
  LOSS=0.
  COREND=.5
  DO 12 I=1,M2
  R4=SOL(1,I)**4
  COS4=SOL(3,I)**4
  SIG=SOL(5,I)**2

```

```

L=SOL(9,I)
NZO2=SOLE(5,I)
NZN2=SOLE(6,I)
TZ=SOLE(10,I)
QO=SOLE(11,I)
IF(K.EQ.2)QO=QO*SOLE(9,I)
CALL RATEL(LMB,TZ,1.38E-13)
BETA=LMB(1,1)*NZN2+LMB(1,2)*NZO2
IF(I.EQ.M2)COREND=.5
CX=COS4*R4/(L*R0*SIG)*DELY*COREND
CONTNT=CONTNT+N(I,J,K)*CX
PRD=PRD+QO*CX
LOSS=LOSS+BETA*N(I,J,K)*CX
12 COREND=1.
RETURN

```

C

C...SET UP TRANSFORMS.....

```

ENTRY COEF2(RE,PHI,AU,ALFO)
MASS=AU*PROTON
CALL ATMST(TINF,TZ,RE-R0,COSTIL,SINTIL)
CALL ATMSD(DTDPH,DTDTH,DTDR)
ALFKT=ALFO*KB*TINF/MASS
DO 13 I=1,M
R=SOL(1,I)
Z=R-R0
COS4=SOL(3,I)**4
SIG=SOL(5,I)**2
STOQ=SOL(6,I)
GRAV=SOL(10,I)
SINI=2.*SOL(2,I)/SOL(5,I)
ALFH0=ALFKT/GRAV
NTOG1=-(WPERP0*COS4/SIG-Z*R/R0*DTDPH/TINF*OMEGA0)/ALFH0
GTRAN=EXP(R*Z/(R0*ALFH0))
SOL(12,I)=NTOG1
SOL(13,I)=ALFH0
SOL(14,I)=GTRAN
IF(M.EQ.M2)GO TO 13
SOL(12,ITWOM-I)=NTOG1
SOL(13,ITWOM-I)=ALFH0
SOL(14,ITWOM-I)=GTRAN
13 CONTINUE
RETURN

```

C

C...TRANSFORM FROM N TO G.....

```

ENTRY CONTOG(G,N,J,K)
DO 15 I=1,M2
GTRAN=SOL(14,I)
IF(N(I,J,K).LT.1.E-30)N(I,J,K)=1.E-30
15 G(I,J,K)=N(I,J,K)*GTRAN
RETURN

```

C

C...GO FROM G TO N.....

```

ENTRY COGTON(N,J,K)
DO 17 I=1,M2
GTRAN=SOL(14,I)
N(I,J,K)=N(I,J,K)/GTRAN
IF(N(I,J,K).GT.1.E-30)GO TO 17
N(I,J,K)=1.E-30
17 CONTINUE
RETURN

```

C

C...COMPUTE ANY ION.....

```

ENTRY COEFN(ZZ,RE,PHI,N,V,IM,K,ITYPE,AU,MOLEC,LONGO,NOTRAN)
I1=IM(1)
IF(I1.NE.1)GO TO 127
IF(QTMDL.NE.0)CALL QTITE(RE,PHI,COSPH,SINPH,N,K)
IF(K.NE.2)GO TO 127
PHIM=0.
CALL ECLPSE(TIME, LONGO, PHI, UT, LONG, SINX, COSX,
1PHIM, THT, NENTRY)
SNPHIM=SIN(PHIM)
CSPHIM=COS(PHIM)
DO 126 I=1, M2
E=1.
IF(NENTRY.EQ.0)GO TO 125
R=SOL(1, I)
SIN1=SOL(2, I)
COS1=SOL(3, I)
SN1=SIN1*COSTIL+COS1*SINTIL
CS1=COS1*COSTIL-SIN1*SINTIL
CALL SUN(SN1, CS1, SNDEL, CSDEL, SINPH, COSPH, R)
CALL MOON(E, SINX, COSX, SNPHIM, CSPHIM)
125 SOLE(9, I)=E
126 CONTINUE
127 MASS=AU*PROTON
DELYX=DELY
J0=0
J1=1
DO 129 I=1, M2
L=SOL(9, I)
STOQ=SOL(6, I)
LSTOQ=L*STOQ
TINF=SOLE(1, I)
KTE=SOLE(2, I)
KTI=SOLE(3, I)
NZO=SOLE(4, I)+NZAO
NZO2=SOLE(5, I)
NZN2=SOLE(6, I)
WIND=SOLE(7, I)
DDSKT=SOLE(8, I)
DSDTT=DDSKT/KTI
IF(I.NE.M2)GO TO 128
J1=0
DELYX=DELY
IF(M.NE.M2) GO TO 128
J1=-1
DELYX=TWODY
128 UTOO=0.
NE=N(I, 1, K)
IF(NOMOL.EQ.1)GO TO 270
DO 27 J=2, NOMOL
UTOO=N(I-J0, IM(J), K)-N(I+J1, IM(J), K)+UTOO
NE=NE+N(I, J, K)
27 CONTINUE
270 CONTINUE
DDSN=LSTOQ*UTOO/DELYX
ALF(I)=1.+ZZ*KTE*N(I, I1, K)/(KTI*NE)
C
C..COMPUTE COLLISION COEFFICIENTS .....
MOLECC=MOLEC
IF(MOLEC.EQ.7)MOLECC=1
CALL RATED(CD, IM, MOLECC, TZ, TINF, KTI, KTE)
DD=NZO/CD(I1, 10)+NZO2/CD(I1, 11)+NZN2/CD(I1, 12)
UTOO=DD

```

```

IF(NOMOL.EQ.1)GO TO 280
DO 28 J=2,NOMOL
UTOO=N(I,IM(J),K)/CD(I1,IM(J))+UTOO
28 CONTINUE
280 CONTINUE
SOUP(1,I)=1./UTOO
UTOO=WIND*DD
IF(NOMOL.EQ.1)GO TO 290
DO 29 J=2,NOMOL
UTOO=V(I,IM(J),K)*N(I,IM(J),K)/CD(I1,IM(J))+UTOO
29 CONTINUE
290 CONTINUE
SOUP(2,I)=DSDTT-UTOO+ZZ*DDSN*KTE/(KTI*NE)
J0=1
129 DELYX=TWODY
JJ=1
L0=L00
J0=0
J1=1
DELYX=DELY
SIGN=1.
E=1.
DO 142 I=1,M2
NE=0.
DO 30 J=1,NOMOL
30 NE=NE+N(I,J,K)
TINF=SOLE(1,I)
KTE=SOLE(2,I)
KTI=SOLE(3,I)
NZO=SOLE(4,I)
NZO2=SOLE(5,I)
NZN2=SOLE(6,I)
NZNO=SOOL(1,I)
NZN=SOOL(2,I)
NZHE=SOOL(3,I)
NZH=SOOL(4,I)
HEPLUS=SOOL(5,I)
NZN2D=SOOL(6,I)
WIND=SOLE(7,I)
DDSKT=SOLE(8,I)
TZ=SOLE(10,I)
R=SOL(1,I)
SIN1=SOL(2,I)
COS1=SOL(3,I)
SQRSIG=SOL(5,I)
STOQ=SOL(6,I)
DELT=SOL(7,I)
DELVEM=SOL(8,I)
L=SOL(9,I)
GRAV=SOL(10,I)
Y=SOL(11,I)
LSTOQ=L*STOQ

```

C

C...RATE COEFFICIENTS.....

```

CALL RATEL(LMB,TZ,KTE)
IF(I.NE.M2)GO TO 131
J1=0
DELYX=DELY
IF(M.NE.M2)GO TO 131
J1=-1
DELYX=TWODY
SIGN=-1

```

```

C
C...COMPUTE T.DEL(N(I)V(I)).....
131 H=KTI/(MASS*GRAV)
    SINI=2.*SIN1/SQRSIG
    SINI2=SINI*SINI
    SIN2=SIN1**2
    COS2=1.-SIN2
    SIG2=SQRSIG**4
    D=SOUP(1,I)
    ALPHA=ALF(I)
    DSDTT=DDSKT/KTI
    ALPHAD=ALPHA*D
    SINIH=SINI/H
    DX=-2.*(SINI2+COS2/SIG2)/R
    DD1=D*(SOUP(2,I)+SINIH)
    DDSD=LSTOQ*(SOUP(1,I-J0)-SOUP(1,I+J1))/DELYX
    DDSAD=LSTOQ*(ALF(I-J0)*SOUP(1,I-J0)-ALF(I+J1)*SOUP(1,I+J1))
1/DELYX
    A2=-LSTOQ*(SOUP(2,I-J0)-SIGN*SOUP(2,I+J1))*D/DELYX
1-DDSD*DD1/D
    2-D*(-DSDTT*SINI+DX)/H
    A3=-DDSAD-DD1
    A4=-ALPHAD

C
C...ADD ON N(I)V(I)*DEL.T.....
    A2=-DELT*DD1+A2
    A3=A3-DELT*ALPHAD

C
C...ADD REST OF CONTINUITY EQUATION.....
    B1=0.
    B2=-DELVEM-A2
    B3=-A3
    B4=-A4

C
C...COMPUTE PRODUCTION AND LOSS TERMS.....
    IF(K.EQ.2)E=SOLE(9,I)
C...THE FOLLOWING VARIABLES STAND FOR THE CORRESPONDING IONS
C...N1...O+
C...N2...NO+
C...N3...O2+
C...N4...N2+
C...N5...N+
C...N6...O++
C...N7...O+2D
    GO TO (132,133,134,135,1361,1362,1363,1364,1365),MOLEC

C
C...FOR O+.....
132 B1=B1+SOLE(11,I)*E+3.E-8*NE*N(I,7,K)
    B2=B2-LMB(1,1)*NZN2-LMB(1,2)*NZO2-LMB(1,3)*NZNO
    2-LMB(1,4)*NE
    GO TO 137

C
C...FOR NO+.....
133 B1=B1+LMB(1,1)*NZN2*N(I,1,K)
    1+(LMB(3,1)*NZNO+LMB(3,2)*NZN+LMB(3,3)*NZN2)*N(I,3,K)
    2+(LMB(4,2)*NZO+LMB(4,3)*NZNO)*N(I,4,K)
    3+(LMB(5,1)*NZO2/2.+LMB(5,2)*NZNO)*N(I,5,K)
    B2=B2-LMB(2,1)*NE
    GO TO 137

C
C...FOR O2+.....
134 B1=B1+SOLE(12,I)*E+(LMB(1,2)*N(I,1,K)+LMB(4,1)*N(I,4,K)

```

```

1+LMB(5,1)/2.*N(1,3,N)/N2O2
B2=B2-LMB(3,1)*NZNO-LMB(3,2)*NZN-LMB(3,3)*NZN2
1-LMB(3,4)*NZN2D-LMB(3,5)*NE
GO TO 137

```

```

C
C...FOR N2+.....
135 B1=B1+LMB(10,2)*SOLE(13,I)*E
1+.3*LMB(7,1)*NZN2*HEPLUS+3.E-10*NZN2*N(I,7,K)
B2=B2-LMB(4,1)*NZO2-LMB(4,2)*NZO-LMB(4,3)*NZNO-LMB(4,4)*NZN
1-LMB(4,5)*NE
GO TO 137

```

```

C
C...FOR N+.....
1361 QN=(1.-LMB(10,2))*SOLE(13,I)*E
B1=B1+QN+LMB(4,4)*NZN*N(I,4,K)+.7*LMB(7,1)*NZN2*HEPLUS
1+LMB(3,4)*NZN2D*N(I,3,K)
B2=B2-LMB(5,1)*NZO2-LMB(5,2)*NZNO
GO TO 137

```

```

C
C...FOR O++.....
1362 B1=B1+SOLE(15,I)*E
B2=B2-LMB(6,1)*NZO2-LMB(6,2)*NZN2
GO TO 137

```

```

C
C...FOR O+2D.....
1363 B1=SOLE(14,I)*E+B1
B2=-3.E-10*NZN2-3.E-8*NE+B2
1364 CONTINUE
1365 CONTINUE
137 CONTINUE
SUMX(MOLEC,I)=B1+(B2+DELVE+M+A2)*N(I,I1,1)
IF(ITYPE.EQ.0)GO TO 139
IF(I.NE.L0)GO TO 139
IF(L00.LE.2.OR.L00.GE.(M2-3))GO TO 139
LSTOQ2=LSTOQ*LSTOQ
AN0=N(L0-2,I1,K)
AN1=N(L0-1,I1,K)
AN2=N(L0,I1,K)
AN3=N(L0+1,I1,K)
AN4=N(L0+2,I1,K)
D1NDY=(AN1-AN3)/TWOY
D2NDY=(-AN0+16.*AN1-30.*AN2+16.*AN3-AN4)/(12.*DELY2)
D1NDS=LSTOQ*D1NDY
D2NDS=LSTOQ2*D2NDY+(-DELVE+Y*LAMBD2*STOQ/L)*D1NDS
UDELNV(JJ)=(DELVE+M+A2)*AN2+A3*D1NDS+A4*D2NDS
UPRO(JJ)=B1

```

```

C
C...SUBTRACT OUT DELVE+M+A2.....
ULOSS(JJ)=- (B2+DELVE+M+A2)*AN2
UAN(JJ)=AN2
IF(JJ.EQ.3)GO TO 138
JJ=JJ+1
L0=L0+1
GO TO 139
138 AN=INTR(UAN(1),UAN(2),UAN(3))
PRO=INTR(UPRO(1),UPRO(2),UPRO(3))
LOSS=INTR(ULOSS(1),ULOSS(2),ULOSS(3))
DELNV=INTR(UDELNV(1),UDELNV(2),UDELNV(3))
SLAT=LATOB/RAD
139 IF(I.NE.M)GO TO 140
ANX=N(M,I1,K)
LOSSX=- (B2+DELVE+M+A2)*ANX

```

```

    PROX=B1
    NEX=NE
    TEX=KTE/KB
C
C...IGNORE G-TRANSFORM IF NOTRAN IS POSITIVE.....
  140 IF(NOTRAN.GT.0)GO TO 141
C
C...N TO G TRANSFORM.....
    NTOG1=SOL(12,I)
    ALFH0=SOL(13,I)
    GTRAN=SOL(14,I)
    SINIAH=SINI/ALFH0
    B1=B1*GTRAN
    B2=B2-B3*SINIAH+B4*(SINIAH**2-DX/ALFH0)-NTOG1
    B3=B3-B4*2.*SINIAH
C
C...S TO Q TRANSFORM.....
  141 B3=STOQ*(B3-DELT*B4)
    B4=STOQ*STOQ*B4
C
C...Q TO Y TRANSFORM.....
    B3=L*B3+Y*(LAMBD2*B4-DYDT)
    B4=L*L*B4
    X(1,I)=LSTOQ
    X(2,I)=-DD1
    X(3,I)=-ALPHAD*LSTOQ
    X(4,I)=B1*GMULT
    X(5,I)=B2*GMULT
    X(6,I)=B3*GMULT
    X(7,I)=B4*GMULT
    DELYX=TWODY
  142 J0=1
    RETURN
C.....
    ENTRY COV(N,V,I1,K,ITYPE)
    J0=0
    J1=1
    DELYX=DELY
    DO 151 I=1,M2
    IF(I.LT.M2)GO TO 150
    DELYX=DELY
    J1=0
    IF(M.EQ.M2)J1=-1
    IF(M.EQ.M2)DELYX=TWODY
  150 DNDY=ALOG(N(I-J0,I1,K)/N(I+J1,I1,K))/DELYX
    J0=1
    DELYX=TWODY
    V(I,I1,K)=X(2,I)+X(3,I)*DNDY
    IF(V(I,I1,K).LT.-300.E2)V(I,I1,K)=-300.E2
    IF(V(I,I1,K).GT.300.E2)V(I,I1,K)=300.E2
  151 CONTINUE
    IF(ITYPE.EQ.0)RETURN
C
C...COMPUTE NDELV.....
    SLAT=0.
    DELVEM=SOL(8,M)
    LSTOQ=SOL(9,M)*SOL(6,M)
    IF(M.NE.M2)GO TO 153
    DO 152 I=1,8
    N(M+I,I1,K)=N(M-I,I1,K)
    X(2,M+I)=X(2,M-I)
  152 X(3,M+I)=X(3,M-I)

```



```

153 DO 154 I=1,9
      DNDY=DER9 (N(M-9+I, I1, K) -N(M-1+I, I1, K) ,
1          N(M-8+I, I1, K) -N(M-2+I, I1, K) ,
2          N(M-7+I, I1, K) -N(M-3+I, I1, K) ,
3          N(M-6+I, I1, K) -N(M-4+I, I1, K) )
      IF (I.EQ.5) DN=DNDY
154 VX(I)=X(2, M-5+I)+X(3, M-5+I)*DNDY/N(M-5+I, I1, K)
      DVX=DER9 (VX(1) -VX(9) , VX(2) -VX(8) , VX(3) -VX(7) , VX(4) -VX(6) )
      DELNV=(VX(5) *DN+N(M, I1, K) *DVX) *LSTOQ+DELVEM*N(M, I1, K)
      RETURN
      END

C
C.....
      SUBROUTINE ATMS(RE, PHI)
$SET OWN
C.....
C THE NEUTRAL ATMOSPHERE USES JACCHIA'S MODELS FOR TEMPERATURE
C AND DENSITY.
C THREE ENTRIES BESIDES THE SUBROUTINE ENTRY ARE USED.
C FOR THE ENTRY TO THE DERIVATIVES BE SURE THAT ATOMIC OXYGEN
C IS BEING USED.
C.....
C TO=680 DEG @ S.S. MIN AND 1140 DEGS @ S.S. MAX
C TO=CT(1), T120= CT(2) AND NZAO=CT(3).
      IMPLICIT REAL*4 (A-Z)
      INTEGER WNDMDL, DRFMDL, QTMDL, ATMS71
      INTEGER I1, NOX, NOMOL
      INTEGER NSET, MU, M2
      INTEGER INDX(32), IN, IM
      COMMON NSET, MU, M2, CS(7), DUM2, DUM3, T0, T120, NZAO
      COMMON CRSCN2, AUO, DUM5, NZ00, NZ002, NZON2,
1DUM6, CK(2), CTH1, A1, A2
      COMMON CTH4, CTE(2), CDO, DUM7, CRSCO, CRSCPH, DELTA, DUM8
      COMMON UPHASE, CUPHI, PHIU, DUM9, DUM10,
1OFFSET, DELPH, PHFNAL, DPHOUT
      COMMON ZEINIT, PHINIT, DUM11, LAMBDA, RBASE, RD,
1DUM12, SPHASE, DUM13
      COMMON DUM14, DBO, DDB
      COMMON R0, DELY, WTH0, WPERP0, OMEGA, B0
      COMMON/PROFL/XZ(100), PRF(8, 100), NOX
      COMMON/CNTRL/WNDMDL, DRFMDL, QTMDL, ATMS71
      COMMON/MOL/NOMOL
      I1=1
      INDX(28)=2
      INDX(32)=3
      INDX(16)=4
      INDX(30)=5
      INDX(14)=6
      INDX(4)=7
      INDX(1)=8
      ZERO=0.
      ONE=1.
      TWO=2.
      FOUR=4.
      H120=120.E5
      R120=H120+R0
      K=1.38054E-16
      PI=3.1415926535
      RAD=PI/180.
      G120=944.655
      HN=K*1130./ (1.67E-24*980.65*14.)
      HNO=HN*14./30.

```

```

BETTA=-45. *RAD
GAMMA=45. *RAD
P=12. *RAD
R=0.3
M=2.5
MR=M*R
N=2.5
M1=M-ONE
AM2=M-TWO
AN1=N-ONE
SINDEL= SIN(DELTA/TWO)
COSDEL= COS(DELTA/TWO)
CEF1= ONE+P* COS(PHI +GAMMA)
CAPPHI=PHI +BETTA+P* SIN(PHI +GAMMA)
1 IF(CAPPHI-PI) 3,5,2
2 CAPPHI=CAPPHI-TWO*PI
GO TO 1
3 IF(CAPPHI+PI) 4,5,6
4 CAPPHI=CAPPHI+TWO*PI
GO TO 3
5 CS1PH=ZERO
GO TO 7
6 CS1PH= COS(CAPPHI/TWO)
7 CSN1PH=CS1PH**AN1
CSNPH=CSN1PH*CS1PH
ZE=RE-RO
RETURN

```

C.....

```

C ENTRY TO NEUTRAL TEMPERATURES
ENTRY ATMST(TINF,TZ,Z,COSINE,SINE)

```

C.....

```

IF(ATMS71.EQ.1)GOTO 19
COS1= SQRT((ONE+COSINE)/TWO)
SIN1=SINE /(TWO*COS1)
SN1TH=SIN1*COSDEL+COS1*SINDEL
DSN1TH= ABS(SN1TH)
CS1TH=COS1*COSDEL-SIN1*SINDEL
CS2TH=CS1TH*CS1TH
SN1ET=SIN1*COSDEL-COS1*SINDEL
CS1ET=COS1*COSDEL+SIN1*SINDEL
CSM2ET=CS1ET**AM2
CSM1ET=CSM2ET*CS1ET
CSMET=CSM1ET*CS1ET
SNM2TH=DSN1TH**AM2
SNM1TH=SNM2TH* SN1TH
SNMTH=SNM1TH* SN1TH
CEF2=ONE+R*SNMTH
CEF3=R*(CSMET-SNMTH)/CEF2
CEF4=CEF3*CSNPH
TINF= T0*CEF2*(ONE+CEF4)
Y0=TINF-800.
Y1=1.722E-4*Y0*Y0
X=Y0/(750. +Y1)
S=0.0291E-5* EXP(-X*X/TWO)
SIG=S+ONE /R120
R120Z=R120/(RO+Z)
R120Z2=R120Z*R120Z
ZETA=(Z-H120)*R120Z
B=(TINF-T120)/TINF
CEFO=ONE-B
Y2=SIG*ZETA
Y3= EXP(-Y2)

```

```

Y7= ABS(ONE-B*Y3)
Y8=CEFO/Y7
TZ=TINF-(TINF-T120)*Y3
HZ=G120/(SIG*K*TINF)*1.67E-24
19 ZX=XZ(I1)
   IF(ZX.LE.Z)GOTO 22
20 I1=I1-1
   IF(I1.LE.0)GOTO 23
   ZX=XZ(I1)
   IF(ZX.GT.Z)GOTO 20
21 FACT=(Z-XZ(I1))/(XZ(I1+1)-XZ(I1))
   GOTO 25
22 I1=I1+1
   IF(I1.GT.NOX)GOTO 24
   ZX=XZ(I1)
   IF(ZX.LE.Z)GOTO 22
   I1=I1-1
   GOTO 21
23 I1=1
   FACT=0.
   GOTO 25
24 I1=NOX-1
   FACT=1.
25 CONTINUE
   IF(ATMS71.NE.1)RETURN
   TINF=PRF(1,NOX)
   TZ=PRF(1,I1)+(PRF(1,I1+1)-PRF(1,I1))*FACT
   RETURN
C.....
C   ENTRY TO DENSITY
C   MASS IN ATOMIC MASS UNITS
C   ENTRY ATMSN(NO,MASS,NZ)
C.....
   IF(ATMS71.EQ.1)GOTO 18
   GAMA=MASS*HZ
   Y5=Y2*GAMA
   Y6= EXP(-Y5)
   ARG=GAMA
   Y9=Y8**ARG
   NZ=NO*Y9*Y8*Y6
   RETURN
18 IN=MASS
   IM=INDX(IN)
   NZ=PRF(IM,I1)+(PRF(IM,I1+1)-PRF(IM,I1))*FACT
   RETURN
C.....
C   ENTRY TO DERIVATIVES OF NEUTRAL TEMPERATURES
C   PH REFERS TO LONGITUDE AND TH REFERS TO COLATITUDE
C   ENTRY ATMSD(DTDPH,DTDTH,DTDR)
C.....
   IF(ATMS71.EQ.1)GOTO 69
   DTDTH=-T0*MR/TWO*(SNM1TH*CS1TH*(ONE+CEF4) -
1CSNPH*(CSM1ET*SN1ET
1 + SNM1TH*CS1TH+CEF3*SNM1TH*CS1TH))
   DTDPH=T0*CEF2*CEF3*N*CSN1PH*CEF1/TWO*( -SIN(CAPPHI/TWO).)
   RETURN
69 DTDPH=0.
   DTDTH=0.
   DTDR=0.
   RETURN
C.....
C   ENTRY ATMSUP(NZNO,NZN,NZHE,NZHEP)

```

```

NZN=3.E6
NZNO=5.E6
IF(Z.LT.250.E5)GO TO 6767
NZN=3.E6*EXP(-(Z-250.E5)/HN)
NZNO=5.E6*EXP(-(Z-250.E5)/HNO)
6767 NZHEP=PRF(8,I1)+(PRF(8,I1+1)-PRF(8,I1))*FACT
RETURN
END

```

C

C.....

```

SUBROUTINE EVALU(PHI,Y,YP,L)
$SET OWN
REAL*4 NZAO,NZOO,NZON2,NZOO2,LAMBDA
INTEGER WNDMDL,DRFMDL,QTMDL
DIMENSION Y(10),YP(20,6)
COMMON NSET,M,M2,CS(7),DUM2,DUM3,T0,T120,NZAO
COMMON CRSCN2,AUO,DUM5,NZOO,NZOO2,NZON2,
1DUM6,CK(2),CTH1,A1,A2
COMMON CTH4,CTE(2),CDO,DUM7,CRSCO,CRSCPH,DELTA,DUM8
COMMON UPHASE,CUPHI,PHIU,DUM9,DUM10,
1OFFSET,DELPH,PHFNAL,DPHOUT
COMMON ZEINIT,PHINIT,DUM11,LAMBDA,RBASE,RD,
1DUM12,SPHASE,DUM13
COMMON DUM14,DBO,ddb
COMMON R0,DELY,WTH0,WPERPO,OMEGA,BO,DWDRE,DWDPH
COMMON/CNTRL/WNDMDL,DRFMDL,QTMDL
1 CONTINUE
IF(DRFMDL.EQ.0)GOTO 10
RE=Y(2)
B=B0*(R0/RE)**3
S2=-B*OMEGA*RE*RE
S= S2
DS2DR=B*OMEGA*RE
CALL VPERP(ZW,PHI,WPERP)
RW=ZW+R0
RW2=RW*RW
RE2=RE*RE
WPERPO=WPERP*RE2/RW2
DWDRE=2.*WPERPO/RE
WTH0=0.
DWDPH =0.
WTHT=( DS2DR)/B
YP(1,L)=RE/WTHT
YP(2,L)=WPERPO*YP(1,L)
RETURN
10 RE=Y(2)
PI2=3.1415926535/2.
COSPH=COS(PHI)
SINPH=SIN(PHI)
IF(RE.GT.RD)GOTO 110
PHID=PI2
DPHID=0.
GOTO 111
110 PHID=ARSIN(SQRT(RD/RE))
DPHID=-SQRT(RD/(RE-RD))/(2.*RE)
111 PHIDS=PI2-PHID
DPHIDS=-DPHID
PSIA=CS(1)+CS(2)*COS(CS(3)*PHIDS)
DPSIA=-CS(2)*CS(3)*SIN(CS(3)*PHIDS)*DPHIDS
PSIB=CS(4)+CS(5)*COS(CS(6)*PHIDS)
DPSIB=-CS(5)*CS(6)*SIN(CS(6)*PHIDS)*DPHIDS
B=B0*(R0/RE)**3

```

```

S1=-CS(7)*R0*(PSIA*SINPH+PSIB*COSPH)
S2=-B*OMEGA*RE*RE
S=S1+S2
DSDTH=-CS(7)*R0*(PSIA*COSPH-PSIB*SINPH)
DS1DR=-CS(7)*R0*(DPSIA*SINPH+DPSIB*COSPH)
DS2DR=B*OMEGA*RE
WPERP0=-DSDTH/(B*RE)
DWDRE=2.*WPERP0/RE+CS(7)*R0*
1(DPSIA*COSPH-DPSIB*SINPH)/(B*RE)
WTH0=DS1DR/B
DWDPH=-CS(7)*R0*(DPSIA*COSPH-DPSIB*SINPH)/B
WTHT=(DS1DR+DS2DR)/B
YP(1,L)=RE/WTHT
YP(2,L)=WPERP0*YP(1,L)
RETURN

```

C.....

```

ENTRY SS(S,COSPH,SINPH,RE)
IF(DRFMDL.EQ.0)GOTO 11
B=B0*(R0/RE)**3
S2=-B*OMEGA*RE*RE
S= S2
RETURN

```

```

11 PI2=3.1415926535/2.
IF(RE.LE.RD)PHID=PI2
IF(RE.GT.RD)PHID=ARSIN(SQRT(RD/RE))
PHIDS=PI2-PHID
PSIA=CS(1)+CS(2)*COS(CS(3)*PHIDS)
PSIB=CS(4)+CS(5)*COS(CS(6)*PHIDS)
B=B0*(R0/RE)**3
S1=-CS(7)*R0*(PSIA*SINPH+PSIB*COSPH)
S2=-B*OMEGA*RE*RE
S=S1+S2
RETURN
END

```

C

C.....

```

SUBROUTINE PHOTO(NHCHO,NHCHO2,NHCHN2,OPLUS,
1Q,QO4S,QO2D,QOO,QO2,
1QN2,QRATIO,NZO,NZO2,NZN2,Z)
$SET OWN
IMPLICIT REAL(A-Z)
INTEGER I,J,K,TAU,LMB,IL
DIMENSION ALMB(25),AA4S(25),AA2D(25),AA2P(25),
1AA4P(25),A2PP(25)
DATA ALMB/734.,700.,663.,650.,600.,550.,500.,450.,435.,
1 425.,400.,1375.,350.,325.,310.,300.,275.,250.,225.,
1 200.,175.,150.,125.,100.,0./
DATA AA4S/1.00,0.46,0.45,0.32,0.30,0.30,0.29,0.28,
1 0.28,0.27,0.27,0.27,0.27,0.27,0.27,0.27,0.27,0.26,
1 0.26,0.26,0.25,0.24,0.23,0.21/
DATA AA2D/0.00,0.54,0.55,0.42,0.45,0.44,0.44,
1 0.44,0.44,0.41,0.41,0.40,0.39,0.38,0.38,0.36,0.35,0.34,
1 0.34,0.33,0.33,0.32,0.31,0.28,0.26/
DATA AA2P/0.00,0.00,0.00,0.26,0.25,0.26,0.27,
1 0.28,0.28,0.25,0.25,10.25,0.25,0.25,0.25,0.23,
1 0.23,0.22,0.21,0.20,0.20,0.19,1.18,0.18,0.15/
DATA AA4P/0.00,0.00,0.00,0.00,0.00,0.00,0.00,
1 0.00,0.00,0.07,0.07,0.08,0.09,0.10,0.10,0.10,0.10,0.11,
1 0.11,0.12,0.12,0.13,0.15,0.18,0.22/
DATA A2PP/0.00,0.00,0.00,0.00,0.00,0.00,0.00,
1 0.00,0.00,0.00,0.00,0.00,0.00,0.00,0.04,0.05,0.06,
1 0.08,0.09,0.09,0.11,0.12,0.14,0.16/

```

```

DIMENSION CRIO2(70), CRIO(70), CRIN2(70)
DIMENSION EX(1000), PH(70), CRAO(70), CRAO2(70), CRAN2(70),
1LAMD(70)
DIMENSION PHCRO(70), PCRO2D(70), PHCRO2(70),
1PHCRN2(70), PHCROO(70)
QO4S=0.
QO2D=0.
QOO=0.
QO2=0.
QN2=0.
DO 1 I=1,K
TAU=(CRAO(I)*NHCHO+CRAO2(I)*NHCHO2+
1CRAN2(I)*NHCHN2)*100.+1.5
IF(TAU.GT.1000)TAU=1000
EXTAU=EX(TAU)
QO4S=QO4S+PHCRO(I)*EXTAU
QO2D=QO2D+PCRO2D(I)*EXTAU
QOO=QOO+PHCROO(I)*EXTAU
QO2=QO2+PHCRO2(I)*EXTAU
1 QN2=QN2+PHCRN2(I)*EXTAU
QO4S=QO4S*NZO*QRATIO
QO2D=QO2D*NZO*QRATIO
QOO=QOO* OPLUS*QRATIO
QO2=QO2*NZO2*QRATIO
QN2=QN2*NZN2*QRATIO
Q=QO4S+QO2D+QOO+QO2+QN2
RETURN
C.....
ENTRY PHOTOO
IL=1
READ(1,1000)K
READ(1,1001)(PH(J),LAMD(J),CRAO(J),CRAO2(J),CRAN2(J),
1CRIO(J),CRIO2(J),CRIN2(J),J=1,K)
WRITE(3,1003)(PH(J),LAMD(J),CRAO(J),CRAO2(J),CRAN2(J),
1 CRIO(J),CRIO2(J),CRIN2(J),J=1,K)
1000 FORMAT(8X,I5)
1002 FORMAT(' SUNSPOT # FOR DATA IS',F5.1,'ACTIVITY IS',F5.1)
1001 FORMAT( 8F5.0)
1003 FORMAT(' ',8F8.2)
C FLUX IS READ IN PHOTONS CM-2 SEC-1
C EFFECTIVE WAVELENGTH IN A
C CROSSECTION IN CM-2/10E-18
DO 765 I=1,K
765 PHCROO(I)=0.
DO 2 I=1,K
69 IF(LAMD(I).GT.ALMB(IL))GO TO 70
IF(IL.EQ.25)GO TO 70
IL=IL+1
GO TO 69
70 CONTINUE
CRAO(I)=CRAO(I)*1.E-18
CRAO2(I)=CRAO2(I)*1.E-18
CRAN2(I)=CRAN2(I)*1.E-18
PHCRO2(I)= PH(I)*CRIO2(I)*1.E-9
PHCRO(I)= PH(I)*CRIO(I)*1.E-9*(AA4S(IL)+AA4P(IL))
PCRO2D(I)=(AA2D(IL)+AA2P(IL)+A2PP(IL))*PH(I)*CRIO(I)*1.E-9
IF(LAMD(I).LT.360.)PHCROO(I)=.5*PHCRO(I)
2 PHCRN2(I)= PH(I)*CRIN2(I)*1.E-9
DELX=.01
X=0.
DO 3 I=1,1000
EX(I)=EXP(-X)

```

```

3 X=X+DELX
  S1=0.
  S12D=0.
  S2=0.
  S3=0.
  S4=0.
  DO 4 I=1,K
    S1=S1+PHCRO(I)
    S12D=S12D+PCRO2D(I)
    S2=S2+PHCROO(I)
    S3=S3+PHCRO2(I)
    S4=S4+PHCRN2(I)
4 CONTINUE
  WRITE(3,5) S1,S12D,S2,S3,S4
5 FORMAT(' PHCRO4S+',1PE10.3,' PHCRO2D+',E10.3,
1'PHCRO++',E10.3,' PHCRO2+',E10.3,' PHCRN2+',E10.3)
  RETURN
  END

```

C

C.....

```

SUBROUTINE ECLPSE(TIME, LONGO, THETA, UT, LONG, SINX, COSX,
1PHIM, THT, NENTRY)

```

\$SET OWN

```

  IMPLICIT REAL*4 (A-Z)
  INTEGER NOECLP, NENTRY
  NENTRY=0

```

```

  T0=(TH0+LONGO-LNGEC)/RAD*240.+TIMEEC

```

C UT IS UNIVERSAL TIME KEPT AT FIELD LINE

```

  UT=T0+TIME

```

C LONGITUDE WEST OF FIELD LINE

```

  LONG=LONGO+TIME/240. *RAD-(THETA-THINIT)

```

C TIMEEC IS UNIVERSAL TIME POINT OF TRANSIT

```

  IF(NOECLP.EQ.1) RETURN

```

```

  IF(UT.LT.FSC.OR.UT.GT.LSC) RETURN

```

```

  NENTRY=1

```

```

  BASS=(UT-TIMEEC)*DTDECS+DECS

```

```

  SNDEL= SIN(BASS*RAD)

```

```

  CSDEL= COS(BASS*RAD)

```

```

  THT=THETA-(UT-TIMEEC)*DTRAS/240.*RAD

```

```

  SINTH= SIN(THT)

```

```

  COSTH= COS(THT)

```

```

  SINX= SIN(((UT-TIMEEC)*(DTDECM+(UT-TIMEEC)*D2TDCM/2.)+
1DECM)*RAD)

```

```

  COSX= SQRT(1. -SINX*SINX)

```

```

  LONGM= LNGEC-(UT-TIMEEC)*(DTRAM+(UT-TIMEEC)*D2TRAM/2.)
1/240.*RAD+

```

```

1OMEGA*(UT-TIMEEC)

```

```

  PHIM=LONGM-LONG

```

```

  RETURN

```

C.....

```

ENTRY SUN(SIN1, COS1, CRUD1, CRUD2, CRUD3, CRUD4, R)

```

```

  B1=R*R+RM2

```

```

  B2=-TWORM*R

```

```

  CSCHIS=SIN1*SNDEL+COS1*CSDEL*COSTH

```

```

  SNCHIS= SQRT(1. -CSCHIS*CSCHIS)

```

```

  IF(SNCHIS.LT.1.E-4) SNCHIS=1.E-4

```

```

  SNETA1=SINTH*CSDEL/SNCHIS

```

```

  CSETA1=(SNDEL-SIN1*CSCHIS)/(COS1*SNCHIS)

```

```

  RETURN

```

C.....

```

ENTRY MOON(F, SNX, CSX, SNPHIM, CSPHIM)

```

```

  F=1.

```

```

CSCHIM=SIN1*SNX+COS1*CSA*CSCHIM
SNCHIM= SQRT(1. -CSCHIM*CSCHIM)
C TEMPORARY CURE FOR ZERO DIVISOR.
IF(SNCHIM.LT.1.E-4)GO TO 16
SNETA2=SNPHIM*CSX/SNCHIM
CSETA2=(SNX-CSCHIM*SIN1)/(SNCHIM*COS1)
CSETA=CSETA2*CSETA1+SNETA2*SNETA1
XX= SQRT(B1+B2*CSCHIM)
K=R*SNCHIM/XX
SQRTK= SQRT(1. -K*K)
CSCHI=SQRTK*CSCHIM-K*SNCHIM
SNCHI=SQRTK*SNCHIM+K*CSCHIM
CSALFA=CSCHIS*CSCHI+SNCHIS*SNCHI*CSETA
ALFA=ARCOS(CSALFA)
DMOON=RM*DLUNA/XX
ALFMIN=(DSUN-DMOON)/TWO
IF(ALFMIN)15,15,17
15 ALFMIN=ALFMIN-ALFA0
IF(ALFA+ALFMIN)16,16,20
16 F=0.
RETURN
17 ALFMIN=ALFMIN+ALFA0
IF(ALFA-ALFMIN)18,18,20
18 F=1. -DMOON2/DSUN2
RETURN
20 IF(ALFA-(DMOON+DSUN)/TWO)22,22,21
21 F=1.
RETURN
22 DMOON2=DMOON*DMOON
C1=(DSUN2-DMOON2)/(4. *ALFA)
C2=DMOON/DSUN
RHO1=(C1+ALFA)/DSUN
RHO2=(-C1+ALFA)/DMOON
F=(PI-ARCOS(RHO1)-C2*ARCOS(RHO2)+
1RHO1* SQRT(1.-RHO1*RHO1)+C2*RHO2* SQRT(1.-RHO2*RHO2))/PI
RETURN
C.....
ENTRY READEC(INTLNG,DELNG,LNGOBS,LATOBS,NOECLP,FSC,LSC)
READ(1,1003)NOECLP
CM5=1.E5
ONE=1.
TWO=2.
PI=3.1415926535
TWOPI=2. *PI
RAD=PI/180.
R0=6378.17E5
D60=60.
D3600=3600.
PERIOD=23. *D3600+56. *D60+4.09054
SEC=PERIOD/360.
OMEGA=TWOPI/(3600.*24.)
OMEGAM=TWOPI/(27.321661 *24. *D3600)
ALFA0=1.E-4*RAD
C MEASURED FROM TRANSIT
C FOR ECLIPSE AT A GIVEN PLACE AND TIME
C L1=INITIAL LONGITUDE OF FIELD LINE
C L2=DELTA LONGITUDE OF THE THREE FIED LINES RUN SIMULTANEOUSLY
C L3=LONGITUDE OF OBSERVOR
C L4=LATOBS
READ(1,1000)L1,L2,L3,L4
WRITE(3,1002)L1,L2,L3,L4
INTLNG=L1*RAD

```



```

DELNG=L2* $\pi$ 
LNGOBS=L3* $\pi$ 
LATOBS=L4* $\pi$ 
C ANGULAR DIAMETERS OF SUN AND MOON
FSC=19.*D3600
FSC=18.*D3600+15.*D60
LSC=23.5*D3600
LSC=21.*D3600+10.*D60
DSUN=(15./D60+53.5/D3600)*TWO* $\pi$ 
DSUN=(16./D60+1.8/D3600)*TWO* $\pi$ 
DLUNA=(15./D60+10.0/D3600)*TWO* $\pi$ 
DLUNA=(16./D60+42.9/D3600)*TWO* $\pi$ 
TIMEEC=19.*D3600+45.*D60+6.
TIMEEC=21.*D3600+3.*D60+55.0
LNGEC=117.+9./D60
LNGEC=139.+21./D60+14./D3600
LNGEC=LNGEC* $\pi$ 
DECM=+(4.+37./D60+57.48/D3600)
DECM=-(7.+46./D60+1.1/D3600)
DECS=+(4.+24./D60+1.59/D3600)
DECS=-(7.+27./D60+9.2/D3600)
DTDECS=-57.17/D3600**2
DTDECS=-56.3/D3600**2
DTRAS=8.983/D3600
DTRAS=9.24/D3600
DTDECM=-(14./D60+56.64/D3600)/D3600
DTDECM=-(11./D60+9.8/D3600)/D3600
DTRAM=111.245/D3600
DTRAM=147.44/D3600
D2TDCM=-1.76/D3600**3
D2TDCM=3.1/D3600**3
D2TRAM=0.00/D3600**2
DSUN2=DSUN*DSUN
PARLXM=(55./D60+39.81/D3600)* $\pi$ 
PARLXM=(61./D60+23.8/D3600)* $\pi$ 
RM=R0/PARLXM
RM2=RM*RM
TWORM=2.*RM
RM3=RM2*RM
RETURN

```

```

C.....
ENTRY ECLINT(THINIT)
THO=THINIT
1 IF(THO- $\pi$ )3,2,2
2 THO=THO-TWO $\pi$ 
GO TO 1
3 RETURN
1000 FORMAT(4(8X,E11.3))
1002 FORMAT(' INTLNG=',1PE11.3,' DELNG=',E11.3,' LNGOBS=',E11.3,
1 ' LATOBS=',E11.3)
1003 FORMAT(8X,I5)
END

```

```

C
C.....
SUBROUTINE CHECK(N,J,M2,K)
$SET OWN
REAL*4 N(100,10,2)
10 CONTINUE
DO 1 I=1,M2
1 IF(N(I,J,K).LT.1.E-10)N(I,J,K)=1.E-10
RETURN
END

```

```

C.....
SUBROUTINE SOLVE(G,J,M2,K)
$SET OWN
DIMENSION G(100,10,2)
REAL*8 XX(100),YY(100),DENOM
COMMON /COEFF/ X(7,100)
1 CONTINUE
XX(1)=X(6,1)/X(5,1)
YY(1)=X(7,1)/X(5,1)
DO 10 I=2,M2
DENOM=X(5,I)-X(4,I)*XX(I-1)
XX(I)=X(6,I)/DENOM
10 YY(I)=(X(7,I)-X(4,I)*YY(I-1))/DENOM
G(M2,J,K)=YY(M2)
NM1=M2-1
DO 20 KK=1,NM1
I=M2-KK
20 G(I,J,K)=YY(I)-XX(I)*G(I+1,J,K)
RETURN
END

```

```

C.....
SUBROUTINE LINCO(N,J,DELYSQ,DELY2,RDELPH,M,M2,K)
$SET OWN
IMPLICIT REAL*4 (A-Z)
INTEGER I,J,M,M2,K
DIMENSION N(100,10,2)
COMMON /COEFF/ X(7,100)
1 CONTINUE
DO 90 I=1,M2
A=X(7,I)/DELYSQ
B=X(6,I)/DELY2
C=X(5,I)
D=X(4,I)
X(4,I)=A+B
X(5,I)=-2.*A+C-RDELPH
X(6,I)=A-B
90 X(7,I)=-D-N(I,J,K)*RDELPH
X(5,1)=X(5,1)+X(4,1)*N(1,J,K)/N(2,J,K)
IF(M.LT.M2)X(5,M2)=X(5,M2)+X(6,M2)*N(M2,J,K)/N(M2-1,J,K)
IF(M.EQ.M2)X(4,M)=X(4,M)+X(6,M)
RETURN
END

```

```

C.....
SUBROUTINE RETHET(S0,RE,PHI)
$SET OWN
IMPLICIT REAL*4 (A-Z)
PHIX=PHI*180./3.14159
COSPH=COS(PHI)
SINPH=SIN(PHI)
DELRE=1.E5
CALL SS(S,COSPH,SINPH,RE)
DELS=S-S0
IF(DELS.GT.0.)GO TO 3
IF(DELS.EQ.0.)RETURN
1 CALL SS(S,COSPH,SINPH,RE+DELRE)
DELS=S-S0
IF(DELS.GT.0.)GO TO 2
RE=RE+DELRE
GO TO 1

```

```

2 IF (DELS.LE.1.E8) GO TO 6
  DELRE=DELRE/2.
  GO TO 1
3 CALL SS(S,COSPH,SINPH,RE-DELRE)
  DELS=S-S0
  IF (DELS.LE.0.) GO TO 4
  RE=RE-DELRE
  GO TO 3
4 IF ((-DELS).LE.1.E8) GO TO 5
  DELRE=DELRE/2.
  GO TO 3
5 RE=RE-DELRE
  GO TO 7
6 RE=RE+DELRE
7 RETURN
  END

```

C

C.....

```

      SUBROUTINE PRDCT(HGT, PHI, LATOBS, DELTA, NZOO, NZOO2, NZON2,
1NZO, NZO2, NZN2, TZ, QRA, QO4S, QN, HO, BETA)
$SET OWN
      IMPLICIT REAL (A-Z)
      DIMENSION LMB(10,5)
      RO=6370.E5
1 CONTINUE
      PROTON=1.67252E-24
      KB=1.38054E-16
      GO=980.655
      UNDRFL=1.E-10
      R=RO+HGT
      CALL ATMS(R, PHI)
      GRAV=GO*RO*RO/(R*R)
      SINOBS=SIN(LATOBS)+UNDRFL
      COSOBS=COS(LATOBS)+UNDRFL
      CALL ATMST(TINF, TZ, HGT, COSOBS, SINOBS)
      CALL ATMSN(NZOO, 16., NZO)
      CALL ATMSN(NZOO2, 32., NZO2)
      CALL ATMSN(NZON2, 28., NZN2)
      HO=KB*TZ/(16.*PROTON*GRAV)
      HO2=HO*16./32.
      HN2=HO*16./28.
      SNDEL=SIN(DELTA)+UNDRFL
      CSDEL=COS(DELTA)+UNDRFL
      CHI=ARCOS(SNDEL*SINOBS+CSDEL*COSOBS*COS(PHI))
      SINCHI=SIN(CHI)
      NHCHO=NZO*HO*CH(R/HO, CHI, SINCHI)
      NHCHO2=NZO2*HO2*CH(R/HO2, CHI, SINCHI)
      NHCHN2=NZN2*HN2*CH(R/HN2, CHI, SINCHI)
      OPLUS=1.E6
      CALL PHOTO(NHCHO, NHCHO2, NHCHN2, OPLUS, QN, QO4S, QO2D, QOO, QO2,
1QN2, QRA, NZO, NZO2, NZN2, HGT)
      CALL RATEL(LMB, TZ, KB*TZ)
      BETA=LMB(1,1)*NZN2+LMB(1,2)*NZO2
      RETURN
      END

```

C

C.....

```

      SUBROUTINE QR(Y, Q, R, SINHQM, COSHQM, P, QMAX, RE)
$SET OWN
      IMPLICIT REAL*4 (A-Z)
      INTEGER NSET, MU, LX, M2
      COMMON NSET, MU, M2, CS(7), DUM2, DUM3, T0, T120, NZAO

```

```

1DUM6, CK(2), CTH1, A1, A2
COMMON CTH4, CTE(2), CDO, DUM7, CRSCO, CRSCPH, DELTA, DUM8
COMMON UPHASE, CUPHI, PHIU, DUM9, DUM10,
1OFFSET, DELPH, PHFNAL, DPHOUT
COMMON ZEINIT, PHINIT, DUM11, LAMBDA, RBASE, RD,
1DUM12, SPHASE, DUM13
COMMON DUM14, DBO, DDB
COMMON R0, DELY, WTH0, WPERP0, OMEGA, B0
C...CALCULATES Q FROM Y AND QMAX.....
C...THEN CALCULATES R FROM P AND Q BY NEWTON-RAPHSON.....
  YSINH=Y*SINHQM
  Q=ALOG(YSINH+SQRT(1.+YSINH*YSINH))/LAMBDA
  IF(Q) 1, 1, 3
1 R=RE
  RETURN
3 PR=1./P
  TOL=.0001
  F=R/R0
  LX=0
  QR2=1./(Q*Q)
  PRQR2=PR*QR2
5 F3=F*F*F
  CORR=((F3+PRQR2)*F-QR2)/(4.*F3+PRQR2)
  F=F-CORR
  IF(ABS(CORR)-TOL) 2, 2, 4
4 LX=LX+1
  IF(LX-100) 5, 5, 6
6 WRITE(3, 1000) F, CORR, TOL, P, Q
  STOP
2 R=F*R0
  RETURN
C.....
  ENTRY QR1(SINHQM, COSHQM, P, QMAX, RE)
  RE=RE
  R02=R0*R0
  P=RE/R0
  QMAX=SQRT(1.-RBASE/RE)*R02/(RBASE*RBASE)
  SINHQM=SINH(LAMBDA*QMAX)
  COSHQM=COSH(LAMBDA*QMAX)
  RETURN
1000 FORMAT(1H, 'R DID NOT CONVERGE', 1P5E15.5)
  END
C
C.....
  SUBROUTINE RKAM(PHI, TIME, RE, DELPH, NEQ, L)
$SET OWN
  IMPLICIT REAL*4 (A-Z)
  INTEGER NEQ, L, I, M
  COMMON DUM1(52), SPHASE
  DIMENSION K(20, 6), YP(20, 6)
  DIMENSION Y(10), YS(10)
  X=PHI
  Y(1)=TIME
  Y(2)=RE
  IF(L-5) 1, 50, 50
C...RUNGE-KUTTA METHOD FOR INITIAL VALUES.....
1 IF(L-1) 2, 7, 3
2 H2=DELPH/2.
  H720=DELPH/720.
  H=DELPH
3 CALL EVALU(X+SPHASE, Y, K, 1)

```

```

      IF(L)100,100,7
      DO 8 I=1,NEQ
      8 YP(I,L)=K(I,1)
      X=X+H2
      DO 10 I=1,NEQ
      10 YS(I)=Y(I)+H2*K(I,1)
      CALL EVALU(X+SPHASE,YS,K,2)
      DO 20 I=1,NEQ
      20 YS(I)=Y(I)+H2*K(I,2)
      CALL EVALU(X+SPHASE,YS,K,3)
      X=X+H2
      DO 30 I=1,NEQ
      30 YS(I)=Y(I)+H*K(I,3)
      CALL EVALU(X+SPHASE,YS,K,4)
      DO 40 I=1,NEQ
      40 Y(I)=Y(I)+H*(K(I,1)+2.*(K(I,2)+K(I,3))+K(I,4))/6.
      TIME=Y(1)
      RE=Y(2)
      100 RETURN
C...ADAMS-MOULTON PREDICTOR-CORRECTOR METHOD.....
      50 CALL EVALU(X+SPHASE,Y,YP,5)
      X=X+DELPH
      DO 60 I=1,NEQ
      60 YS(I)=Y(I)+H720*(1901.*YP(I,5)-2774.*YP(I,4)+2616.*YP(I,3)-
      1 1274.*YP(I,2)+251.*YP(I,1))
      CALL EVALU(X+SPHASE,YS,YP,6)
      DO 70 I=1,NEQ
      70 Y(I)=Y(I)+H720*(251.*YP(I,6)+646.*YP(I,5)-264.*YP(I,4)+
      1 106.*YP(I,3)-19.*YP(I,2))
      DO 80 I=1,NEQ
      DO 80 M=1,4
      80 YP(I,M)=YP(I,M+1)
      TIME=Y(1)
      RE=Y(2)
      RETURN
      END
C
C.....
      SUBROUTINE GCALC(RE,PHI,DELPH,COSPH,SINPH,LONGO,DELY,G,N,V,
      1NOECLP)
$SET OWN
      IMPLICIT REAL*4 (A-Z)
      INTEGER MOLEC
      INTEGER MOL,REP,I1,II,III,ITYPE,IM(10),ITYP
      INTEGER I,M,M2,K,J,NSET,K1,NOECLP,NOMOL
      COMMON NSET,M,M2,CS(7),DUM1,DUM2,T0,T120,NZAO
      COMMON CRSCN2,AUO,DUM3,NZ00,NZ002,NZ0N2,
      1DUM4,CK(2),CTH1,A1,A2
      COMMON CTH4,CTE(2),CDO,DUM6,CRSCO,CRSCPH,DELTA,DUM8
      COMMON UPHASE,CUPHI,PHIU,DUM9,DUM10,
      1OFFSET,BBBB1,PHFNAL,DPHOUT
      COMMON ZEINIT,PHINIT,DUM11,LAMBDA,RBASE,RD,
      1DUM12,SPHASE,DUM13
      COMMON SCLN,DB0,ddb
      COMMON RO,BBB2,WTH0,WPERPO,OMEGA,B0,DWDRE,DWDPH,TIME
      COMMON INTLNG,DELNG,LNGOBS,UT,LONG,LATOBS,QRA,OMEGA0
      COMMON /COEFF/ X(7,100)
      COMMON /MOL/ NOMOL,MOL(10,2)
      COMMON /OPR/ REP
      DIMENSION N(100,10,2),V(100,10,2),G(100,10,2)
C...NO ECLIPSE: NOECLP=1.....
C.....ECLIPSE: NOECLP=2.....

```

```

PROTON=1.67252E-24
DELYSQ=DELY**2
DELY2=DELY*2.
RDELPH=1./DELPH
DO 4 K=1,NOECLP
ITYP=0
ITYPE=0
DO 4 III=1,REP
IF(III.EQ.REP)ITYPE=1
IF(III.EQ.REP)ITYP=INBED
DO 5 J=1,NOMOL
5 IM(J)=J
DO 4 II=1,NOMOL
I1=IM(1)
AMU=MOL(II,1)
MOLEC=MOL(II,2)
C...ATOMIC MASS OF ATOM OR MOLECULE.....
C...BIN NUMBER (LOCATION OF MOLECULE IN TABLES.
C SEE MAIN, COEFF, RATES)
Z=1.
IF(MOLEC.EQ.6)Z=2.
IF(I1.EQ.1)CALL COEFN(Z,RE,PHI,N,V,IM,K,ITYP,
1AMU,MOLEC,LONGO,0)
IF(I1.NE.1)CALL COEFN(Z,RE,PHI,N,V,IM,K,ITYP,
1AMU,MOLEC,LONGO,1)
CALL LINCO(G,I1,DELYSQ,DELY2,RDELPH,M,M2,K)
CALL SOLVE(N,I1,M2,K)
IF(I1.EQ.1)CALL COGTON(N,I1,K)
CALL CHECK(N,I1,M2,K)
CALL COV(N,V,I1,K,ITYPE)
IF(NOMOL.EQ.1)GO TO 4
DO 33 I=2,NOMOL
33 IM(I-1)=IM(I)
IM(NOMOL)=I1
4 CONTINUE
NSET=NSET+1
RETURN
END
C
C.....
SUBROUTINE RATES
$SET OWN
IMPLICIT REAL (A-Z)
INTEGER I,J,I1,NSET,M,M2
INTEGER IM(10),MOLEC,NOMOL
DIMENSION CD(10,15),BCD(10,15),LAMB(10,5)
C...ALPHC IS FOR CORRECTING RECOMBINATION RATES.....
C...BETAC IS FACTOR FOR CORRECTING LOSS COEFFICIENT BETA.....
COMMON /BETAC/ BETAC,ALPHC
COMMON /MOL/ NOMOL,MOL(10,2)
COMMON /CHEM/ LM(10,5)
COMMON NSET,M,M2,DUM(27),CDO
KB=1.38054E-16
DO 111 I=1,6
DO 111 J=1,15
111 CD(I,J)=1.E22
CXT=8.4E15/1500.**2.5*(16./17.)**.5
XT=300.**.5
MUONO=((16.+30.)/(16.*30.))**.5
MUOO2=((16.+32.)/(16.*32.))**.5
MUON2=((16.+28.)/(16.*28.))**.5
MUOFE=((16.+56.)/(16.*56.))**.5

```

```

MUNOO2=((30.+32.)/(30.*32.))**.5
MUNON2=((30.+28.)/(30.*28.))**.5
MUNOFE=((30.+56.)/(30.*56.))**.5
MUO2N2=((32.+28.)/(32.*28.))**.5
MUO2FE=((32.+56.)/(32.*56.))**.5
MUN2FE=((30.+56.)/(30.*56.))**.5
MUNO=((14.+16.)/(14.*16.))**.5
MUNNO=((14.+30.)/(14.*30.))**.5
MUNO2=((14.+32.)/(14.*32.))**.5
MUNN2=((14.+28.)/(14.*28.))**.5
C...B(O+,NO+)
  CD(1,2)=CXT*MUONO
C...B(O+,O2+)
  CD(1,3)=CXT*MUOO2
C...B(O+,N2+)
  CD(1,4)=CXT*MUON2
C...B(O+,O)
  CD(1,10)=CDO/1000.**.5
C...B(O+,O2)
  CD(1,11)=3.3E18/XT
C...B(O+,N2)
  CD(1,12)=3.4E18/XT
C...B(NO+,O+)
  CD(2,1)=CD(1,2)
C...B(NO+,O2+)
  CD(2,3)=CXT*MUNOO2
C...B(NO+,N2+)
  CD(2,4)=CXT*MUNON2
C...B(NO+,O)
  CD(2,10)=3.3E18/XT
C...B(NO+,O2)
  CD(2,11)=1.9E18/XT
C...B(NO+,N2)
  CD(2,12)=1.8E18/XT
C...B(O2+,O+)
  CD(3,1)=CD(1,3)
C...B(O2+,NO+)
  CD(3,2)=CD(2,3)
C...B(O2+,N2+)
  CD(3,4)=CXT*MUO2N2
C...B(O2+,O)
  CD(3,10)=3.3E18/XT
C...B(O2+,O2)
  CD(3,11)=1.3E18/XT
C...B(O2+,N2)
  CD(3,12)=1.9E18/XT
C...B(N2+,O+)
  CD(4,1)=CD(1,4)
C...B(N2+,NO+)
  CD(4,2)=CD(2,4)
C...B(N2+,O2+)
  CD(4,3)=CD(3,4)
  CD(4,10)=CD(3,10)
  CD(4,11)=CD(3,11)
  CD(4,12)=CD(3,12)
C...B(N+,O+)
  CD(5,1)=1.08E15/(1000.**2.5)
C...B(N+,NO+)
  CD(5,2)=CXT*MUNNO
C...B(N+,O2+)
  CD(5,3)=CXT*MUNO2
C...B(N+,N2+)

```

```

      CD(5,4)=CXT*MUNN2
C...B(N+,0)
      CD(5,10)=8.64E18/SQRT(1000.)
C...B(N+,02)
      CD(5,11)=5.23E18/SQRT(1000.)
C...B(N+,N2)
      CD(5,12)=5.08E18/SQRT(1000.)
      CD(6,10)=CD(1,10)
      CD(6,11)=CD(1,11)
      CD(6,12)=CD(1,12)
      RETURN
C.....
      ENTRY RATED(BCD,IM,MOLEC,TZ,TINF,KTI,KTE)
      TI=KTI/KB
      TE=KTE/KB
      CXT=TI**2.5
      XT=TINF**.5
      I1=IM(1)
      DO 56 I=1,NOMOL
56  BCD(I1,IM(I))=CD(MOLEC,IM(I))*CXT
      BCD(I1,10)=CD(MOLEC,10)*XT
      BCD(I1,11)=CD(MOLEC,11)*XT
      BCD(I1,12)=CD(MOLEC,12)*XT
      IF(MOLEC.NE.6)RETURN
      GAM=9.43
      LNGAM=ALOG(GAM)
      BEE=1.02E8/LNGAM*CXT
      BCD(I1,1)=BEE
      RETURN
C.....
      ENTRY RATEL(LAMB,TZ,KTE)
      TTN=300./TZ
      IF(TZ.GT.900.)TTN=300./900.
      TE=KTE/KB
      TTE=300./TE
      DO 60 I=1,10
      DO 60 J=1,5
      LAMB(I,J)=LM(I,J)
60  CONTINUE
      TENORM=1000./TE
      LAMB(2,1)=LAMB(2,1)*TENORM**1.2
      LAMB(3,5)=LAMB(3,5)*TENORM**.63
      LAMB(4,5)=LAMB(4,5)*TENORM**.37
      RETURN
      END
C
C.....
      SUBROUTINE QTITE(RE,PHI,COSPH,SINPH,N,K)
$SET OWN
      REAL L,LSTOQ,KB,LAMBDA,NZAO,NZON2,NZOO2,
1NZOO,N(100,10,2),NZO,NE
      COMMON NSET,M,M2,CS(7),DUM2,DUM3,T0,T120,NZAO
      COMMON CRSCN2,AUO,B0EQ,NZOO,NZOO2,NZON2,
1DUM6,CK(2),CTH1,A1,A2
      COMMON CTH4,CTE(2),CDO,DUM7,CRSCO,CRSCPH,DELTA,TILT
      COMMON UPHASE,CUPHI,PHIU,DUM9,DUM10,
1OFFSET,DELPH,PHFNAL,DPHOUT
      COMMON ZEINIT,PHINIT,DELPHO,LAMBDA,RBASE,RD,
1DUM12,SPHASE,PUNCH
      COMMON SCLN,DBO,DDB
      COMMON R0,DELY,WTH0,WPERPO,OMEGA,B0,DWDRE,DWDPH,TIME
      COMMON /SO/ SOL(15,100),SOLE(15,100)

```



```

COMMON /TE/ TEMP(2,100)
COMMON /EPSLN/ EPS(100),HGT(100),CNEBYO(100),II
KB=1.38054E-16
90 CONTINUE
ITWOM=2.*M
TOL=5.
IX2=1
IF(M.NE.M2) IX2=2
DO 20 IX=1,IX2
C0=CNEBYO(1)
EPSLN0=EPS(1)
I0=1
JX=2
9 J=I0
IF(IX.EQ.2) J=ITWOM-I0
NE=N(J,1,K)+N(J,2,K)+N(J,3,K)+N(J,4,K)
NZO=SOLE(4,J)
C=NE/NZO
IF(C.GT.C0) GO TO 10
TZ=SOLE(10,J)
SOLE(2,J)=TZ*KB
SOLE(3,J)=TZ*KB
TEMP(K,J)=TZ
I0=I0+1
IF(I0.GT.M) GO TO 20
GO TO 9
10 DO 19 I=I0,M
J=I
IF(IX.EQ.2) J=ITWOM-I
NE=N(J,1,K)+N(J,2,K)+N(J,3,K)+N(J,4,K)
NZO=SOLE(4,J)
C=NE/NZO
11 IF(JX.GT.II) GO TO 18
C1=CNEBYO(JX)
IF(C.LT.C1) GO TO 12
C0=C1
EPSLN0=EPS(JX)
JX=JX+1
GO TO 11
12 X=(C-C0)/(C1-C0)
EPSLN=EPSLN0+(EPS(JX)-EPSLN0)*X
LX=1
TE=TEMP(K,J)
TZ=SOLE(10,J)
DEL=TE-TZ
IF(DEL.LT.0.) DEL=0.
CNE2=4.8E-7*NE*NE
CNZO=3.E-12*NZO*NE/TZ
QN=SOLE(14,J)
IF(K.EQ.2) QN=QN*SOLE(9,J)
QEI=QN*EPSLN
14 X=TZ+DEL
IF(X.GT.0) GO TO 31
DEL=DEL/2.
GO TO 14
31 SQRTX=SQRT(X)
XSQRTX=X*SQRTX
F=QEI-(CNE2/XSQRTX+CNZO)*DEL
DF=CNE2/XSQRTX*(1.5*DEL/X-1.)-CNZO
CORR=F/DF
DEL=DEL-CORR
IF(ABS(CORR)-TOL) 17,17,15

```

```

15 LX=LX+1
   IF(LX.GT.20)GO TO 16
   GO TO 14
16 WRITE(3,100)CORR
100 FORMAT(' CORR=',F11.3)
   DEL=0.
17 TE=TZ+DEL
   SOLE(2,J)=KB*TE
   TI=TZ
   SOLE(3,J)=KB*TI
   TEMP(K,J)=TE
   GO TO 19
18 TZ=SOLE(10,J)
   SOLE(2,J)=TZ*KB
   SOLE(3,J)=TZ*KB
   TEMP(K,J)=TZ
19 CONTINUE
20 CONTINUE
   TWODY=DELY*2.
   J0=0
   J1=1
   DELYX=DELY
   DO 2 I=1,M2
   IF(I.LT.M2)GO TO 1
   DELYX=DELY
   J1=0
   IF(M.EQ.M2)J1=-1
   IF(M.EQ.M2)DELYX=TWODY
1 DTDY=(SOLE(2,I-J0)-SOLE(2,I+J1)
1     +SOLE(3,I-J0)-SOLE(3,I+J1))/DELYX
   J0=1
   DELYX=TWODY
   STOQ=SOL(6,I)
   L=SOL(9,I)
   LSTOQ=L*STOQ
   DTDS=LSTOQ*DTDY
2 SOLE(8,I)=DTDS
   RETURN

```

C.

```

ENTRY QUNT(NOECLP)
KB=1.38054E-16
DO 3 K=1,NOECLP
DO 3 I=1,M2
TZ=SOLE(10,I)
SOLE(2,I)=TZ*KB
SOLE(3,I)=TZ*KB
3 TEMP(K,I)=TZ
TWODY=DELY*2.
J0=0
J1=1
DELYX=DELY
DO 5 I=1,M2
IF(I.LT.M2)GO TO 4
DELYX=DELY
J1=0
IF(M.EQ.M2)J1=-1
IF(M.EQ.M2)DELYX=TWODY
4 DTDY=(SOLE(2,I-J0)-SOLE(2,I+J1)
1     +SOLE(3,I-J0)-SOLE(3,I+J1))/DELYX
   J0=1
   DELYX=TWODY
   STOQ=SOL(6,I)

```

```

L=SOL(9,I)
LSTOQ=L*STOQ
DTDS=LSTOQ*DTDY
5 SOLE(8,I)=DTDS
RETURN
END

```

C

C.....
SUBROUTINE UU0(PHI)

\$SET OWN

C...VARIABLE WIND. DIURNAL FACTOR IS READ IN S.R. IN2.....

```

INTEGER WNDMDL,DRFMDL,QTMDL
REAL*4 NZAO,NZOO,NZON2,NZOO2,LAMBDA
COMMON NSET,M,M2,CS(7),DUM2,DUM3,T0,T120,NZAO
COMMON CRSCN2,AUO,DUM5,NZOO,NZOO2,NZON2,
1DUM6,CK(2),CTH1,A1,A2
COMMON CTH4,CTE(2),CDO,DUM7,CRSCO,CRSCPH,DELTA,DUM8
COMMON UPHASE,CUPHI,PHIU,DUM9,DUM10,
1OFFSET,DELPH,PHFNAL,DPHOUT
COMMON ZEINIT,PHINIT,DUM11,LAMBDA,RBASE,RD,
1DUM12,SPHASE,DUM13
COMMON DUM14,DBO,ddb
COMMON RO,DELY,WTHO,WPERPO,OMEGA,BO,DWDRE,DWDPH
COMMON /CNTRL/ WNDMDL,DRFMDL,QTMDL
CUPH=CUPHI/(1.-COS(PHIU))
IF(WNDMDL.EQ.0)GO TO 10
CALL VWIND(PHI,UPH)
GO TO 11
10 UPH=COS(PHI+UPHASE)+OFFSET
11 CSDEL=COS(DELTA)
SNDEL=SIN(DELTA)
RETURN

```

C.....

```

ENTRY UU(SIN1,COS1,U)
IF(WNDMDL.EQ.0)GO TO 12
SINX=SIN1*CSDEL-COS1*SNDEL
COSX=COS1*CSDEL+SIN1*SNDEL
GO TO 13
12 CONTINUE
SINX=SIN1*CSDEL-COS1*SNDEL
COSX=COS1*CSDEL+SIN1*SNDEL
13 CONTINUE
U=CUPH*(1.-COSX)*UPH
IF(SINX.LT.0.)U=-U
RETURN
END

```

C

C.....
REAL FUNCTION CH0(CNEW)

\$SET OWN

```

IMPLICIT REAL*8 (A-Z)
REAL*4 CNEW,X,CHI,SNCHI,CH
INTEGER I
DIMENSION A(48),Y(48)
10 CONTINUE
A(1)=.20615171495780099
A(2)=.33105785495088417
A(3)=.26579577764421415
A(4)=.13629693429637754
A(5)=.4732892869412521D -1
A(6)=.1129990008033945D -1
A(7)=.1849070943526310D -2

```

```

A(8)=.2042719153082784D -3
A(9)=.1484458687398129D -4
A(10)=.6828319330871196D-6
A(11)=.1881024841079673D-7
A(12)=.2862350242973881D-9
A(13)=.2127079033224103D-11
A(14)=.6297967002517867D-14
A(15)=.5050473700035512D-17
A(16)=.4161462370372855D-21
Y(1)=.8764941047892784D -1
Y(2)=.46269632891508083
Y(3)=.1141057774831226D +1
Y(4)=.2129283645098380D +1
Y(5)=.3437086633893206D +1
Y(6)=.5078018614549767D +1
Y(7)=.7070338535048234D +1
Y(8)=.9438314336391938D +1
Y(9)=.1221422336886615D +2
Y(10)=.1544152736878161D+2
Y(11)=.1918015685675313D+2
Y(12)=.2351590569399190D+2
Y(13)=.2857872974288214D+2
Y(14)=.3458339870228662D+2
Y(15)=.4194045264768833D+2
Y(16)=.5170116033954331D+2
A(17)=.2715245941175409D-1
A(18)=.6225352393864789D-1
A(19)=.9515851168249278D-1
A(20)=.12462897125553387
A(21)=.14959598881657673
A(22)=.16915651939500253
A(23)=.18260341504492358
A(24)=.18945061045506849
Y(17)=.98940093499164993
Y(18)=.94457502307323257
Y(19)=.86563120238783174
Y(20)=.75540440835500303
Y(21)=.61787624440264374
Y(22)=.45801677765722738
Y(23)=.28160355077925891
Y(24)=.9501250983763744D-1
PI=3.1415926535
ONE=1.DO
TWO=2.DO
CH0=0.0
RETURN

```

C.....

```

ENTRY CH(X,CHI,SNCHI)
XSN=X*SNCHI
XSN2=XSN*XSN
CHX=0.DO
PHI0=80.DO*PI/180.DO
IF(CHI-PHI0)1,3,3
1 DO 2 I=1,16
2 CHX=CHX+A(I)/DSQRT(ONE-XSN2/(Y(I)+X)**2)
CH=CHX
RETURN
3 IF(CHI-PI/TWO)4,5,5
4 PHI0=CHI-10.DO*PI/180.DO
GO TO 6
5 PHI0=80.DO*PI/180.DO
6 SNPHI0=DSIN(PHI0)

```

```

XX=XSN/SNPHI0
XXSN=XSN
XXSN2=XXSN*XXSN
DO 7 I=1,16
7 CHX=CHX+A(I)/DSQRT(ONE-XXSN2/(Y(I)+XX)**2)
  CHX=CHX*DEXP(X*(ONE-SNCHI/SNPHI0))
  A1=(CHI-PHI0)/TWO
  A2=(CHI+PHI0)/TWO
  A3=XSN*A1
  DO 8 I=17,24
  SNPHI1=DSIN(-A1*Y(I)+A2)
  SNPHI2=DSIN(A1*Y(I)+A2)
8 CHX=CHX+A3*A(I)*(DEXP(X*(ONE-SNCHI/SNPHI1))/(SNPHI1*SNPHI1)
1+DEXP(+X*(ONE-SNCHI/SNPHI2))/(SNPHI2*SNPHI2))
  CH=CHX
  RETURN
END

```